THE EFFECT OF INTERNAL WAVES ON LONG RANGE ACOUSTIC PROPAGATION IN THE OCEAN

by

RICHARD JAY JAFFEE

Sc.B., Brown University
(1970)

SUBMITTED IN PARTIAL FULFILLMENT OF THE
REQUIREMENTS FOR THE DEGREE OF
DOCTOR OF PHILOSOPHY

at the

MASSACHUSETTS INSTITUTE OF TECHNOLOGY

and the

WOODS HOLE OCEANOGRAPHIC INSTITUTION

May, 1976

Signature of Author.....
Joint Program in Ocean Engineering, Massachusetts Institute of Technology - Woods Hole Oceanographic Institution, May, 1976

Certified by.....
Thesis Supervisor

Accepted by.....
Chairman, Joint Committee on Ocean Engineering, Massachusetts Institute of Technology - Woods Hole Oceanographic Institution

THE EFFECT OF INTERNAL WAVES ON LONG RANGE ACOUSTIC PROPAGATION IN THE OCEAN

by

RICHARD JAY JAFFEE

Submitted to the Department of Ocean Engineering in partial fulfillment of the requirements for the degree of Doctor of Philosophy

ABSTRACT

The acoustic-internal wave interaction in an acoustic waveguide is investigated using wave techniques. Refractive index fluctuations due to the vertical displacements of the internal waves create an inhomogeneous waveguide. The analysis uses weak scattering theory based upon the Rytov perturbation technique. It is found that the internal wave field acts as a diffraction grating in permitting only certain scattered acoustic waves to propagate through the waveguide. Since the internal waves are continuously distributed in wavenumber space, the acoustic fluctuations become a statistical average with a bias toward particular spatial internal wavelengths.

The multimode nature of acoustic propagation precludes the linear relationship of internal wave statistics to acoustic amplitude and phase fluctuations. Assuming statistical independence between amplitude and phase fluctuations within a mode and between different modes, it is shown that the total phase-rate fluctuation is a weighted sum of the phase-rate fluctuations in the individual modes.

Using a statistical internal wave model [C. Garrett and W. Munk, Geophys. Fluid Dynam., 2, 225-264 (1972)] predictions of acoustic fluctuations are made. Over much of the internal wave frequency band the slope of the phase rate frequency spectrum is between -0.5 and -1.0. The depth dependence for the mean-square phase rate fluctuation has been found. Largest fluctuations occur for shallow and deep receivers. The predicted fluctuations compare favorably with experimental data.

Thesis Supervisor: Robert P. Porter
Title: Associate Scientist of Ocean Engineering at the Woods Hole Oceanographic Institution

ACKNOWLEDGEMENTS

I am greatly indebted to my adviser, Dr. Robert Porter, for his many helpful discussions and valuable guidance. I would like to thank the various members of my thesis committee for their constructive comments and suggestions. I am especially grateful to my many friends for their encouragement and support. I would also like to thank Karen Pires for her excellent typing of the manuscript. I am happy to acknowledge Woods Hole Oceanographic Institution for its financial support.

TABLE OF CONTENTS

LIST OF FIGURES

LIST OF SYMBOLS

B	1/e depth for exponential Brunt-Väisälä profile
c	sound speed
$d_m(z)$	eigenfunction for mode m
D	width of waveguide
$E(\alpha,\omega)$	internal wave energy density spectrum
$F_{mn}(r)$	function of mode number and range
$F_\zeta(\alpha,\omega)$, $F_\sigma(\alpha,\omega)$	spectral density for vertical displacement, refractive index
g	acceleration of gravity
$G(r\|r_o)$	Green's function
h_{mn1}, h_{mn2}	functions of mode number and depth
j	number of internal wave modes containing energy at the inertial frequency
K_o	acoustic wavenumber
ℓ_z, ℓ_H	vertical, horizontal correlation scales
m,n	incident, scattered acoustic modes
$n_o(z)$	static refractive-index variation with depth
N	Brunt-Väisälä frequency
N_o	peak Brunt-Väisälä frequency for exponential profile
P,W	Rytov perturbation parameters
q_u, q_ℓ	slopes for n_o^2 bilinear profile
r	horizontal distance

S_z	salinity gradient
$S_m, \dot{S}_m$	phase fluctuation, phase rate fluctuation for mode m
T_{pz}	potential temperature gradient
Tu	Turner number
χ	horizontal distance in propagation direction
y	horizontal distance perpendicular to propagation direction
z, z_s	receiver depth, acoustic source depth
$\overline{Z^2(z)}$	mean-square vertical wave function
α	horizontal internal wavenumber
α_m	horizontal acoustic wavenumber in mode m
$\alpha^{(1)}(\omega)$	dispersion relation for internal wavenumber in first order mode
β	vertical internal wavenumber
γ_m	vertical acoustic wavenumber in mode m
$\Gamma(z_o), \Gamma(z_T)$	magnitude of refractive index fluctuations at depth z_o, acoustic thickness
δ	Dirac delta function
Δ	horizontal acoustic wavenumber difference between incident and scattered modes = $\lvert\alpha_m - \alpha_n\rvert$
$\theta_m(z_u, z)$	phase integral = $\int_z^{z_u} \gamma_m dz$
Λ	ray cycle length
μ	function of the Turner number relating refractive index fluctuations to the Brunt-Väisälä frequency
ν_m	normalization factor for mode m

ξ	vertical displacement fluctuation
ρ	density
σ	refractive index fluctuation
ψ	velocity potential
ω, ω_i	internal wave frequency, inertial frequency
ω_s	acoustic source frequency

1. INTRODUCTION

The passage of an acoustic wave through an inhomogeneous medium, such as the ocean, results in the presence of amplitude and phase fluctuations at the receiver. In an acoustical study these fluctuations may themselves be the quantity of interest or may instead be an undesirable by-product of the propagation path which seriously degrades the usefulness of the received signal. In either event, an understanding of the fluctuations and their causes is important in the study of underwater sound propagation and in the design and operation of underwater communication and detection systems.

Many mechanisms have been postulated to account for the observed acoustic fluctuations. Acoustic waves propagating over long paths in the ocean undoubtedly encounter many different types and scales of spatial and temporal variations in the medium. It is unlikely, therefore, that one theory will be able to predict all the characteristics of the acoustic signal present at the receiving hydrophone.

Early work on acoustic fluctuations has drawn heavily from its counterpart in electromagnetic propagation through the atmosphere. The literature contains numerous references to propagation through an infinite medium containing random, spherical inhomogeneities or homogeneous, isotropic turbulence (Ellison, 1951; Mintzer, 1953, 1954; Batchelor, 1956; Chernov, 1960; Tatarski, 1961; Tatarski, 1971). The emphasis in most of the acoustic studies was to predict amplitude and phase fluctuations at high frequencies and short ranges given the statistical nature of the turbulence or inhomogeneities.

The application of theories treating isotropic turbulence or random inhomogeneities to long range acoustic propagation in the ocean is a questionable procedure. Because of its density variation with depth, the ocean can be considered essentially as a horizontally stratified fluid. Most oceanic motions are therefore likely to possess differing spatial scales in the horizontal and vertical directions. As such, the assumption of variations in the medium possessing isotropic properties will limit a theory's range of validity in the ocean.

Recent acoustical studies at low frequencies and at long ranges have suggested that phenomena other than turbulence or inhomogeneities may be responsible for the observed acoustic fluctuations (Kennedy, 1969; Steinberg et al., 1972; Spindel et al., 1974; Stanford, 1974; Clark and Kronengold, 1974). The investigations have shown that on time scales of the order of several minutes or greater the acoustic phase is fairly stable while the acoustic amplitude exhibits a random character and fluctuates rapidly. Theoretical analysis predicts that temporal characteristics of amplitude and phase fluctuations due to turbulence or random inhomogeneities should be comparable (Chernov, 1960). Furthermore, experimental results have indicated that the principal cause of acoustic fluctuations over long ranges are dynamical processes in the ocean which are spatially coherent over many wavelengths of the acoustic signal (Steinberg et al., 1972), while spatial scales of isotropic turbulence or inhomogeneities in the ocean are at most on the order of meters (Liebermann, 1951; Benilov, 1969). It is reasonable therefore to hypothesize that some other mechanism(s) is

responsible for acoustic fluctuations in long range propagation studies. Some of the mechanisms which have been proposed include tidal influences (Weston et al, 1969; Urick et al., 1969), ocean currents effects (Franchi and Jacobson, 1972; Franchi and Jacobson, 1973), current shear (Sanford, 1974), biological activity (Weston, et al, 1969), Rossby waves (Baer and Jacobson, 1974), and internal waves (Lee, 1961; Barakos, 1965; Chuprov, 1966; Weston and Andrews, 1973; Porter et al., 1974; Weinberg et al., 1974; Munk and Zachariasen, 1976).

An acoustic wave propagating through any one of the above mentioned mechanisms will experience amplitude and phase fluctuations. For short range single path conditions the acoustic fluctuations can be directly related to the oceanic fluctuations. In moderate and long range propagation a hydrophone will detect acoustic signals arriving from many paths. The interaction of the various mechanisms with the multipath transmission structure causes a time-varying multipath interference at the receiver. The measured fluctuations are thus due to the direct interaction of the inhomogeneities with the acoustic waves as well as the spatial and temporal modification of the multipath structure.

Internal gravity waves generally are believed to be the dominant force causing oceanic motions and environmental fluctuations with time scales on the order of several minutes to many hours (Garrett and Munk, 1972; Garrett and Munk, 1975). Typical spatial scales of internal waves range from tens of meters to tens of kilometers horizontally and meters to hundreds of meters vertically. Their large scale motions and their pervasiveness throughout the world's oceans would likely

dominate the acoustic effects of any other inhomogeneities in this frequency-wavenumber band. As such, this study will investigate the nature of acoustic-internal wave interaction on long range acoustic propagation.

Many investigators have studied various aspects of the effect internal waves have on sound propagation. These have consisted of field experiments, theoretical studies, as well as laboratory experiments. The field experiments have found significant acoustic fluctuation energy at time scales where internal waves are expected to be present and have revealed that the spectral energy of amplitude fluctuations contains a higher frequency content than that of the phase fluctuations (Clark and Kronengold, 1974; Spindel et al., 1974). Much of the theoretical work has simplified the acoustic-internal wave interaction by treating the case of a single sinusoidal internal wave located at the interface between two different density fluids. This has been the approach adopted by Barakos (1965) and Malyuzhinits (1959) in their theoretical studies and Barkhatov and Cherkashin (1962; 1963) in their laboratory experiments concerned with the scattering and refraction of an acoustic plane wave by an internal wave. Assuming finite thickness for the internal wave Lee (1961) and Katz (1967) have developed a three layer model which they have studied using ray acoustics and computer simulations. Their analyses have shown that internal waves can cause significant focusing (and defocusing) of the acoustic signals resulting in large amplitude fluctuations. Stanford (1971) has developed a model which separates the horizontal distance between

the source and receiver into fluid columns in which each has a different width, mean sound velocity, internal wave magnitude, and internal wave frequency. The model phase-modulates the acoustic signal and produces fluctuations which agree quite well with his measured data. Using geometrical acoustics, a bilinear sound velocity profile, and horizontally varying internal waves introduced by numerical techniques, Deferrari (1974) predicted the horizontal scales of internal waves that most strongly affect an acoustic signal. He showed that internal waves with wavelengths comparable to the acoustic ray cycle length would produce large phase fluctuation at the internal wave frequencies. Also using geometrical acoustics Porter et al. (1974) developed a theory for acoustic-internal wave interaction based upon the internal wave model of Garrett and Munk (1972). With the assumption that the influence of the internal wave on the acoustical wave is concentrated over a small depth, they predicted phase and amplitude fluctuations as a function of space and time which basically agree with actual measurements. Recently, statistical models of the internal wave field have been utilized with ray acoustics (Munk and Zachariasen, 1976; Dyson et al., 1976) in an attempt to explain fluctuations of single path (Ewart, 1976) as well as multipath (Clark and Kronengold, 1974) propagation experiments. The close agreement between the theoretical predictions and the actual data lend strong evidence to the belief that internal waves are the principal cause of acoustic fluctuations in this spatial-temporal band.

Most of the studies of acoustic-internal wave interaction mentioned above have been based upon ray (geometrical optics) techniques. Acoustic phase fluctuations are assumed to be caused by changes in travel time for rays passing through refractive index fluctuations. Amplitude fluctuations generally are interpreted as being caused by temporal variations in multipath interference as the rays pass through the internal wave field. The theories based upon geometrical acoustics suffer from the usual limitations of ray methods. Among these are:

1. the restriction to high acoustic frequencies
2. the limitation to small index of refraction variations over the distance of an acoustic wavelength
3. the failure to represent accurately the field near turning points, caustics, and focal points
4. the failure to account for diffraction effects.

Weighted against the limitations and deficiencies of ray theory are its ease in implementation as well as its clear physical interpretation. Nevertheless, since geometrical optics is in fact an approximation to the wave equation, it would be desirable to study the acoustic-internal wave interaction from the wave point of view.

The existence of a minimum sound speed at a mid-water depth in the ocean creates an acoustic waveguide which can support sound propagation over very long ranges with little attenuation. Since horizontal sound speed variations are usually small compared to the depth-dependent variations, most acoustic propagation studies in the ocean involve the assumption of a horizontally stratified medium. Any

refractive index perturbations induced by the internal waves become superimposed on the static sound speed profile. Under the assumption of horizontal homogeneity and isotropy, the internal wave field's interaction with the sound speed profile creates a stratified inhomogeneous waveguide which is assumed to be homogeneous and isotropic within a horizontal strata.

It has long been known that inhomogeneities in a waveguide can strongly affect propagation through the duct (Isakovich, 1957; Lapin, 1958; Samuels, 1959; Clay, 1964; Pierce, 1965). Under the influence of the waveguide, the inhomogeneities cause scattering to take place in discrete directions. As a result, both the incident and scattered waves can propagate through the waveguide with little attenuation.

At the receiver a complicated multimode structure will be present. Each incident mode is capable of generating a complete set of scattered modes each with a different amplitude and phase. Numerical techniques are necessary for determining the full multimode summation but it will be shown that only a few of the scattered modes contribute appreciably to the sum. The effect of the multimode structure on acoustic fluctuations will be discussed. It will be shown that, unlike amplitude and phase fluctuations, the total phase rate fluctuation can be simply related to the phase rate fluctuation in the individual modes.

A statistical representation for the internal wave field based on the work of Garrett and Munk (1972; 1975) will be used in this study. As such, the stochastic nature of the internal waves will

create a random inhomogeneous waveguide through which acoustic waves will propagate. The density stratification in the ocean permits the existence of internal waves and leads to their highly anisotropic behavior whereby horizontal scales are typically an order of magnitude larger than vertical scales. The induced refractive index fluctuations are assumed to be caused by the vertical motions of the internal waves. Linearized theories of internal wave motion reveal that the refractive index fluctuations are greatest near the top of the main thermocline and generally decrease with depth. Typical values for the fluctuations of internal waves in the main thermocline are a rms vertical displacement value of 7 meters and a resultant rms perturbation on the refractive index of 5×10^{-4} or approximately 1 meter/sec.

As is suggested by the small refractive index fluctuations, internal waves represent a weak scattering process to acoustic waves. The scattering does not occur at discrete points but rather it takes place throughout the weakly inhomogeneous medium. A perturbation technique known as Rytov's method [method of smooth perturbations (Tatarski, 1961)] will be used in the determination of the scattered waves. The modification of Rytov's method as it applies to an inhomogeneous waveguide and the range of validity of the weak scattering process will be discussed.

Before treating the actual variable-sound-speed waveguide in the ocean, we shall perform a preliminary analysis on two dimensional and three dimensional isospeed waveguides. This will permit us to interpret the nature of the acoustic-internal wave interaction while laying the

mathematical basis for the general waveguide with depth-varying sound speed. Superimposing typical refractive index fluctuations induced by internal waves will allow us to model the isospeed waveguide as an inhomogeneous waveguide. Straightforward analytical expressions will be obtained for the incident waves, scattered waves, and the acoustic fluctuations at any point in the waveguide.

The transition from the two dimensional isospeed waveguide to the three dimensional isospeed waveguide to the three dimensional variable-sound-speed waveguide involves increasing degrees of complexity. The analysis in the two dimensional waveguide results in plane waves with trigonometric functions for the eigenfunctions. In the three dimensional isospeed waveguide we assume cylindrical symmetry which leads to cylindrical waves and expansions in terms of Hankel functions. The eigenfunctions are again in trigonometric form. The three dimensional variable-sound-speed waveguide also involves Hankel functions, but exact eigenfunctions can only be determined for special sound-speed profiles. We shall use the WKB approximation to permit the treatment of more general sound-speed distributions, although we shall assume a bilinear squared-refractive-index profile for comparisons with experimental data.

The random nature of the internal wave field precludes the precise determination of the acoustic field at any time or point in space. Based upon the theoretical internal wave model of Garrett and Munk (1972, 1975), statistical estimates of the acoustic fluctuations will be determined. Root-mean-square multimode phase rate fluctuations will be calculated and compared with actual experimental values. The similarities

and differences will be analyzed and the various possible model modifications will be discussed.

The thesis is structured in the following manner. Section 2 contains the statistical internal wave model and discusses the induced refractive index fluctuations. Section 3 is composed of the acoustic model with a treatment of the perturbation technique and with a discussion of the inhomogeneous waveguide. The two dimensional and three dimensional isospeed waveguides are treated in sections 4 and 5. Section 6 contains the discussion of the multimode waveguide. The analysis of the variable-sound-speed waveguide and comparisons with experimental results are in section 7. Section 8 contains the conclusions of the thesis.

2. INTERNAL WAVE MODEL

The existence of internal waves is possible in any stratified medium where the density varies as a function of depth. Motions in the ocean and fluctuations in environmental parameters (such as temperature and salinity) with periods between the buoyancy and inertial periods are generally considered to be caused by internal waves. The waves cause significant horizontal as well as vertical variations in the ocean with horizontal scales on the order of tens of meters to tens of kilometers and vertical scales from meters to hundreds of meters (Garrett and Munk, 1972).

Due to the stratification of the ocean, the linearized equations of motion for internal waves can be separated into horizontal and vertical components. The equation for vertical motion reveals that internal waves can establish modes in the vertical direction with frequencies restricted to lie between the buoyancy (Brunt-Väisälä) frequency N and the inertial frequency ω_i (Phillips, 1969). The Brunt-Väisälä frequency is the natural frequency of oscillation for an element of water which has been transferred adiabatically from its equilibrium depth to another depth. It is a measure of the gravitational stability of the water column or the magnitude of the density stratification and may be imaginary in some instances indicating an instability in the water (Eckart, 1960, p. 60). The period of oscillation varies typically from a value of tens of minutes near the top of the main thermocline to several hours in the depths of the oceans. The inertial frequency sets the lower frequency bound for internal

waves with its period given by the expression 12 hrs/sin θ where θ is the latitude of interest (e.g. 24 hours at 30° latitude). The horizontal component of the equations of motion reveals that the internal wave modes propagate horizontally with wavelengths determined by dispersion relations.

Internal waves have been found to exist throughout the world's oceans. Some of the mechanisms attributed to the generation of internal waves are atmospheric disturbances, flow over an irregular bottom, tidal forces, shear flow, and surface wave interactions (Phillips, 1969). Measurements and observations of internal waves have been made by many investigators and various theories and ideas have been proposed to explain their effect.

In 1972 Garrett and Munk proposed a statistical model that contained the essential features of the internal wave field in the ocean (Garrett and Munk, 1972). It has subsequently been modified and refined (Garrett and Munk, 1972). Their model proposed a universal frequency-wavenumber spectrum for internal waves throughout the world's oceans. Frequency and wavenumber spectra that have been measured at various places, times, and depths exhibit differences from one another. The Garrett and Munk (GM) model proposes that nearly all the frequency and wavenumber spectra fall on the same universal curve when appropriately scaled by the local Brunt-Väisälä frequency.

Under the assumption of a stationary homogeneous, and horizontally isotropic internal wave field Garrett and Munk have postulated an analytical expression for the horizontal wavenumber - frequency energy

density $E(\alpha,\omega)$. In dimensional form the 1972 expression is

$$E_{72}(\alpha,\omega) = \begin{cases} \dfrac{4EB^3N_o^3\omega_i}{j\pi\omega(\omega^2-\omega_i^2)} & \text{for } \omega_i < \omega < N(z) \\ & \text{and } \alpha^{(1)}(\omega) < \alpha < j\alpha^{(1)}(\omega) \\ 0 & \text{otherwise.} \end{cases} \qquad 2.1$$

In equation 2.1 j is the number of modes containing energy at the inertial frequency and $\alpha^{(1)}(\omega)$ is the dispersion relation for the lowest order mode:

$$\alpha^{(1)}(\omega) = (\omega^2-\omega_i^2)/2BN_o \quad . \qquad 2.2$$

In fitting this expression to actual observations, Garrett and Munk have chosen the dimensionless constant E to be $2\pi \times 10^{-5}$ and have taken j to be 20. The quantities N_o and B are associated with their choice of an exponentially decaying Brunt-Väisälä profile to model most of the world's oceans

$$N(z) = N_o \exp(-z/B). \qquad 2.3$$

The projection of the energy density spectrum on the frequency axis exhibits a peak at the inertial frequency ω_i and a sharp cutoff at the local Brunt-Väisälä frequency N (See Figure 1). In the 1972 model Garrett and Munk assumed that all modes from 1 to 20 were equally excited and that the wavenumber dependence was constant up to a high wavenumber cutoff.

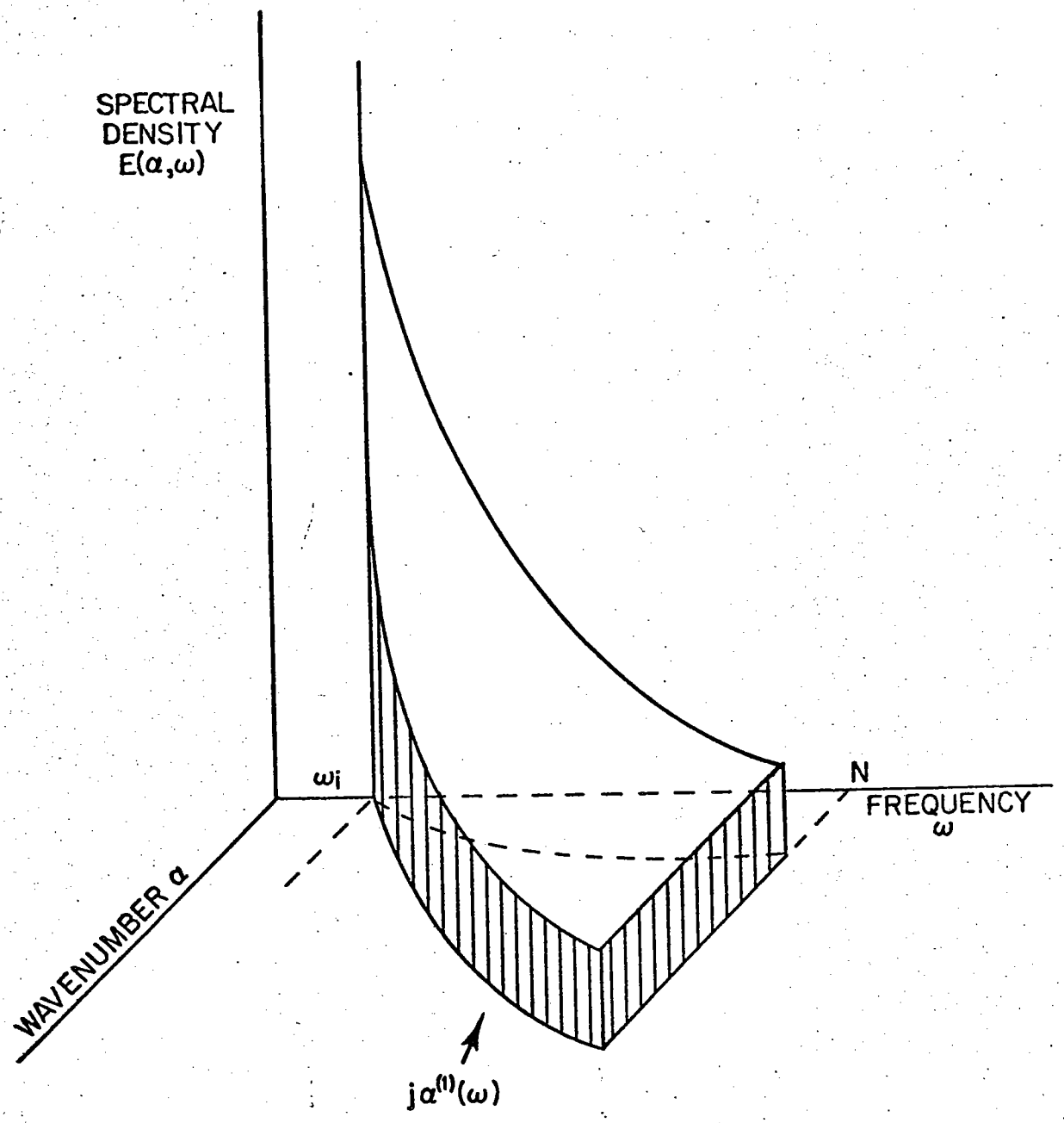

Figure 1: 1972 Garrett and Munk model for the spatial and temporal distribution of the energy spectral density. Sharp cutoffs occur at $\omega = N$ and $\alpha = j\alpha^{(1)}$.

Recognizing that some refinements were needed in their 1972 model to explain subsequent data, Garrett and Munk proposed their 1975 model:

$$E_{75}(\alpha,\omega) = \begin{cases} \dfrac{6EB^3N_o^3\omega_i}{j_*\pi\omega(\omega^2-\omega_i^2)}\left(\dfrac{\alpha_*}{\alpha+\alpha_*}\right)^{2.5} & \text{for } \omega_i<\omega<N \\ 0 & \text{otherwise.} \end{cases} \qquad 2.4$$

In equation 2.4 j_* is a mode scale number (chosen to be 6) with its associated wavenumber

$$\alpha_*(\omega) = j_*(\omega^2-\omega_i^2)^{1/2}/2BN_o \quad . \qquad 2.5$$

Most of the energy in the spectrum is located in modes less than j_* and wavenumbers less than α_* . For large wavenumbers $E_{75}(\alpha,\omega)$ is proportional to $\alpha^{-2.5}$ with no high wavenumber cutoff. The frequency dependence is identical with that of $E_{72}(\alpha,\omega)$. The constant E is again chosen to be $2\pi \times 10^{-5}$. The energy density representation in horizontal wavenumber-frequency space of equation 2.4 can easily be transformed to a vertical wavenumber-frequency representation by

$$E(\beta,\omega) = [E(\alpha,\omega)]\, d\alpha/d\beta \quad . \qquad 2.6$$

It will subsequently be shown that the contribution of vertically propagating internal waves to the acoustic scattering is secondary in comparison to that of the horizontally propagating internal waves.

As such, the precise nature of the vertical wavenumber dependence is not critical to the acoustic-internal wave interaction. We shall later find it convenient to introduce a vertical correlation function of the form exp $(-z^2/\ell_z^2)$ for the induced refractive index fluctuations. The form chosen is not meant to model exactly the vertical flucutations, but rather it gives a reasonable representation while being analytically tractable.

Measurements of low coherence between vertically spaced sensors suggest that many modes of varying amplitude and phase are being excited by the internal waves in each frequency band. Rapid and random oscillations of the index of refraction are due to the small vertical wavelengths of the internal waves and the small vertical correlation scales. Garrett and Munk circumvent the problem of multimode summation by substituting the root mean square (rms) behavior of the vertical wave function and by using a statistical description of the internal wave field. In effect they have introduced a smoothing or averaging operation over small intervals of depth while leaving intact the slowly varying depth dependencies. In the horizontal direction the internal wave field retains its properties of homogeneity and isotropy. This replacement of the multi-mode structure by the random variable representation permits spectral relationships to be established between various variables without retaining the details of the complicated vertical structure.

In terms of the mean square vertical wave function $\overline{Z^2(z)}$, the mean-square vertical displacement $\overline{\xi^2}$ can be written as (Garrett and

Munk, 1972, eq. 4.4; Porter et al, 1974, eq. 6)

$$\overline{\xi^2} = \iint N_0^{-2}\, \overline{Z^2(z)}\, E(\alpha,\omega)\, d\alpha\, d\omega \qquad 2.7$$

where $$\overline{Z^2(z)} = N_0 \left(\omega^2 - \omega_i^2\right)/N\omega^2 .$$

Recognizing that

$$\overline{\xi^2} = \iint F_\xi(\alpha,\omega)\, d\alpha\, d\omega ,$$

we can relate the vertical displacement spectral density $F_\xi(\alpha,\omega)$ to the energy density spectrum $E(\alpha,\omega)$:

$$F_\xi(\alpha,\omega) = N_0^{-2}\, \overline{Z^2(z)}\, E(\alpha,\omega) . \qquad 2.8$$

In terms of the 1972 and 1975 GM models we have

$$F_{\xi 72}(\alpha,\omega) = \frac{4EB^3N_0^2\omega_i}{j\pi N\omega^3} \qquad 2.9$$

and $$F_{\xi 75}(\alpha,\omega) = \frac{6EB^3N_0^2\omega_i}{j_*\pi N\omega^3}\left(\frac{\alpha_*}{\alpha+\alpha_*}\right)^{2.5}$$

where the limits on frequency and wavenumber are identical to those for the energy density spectrum. If we substitute $E_{72}(\alpha,\omega)$ or $E_{75}(\alpha,\omega)$ into equation 2.7 and perform the double integration, we obtain a root-mean-square vertical displacement $(\overline{\xi^2})^{\frac{1}{2}}$ of 7.3 meters near the top

of the main thermocline (i.e. where $N(Z) = N_o$). It is important to note that rms vertical displacement is proportional to $N^{-\frac{1}{2}}$ so that the internal wave field will cause larger vertical displacements in deeper water.

Since the phase velocity of an acoustic wave is much faster than that of the fastest internal wave (Garrett and Munk, 1972), a propagating acoustic wave will experience a "frozen" internal wave field. Internal wave fields sampled by rapidly towed instruments are also considered to be "frozen." We could therefore expect both processes to measure similar internal wavenumber spectra. The measurement of vertical displacement by a horizontal tow in the x direction would give the wavenumber spectra

$$F_j(\alpha_x) = N_o^{-2} \int_{\omega_i}^{N} d\omega\, \overline{Z^2(z)} \int_{-\infty}^{\infty} d\alpha_y \left[E(\alpha_x, \alpha_y, \omega) + E(-\alpha_x, \alpha_y, \omega) \right] . \qquad 2.10$$

Assuming horizontal isotropy,

$$E(\alpha, \omega) = 2\pi\alpha\, E(\alpha_x, \alpha_y, \omega) ,$$

and substituting $\alpha_y^2 = \alpha^2 - \alpha_x^2$,

we can write equation 2.10 as

$$F_j(\alpha_x) = 2N_o^{-2}\pi^{-1} \int_{\omega_i}^{N} d\omega\, \overline{Z^2(z)} \int_{\alpha_x}^{\infty} d\alpha \left(\alpha^2 - \alpha_x^2\right)^{-\frac{1}{2}} E(\alpha, \omega) \qquad 2.11$$

(see Garrett and Munk, 1972, eqs. 4.8 and 4.9).

If we now substitute $E_{72}(\alpha, \omega)$ into equation 2.11 and perform the indicated

integrations, the vertical displacement spectrum becomes proportional to α_x^{-2} over much of horizontal wavenumber space (Garrett and Munk, 1972, eq. 6.22). Using $E_{75}(\alpha,\omega)$ the spectrum is proportional to $\alpha_x^{-1.5}$ for small wave numbers and $\alpha_x^{-2.5}$ for large wavenumbers. Although the precise details of the wavenumber spectra vary with the two models, the general result is that spectral density levels decrease rapidly with increasing wavenumber. We shall later use this result in explaining why small internal wavenumbers (large internal wavelengths) form the major contribution to the acoustic-internal wave interaction process.

The presence of internal waves will have a significant effect on the sound speed distribution. The fluctuation in the index of refraction due to the passage of an internal wave which vertically displaces an element of water at depth z by a distance ξ is (Munk and Rosenbluth, 1973, personal communication; Porter et al., 1974)

$$\frac{\Delta C}{C} = \varepsilon \xi T_{pz} + \beta \xi S_z + \gamma \frac{\Delta \rho}{\rho} (\rho g \xi) \qquad 2.12$$

where c is the sound velocity

T_{pz} is the potential temperature gradient

S_z is the salinity gradient

ρ is the density

g is the acceleration of gravity

$\varepsilon, \beta, \gamma$ are constants.

The potential temperature gradient T_{pz} is equal to the "in situ" minus the adiabatic temperature gradient. The third term in the above equation

is the internal-wave-induced pressure fluctuations at a fixed depth z and is reduced by the factor $\Delta\rho/\rho$ ($\approx 10^{-3}$) over the pressure fluctuations experienced by a fixed water particle. This term is small in comparison to the first two terms and will be neglected in subsequent calculations.

The sound velocity fluctuations can also be related to the Brunt-Väisälä frequency N:

$$N^2(z) = g\rho_p^{-1}\rho_{pz} = g(-hT_{pz} + wS_z) = -ghT_{pz}(1-Tu) \qquad 2.13$$

where ρ_p is the potential density

ρ_{pz} is the potential density gradient

h,w are volume expension coefficients

and Tu is the Turner number = wS_z/hT_{pz} .

The Turner number describes the relative contributions of salinity and potential temperature to the potential density stratification. The fluctuation in the index of refraction can then be expressed as

$$\sigma = \frac{\Delta C}{C} = \varepsilon\xi T_{pz}(1+dTu) = -N^2\xi\mu/g \qquad 2.14$$

where d is a constant much less than one and

$$\mu = \frac{\varepsilon(1+dTu)}{h(1-Tu)} \qquad 2.15$$

.

It is important to note that μ is not a constant since the value of the Turner number can vary throughout the water column indicating a

varying T-S relationship.

We mentioned earlier that the root-mean-square displacement of internal waves is proportional to $N^{-\frac{1}{2}}$. For a constant Turner number the rms fluctuation in index of refraction then varies as $N^{3/2}$. Therefore the acoustic influence of internal waves is concentrated where N is maximum (usually near the top of the main thermocline), although the 3/2 dependence implies a significant influence throughout depth. Using the rms vertical displacement of 7.3 meters at the top of the main thermocline, the resultant rms perturbation on refractive index is 5×10^{-4} or approximately 1 meter/sec sound speed fluctuation.

Spectral relationships can be established between refractive index fluctuations and vertical displacement fluctuations. Using equations 2.14, 2.7 and 2.8, we can write

$$\overline{\sigma^2} = \frac{N^4 \mu^2}{g^2} \overline{\zeta^2} = \frac{N^4 \mu^2}{g^2} \iint N_0^{-2} \overline{Z^2(z)} E(\alpha,\omega) = \iint F_\sigma(\alpha,\omega)\, d\alpha\, d\omega \qquad 2.16$$

where the refractive index spectral density $F_\sigma(\alpha,\omega)$ is

$$F_\sigma(\alpha,\omega) = N^4 \mu^2 g^{-2} N_0^{-2} \overline{Z^2(z)} E(\alpha,\omega). \qquad 2.17$$

In terms of the 1972 and 1975 GM models we have

$$F_{\sigma 72}(\alpha,\omega) = \frac{4 E B^3 N_0^2 \omega_i \mu^2 N^3}{j \pi g^2 \omega^3} \qquad 2.18$$

and $$F_{675}(\alpha,\omega) = \frac{6EB^3N_o^2\omega_i\mu^2N^3}{j_*\pi g^2\omega^3}\left(\frac{\alpha_*}{\alpha+\alpha_*}\right)^{2.5}$$

where again the limits on frequency and wavenumber are identical with the respective energy density spectrum.

All the previous discussions have assumed that the internal-wave induced refractive index fluctuations have been caused solely by the vertical displacements of the internal waves. In actual fact the sound speed will also be perturbed by the horizontal currents associated with the internal waves. These horizontal currents are on the order of a few cm/sec (Mooers, 1975) with a corresponding refractive index fluctuation of approximately 1×10^{-6}. Because of the $N^{3/2}$ dependence, the refractive index fluctuations due to vertical displacements approach 1×10^{-6} for very deep water (5000 meters). Over the rest of the water column the refractive index fluctuations associated with vertical displacements are clearly dominant over those associated with horizontal currents, and we shall ignore the horizontal currents in this study.

3. ACOUSTIC MODEL

As was mentioned in the previous section, rms fluctuations in sound speed due to the passage of an internal wave are typically at most 1 meter/sec or less than 1 part in 10^3 change in the static sound-speed profile. The continuous spatial distribution of internal waves creates a medium with a weakly inhomogeneous refractive index. The relatively small effect on the sound speed then suggests the use of a perturbation approach in determining the effect of internal wave activity on an acoustic wave field.

The stochastic nature of the internal wave field precludes any exact determination of the acoustic field at any point in time or space. The approximate solution offered by a perturbation expansion will then only provide estimates of the field's statistical quantities.

Historically, two types of perturbation techniques have been used in studies involving wave propagation through an inhomogeneous medium. These are the Born expansion or the method of small perturbations and the Rytov method or the method of smooth perturbations. As in any perturbation technique, the solution to the full problem is represented by an infinite summation of terms in the perturbation expansion. The usual perturbation solution, however, is to consider only the first two terms in the expansion. Although the inclusion of only the first two terms in the perturbation solution usually leads to a straightforward determination of the wave field, the restriction to a limited number of terms leads to a solution which possess finite regions of validity and which breaks down in regions of nonuniformity.

The Born perturbation technique involves the expansion of the wave field directly into an unperturbed zero-order term and a first-order term to account for the scattering caused by the inhomogeneity. The zero-order term determines the field in the absence of any inhomogeneity, while the first-order term accounts for the interaction between the zero-order field and the inhomogeneity. The expansion is a single scattering approximation which is known to be valid only over distances where the amplitude and phase fluctuations remain small.

The Rytov perturbation technique was first used in the study of diffraction of light by ultrasonic waves (Chernov, 1960; Tatarski, 1961). It involves a transformation of the wave equation to employ logarithms of the field variables with the perturbation expansions then made on the logarithms. The relationship between the two perturbation expansions is very close, evidenced by the fact that the Rytov series can be obtained by expressing the Born series as an exponential expansion. According to Nayfeh (1973) the Rytov series is a renormalized Born expansion which should lead to a greater region of validity.

The contention that Rytov's perturbation procedure can be applied to longer range studies than that permitted by the Born expansion has been a center of controversy for many years (Brown, 1967; DeWolf, 1967; Heidbreder, 1967; Taylor, 1967; Strohbehn, 1968; Keller, 1969; Sancer and Varvatsis, 1970; Neubert, 1970). Most wave propagation studies using the Rytov technique limit the expansion to the first two terms for computational efficiency. Early advocates of Rytov's method contended that the method placed no restriction on the total phase and

amplitude change of a wave whenever the phase and amplitude change per wavelength remained small (Chernov, 1960; Tatarski, 1961). However, examinations of the second term in the perturbation expansion revealed a much smaller range of validity for the first two terms in the expansion than had been originally proposed (Pisareva, 1960). Much effort has been expended in comparing the validity of the first order solutions for the Born and Rytov methods. Although no universally accepted conclusion has been reached, it is generally agreed that the first order Rytov term fails to extend the region of validity for log-amplitude measurements but does allow a more widespread region for phase calculations. It is important to realize, however, that the solution offered by the first-order Rytov series represents the field resulting from a single or weak scattering environment. A more precise determination of the acoustic variations would have to involve multiple scattering with its inherent complications. Nevertheless, a comparison with experimental data will indicate that the weak scattering solution can roughly predict the effect of internal waves on long-range acoustic propagation.

The Rytov derivation shown below is adapted from Tatarski (1971). It lays the basis for modifications required for propagation in waveguides and in stratified medium.

The acoustic field due to a point source in an inhomogeneous medium can be described in terms of the velocity potential Φ with the standard wave equation

$$\nabla^2 \Phi - \frac{1}{c^2} \Phi_{tt} = -\delta\left(\vec{r} - \vec{r}_s\right) \quad . \qquad 3.1$$

It is assumed that during the passage of the acoustic wave through a region of internal wave activity the internal wave field is frozen in space and time, although the refractive index fluctuations will vary along the transmission path. The source term is denoted by

$$\delta\left(\vec{r} - \vec{r}_s\right)$$

where δ is the Dirac delta function, c is the sound speed, $\vec{r}_s$ is the source coordinate, and $\vec{r}$ is the observation point. Assuming a continuous wave source of frequency ω_s so that

$$\Phi = \psi e^{-i\omega_s t} \quad ,$$

equation 3.1 becomes

$$\nabla^2 \psi + \frac{\omega_s^2}{c^2} \psi = -\delta\left(\vec{r} - \vec{r}_s\right) . \qquad 3.2$$

The index of refraction n is equal to c_o/c where c_o is a refence sound speed. A perturbation expansion can be made on n

$$n = n_0 + \sigma + \ldots$$

where n_o is deterministic and due to the static sound velocity distribution in space and σ is stochastic and induced by the internal wave field which is a random function of space and time. We note that $\sigma << n_o$. To first-order equation 3.2 becomes

$$\nabla^2\psi + k_o^2\left(n_o^2 + 2n_o\sigma\right)\psi = -\delta\left(\vec{r}-\vec{r}_s\right) \qquad 3.3$$

where $k_o = \omega_s/c_o$ is the acoustic wavenumber in a medium with reference sound speed c_o. Taking $\psi = \exp(p)$, equation 3.3 becomes

$$\nabla^2 p + (\nabla p)^2 + k_o^2\left(n_o^2 + 2n_o\sigma\right) = -\delta\left(\vec{r}-\vec{r}_s\right). \qquad 3.4$$

Expanding p, so that $p = p_o + p_1$ (where $p_1 << p_o$), and equating terms with equal orders of magnitude gives

$$\nabla^2 p_o + (\nabla p_o)^2 + k_o^2 n_o^2 = -\delta\left(\vec{r}-\vec{r}_s\right) \qquad 3.5$$

and

$$\nabla^2 p_1 + 2\nabla p_o \nabla p_1 = -2k_o^2 n_o \sigma \; . \qquad 3.6$$

Setting $p_o = \ln\psi_o$, equation 3.5 can be directly reduced to

$$\nabla^2\psi_o + k_o^2 n_o^2 \psi_o = -\delta\left(\vec{r}-\vec{r}_s\right) \qquad 3.7$$

which is the wave equation for a medium without fluctuations. The first order equation 3.6 can be simplified by substituting

$$p_1 = W_1/\psi_o \qquad 3.8$$

which leads to

$$\nabla^2 W_1 + k_o^2 n_o^2 W_1 = -2k_o^2 n_o \sigma \psi_o \; . \qquad 3.9$$

This latter equation can then be solved by Green's function techniques

$$P_1(r) = \int_{r_0} dr_0\, G(r|r_0) 2k_0^2 n_0(r_0) \sigma(r_0) \psi_0(r_0)/\psi_0(r) \qquad 3.10$$

where $G(r|r_o)$ is the Green's function.

The first order perturbation equation (equation 3.9) reveals the nature of the acoustic-internal wave interaction. The equation is recognized as an inhomogeneous Helmholtz equation where the driving force or source term is composed of the zero-order field, the static sound velocity profile, and the refractive index fluctuations induced by the internal wave. The only solution is the inhomogeneous one since the homogeneous solution is lumped into the zero-order field which is given by equation 3.7.

Most previous studies involving wave propagation through an inhomogeneous medium have assumed the inhomogeneous medium to be infinite in extent (Tatarski, 1971; Liu, 1968; Schmeltzer, 1966). The inhomogeneities cause a scattering of the incident wave which results in the presence of amplitude and phase fluctuations at any point in space. The assumption of an infinite inhomogeneous medium is probably valid for short range studies but must be seriously questioned for long-range acoustic propagation in the ocean.

It has been known for many years that sound energy can propagate for thousands of kilometers in the ocean with little attenuation. This

property is due to the depth-varying dependence of the sound speed. Under the dominant influences of temperature and pressure, sound speed profiles typically exhibit a minimum at some mid-water depth with increasing sound speeds toward the surface and bottom. Horizontal variations of sound speed are usually secondary compared to the vertical variations so that acoustic propagation studies usually assume the ocean to be horizontally stratified. The structure of the sound-speed distribution causes acoustic radiation to be strongly refracted within the water column so that a waveguide is established. Acoustic energy that reflects off the ocean surface or bottom becomes attenuated and scattered in many directions. As a result, most of the acoustic energy reaching a receiver which is farther than a few hundred kilometers from the source will have been totally refracted through the waveguide.

The presence of any fluctuations in the water column (such as those due to internal waves) will likely affect long range acoustic propagation. As was indicated previously, the principal effect internal waves have on acoustic propagation is to cause a displacement of the isotherms with their motion resulting in sound-speed variations in space and time. These perturbations induced by the internal wave field are superimposed on the static sound speed profile in the waveguide.

It has long been known, both theoretically and experimentally, that the presence of any inhomogeneities in a waveguide can cause large variations in the wave field supported by the duct. This phenomenon occurs since both the incident wave and the scattered waves resulting from the inhomogeneous region can propagate through the waveguide for very long distances (Isakovich, 1957; Nayfeh, 1974).

We shall later show that the effect of an internal wave in the waveguide is equivalent to that of a diffraction grating. Scattered waves will only result from an acoustic wave incident to the internal wave at a certain angle. With a continuous wavenumber spectrum of internal waves, a given acoustic wave will interact with only those elements of the internal wave field which satisfy the scattering condition of the diffraction grating.

In the terminology of mode theory the sound-speed variations caused by the internal waves can be considered as secondary sources for normal modes of varying wave numbers. A transfer of energy occurs from the incident normal wave of a specified mode number to the scattered waves of different mode numbers. In order to travel for long distances with little attenuation the scattered waves are restricted by the waveguide to propagate in certain specific directions.

The resultant acoustic field in the waveguide is then composed of the sum of the incident and scattered waves. The field is a complicated mode interference summation with many incident normal modes possible, each of which can generate a set of scattered waves. For simplicity the restriction to forward scattering will be made as is suggested by the relatively weak sound-speed inhomogeneities induced by the internal waves and their larger scale sizes as compared to acoustic wavelengths. We should realize, though, that at very long ranges backscattered contributions will become significant so that the forward scattering solution no longer remains valid.

In order to determine the acoustic field in an inhomogeneous waveguide by means of Rytov's method, it is necessary to modify the solution

for the first order term as given by equations 3.6 - 3.10. At every node of the incident normal mode we note that $\psi_o = 0$. It is then evident from equation 3.8 that the first order perturbation term (and all higher order terms) will become infinite at these points. This is a physically untenable result and is due to a singularity of the standard Rytov method at that point. This singularity in the Rytov method can be treated by a straight-forward procedure. Any normal mode in a waveguide can be considered as a sum of two traveling waves which are propagating vertically as well as horizontally through the waveguide. A given mode is therefore treated as two incident waves each of which interacts with the internal wave field to produce scattered waves (Lapin, 1958). The standard Rytov method is applied to each of the incident waves, the first order scattered field is determined, and superposition is used to determine the total scattered field due to the mode.

The sound field in a waveguide without inhomogeneities can be expressed as a sum of normal modes

$$\psi = \sum_m \psi_{om} \qquad 3.11$$

Each zero order mode ψ_{om} can be broken into an upward and downward traveling wave in the waveguide, ψ_{om}' and ψ_{om}'' respectively. Each of these waves and the scattered fields which they produce can be examined by equations similar to 3.6 - 3.10. With the subscript one (1) understood, the first order term resulting from the upward traveling incident wave is given by

$$P_m' = W_m' / \psi_{om}' \qquad 3.12$$

where W_m' satisfies

$$\nabla^2 W_m' + K_0^2 n_0^2 W_m' = -2K_0^2 n_0 \sigma \psi_{om}' \qquad 3.13$$

Similar expressions exist for the scattered waves from the downward traveling incident wave. The total acoustic field in an inhomogeneous waveguide resulting from a set of normal modes m can then be expressed as

$$\psi = \sum_m \left(\psi_{om}' e^{P_m'} + \psi_{om}'' e^{P_m''} \right) \qquad 3.14$$

We have attempted in this section to construct the acoustic model which will be used in this study. The effect of the internal wave field will be treated as a weak scattering process with the acoustic fluctuations being determined by the Rytov perturbation technique. The induced refractive index fluctuations cause an inhomogeneous waveguide to be created where both incident and scattered waves can propagate to long ranges with little attentuation. In the sections that follow we shall investigate the nature of acoustic-internal wave interaction in various acoustic waveguides. We shall first examine the two dimensional

isospeed waveguide, since the interaction process can be clearly understood and since analytical expressions can be readily obtained.

4. TWO DIMENSIONAL ISOSPEED WAVEGUIDE

The nature of the acoustic-internal wave interaction in long range propagation studies can be revealed by treating the case of a static homogeneous waveguide with a free surface and hard bottom. Within the waveguide the sound velocity is assumed to be constant over depth and range. The isospeed waveguide permits fairly simple analytical expressions in describing the acoustic field while retaining the peculiarities of waveguide propagation.

As was mentioned earlier, the passage of an internal wave causes a vertical displacement of water with a resultant variation on the sound velocity field. Since the homogeneous waveguide contains constant sound speed water, refractive index fluctuations must be introduced artificially. These fluctuations will simulate both the dynamics and the statistics of internal-wave-induced refractive index fluctuations in a real ocean. The perturbations on the sound speed create an inhomogeneous waveguide which is then treated with the Rytov perturbation technique. The analysis of the acoustic-internal wave interaction in the isospeed waveguide will be undertaken with various degrees of complexity. These will range from the simplified problem of a single incident acoustic mode in a two-dimensional channel interacting with a single frequency internal wave to the general problem of multimode summation in a three-dimensional waveguide with a continuous spectrum of internal waves in wavenumber-frequency space.

The case of the two-dimensional isospeed waveguide as shown below will first be treated.

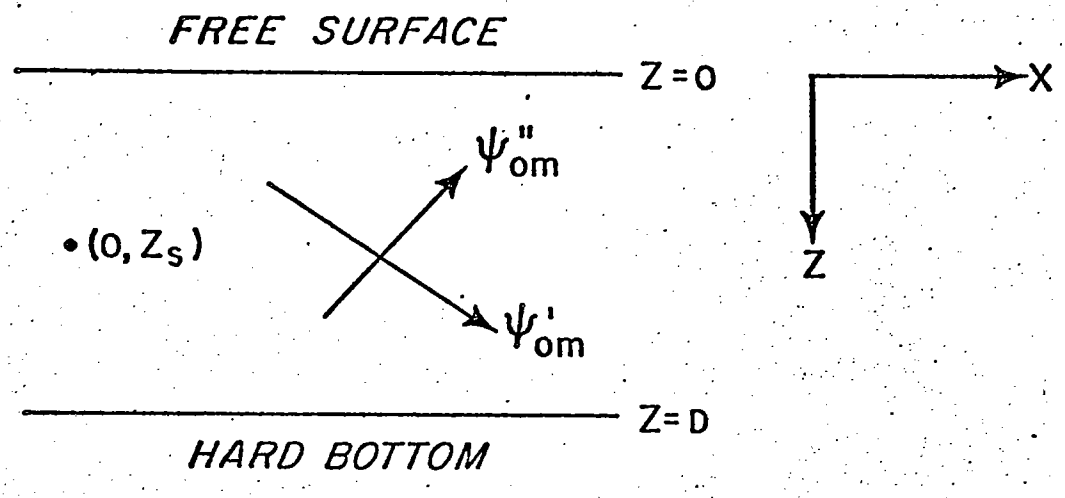

Figure 2: Two dimensional isospeed waveguide. The velocity potential in mode m is decomposed into two traveling waves ψ_{om}' and ψ_{om}''.

Neither the properties of the artificial internal wave field nor of the waveguide are assumed to be a function of the coordinate y, so that all motion occurs parallel to the x-z plane. A continuous wave (CW) source of frequency ω_s is assumed to lie within the waveguide at a location $(0, z_s)$. The induced refractive index fluctuations are assumed to be horizontally homogeneous.

In the absence of internal waves the acoustic field at any point in the waveguide can be described by a sum of normal modes.

$$\psi(x,z) = \sum_m \psi_m = \frac{i}{2} \sum_m \frac{1}{\alpha_m} h_m(z) h_m(z_s) e^{i\alpha_m x} \qquad 4.1$$

where the ortho-normal eigenfunctions are

$$h_m(z) = (2/D)^{1/2} \sin \gamma_m z$$

and the horizontal wavenumber of the m^{th} mode is α_m. The orthonormality condition for the eigenfunction is

$$\int_0^D h_m(z) h_n(z)\, dz = \begin{cases} 1, & n = m \\ 0, & n \neq m \end{cases} .$$

For a free surface and hard bottom the eigenvalues are

$$\gamma_m = \left(m - \frac{1}{2}\right)\frac{\pi}{D}$$

where the mode summation extends from m = 1 to m = ∞ . Substituting the eigenfunction value into equation 4.1 gives the normal mode summation in the isospeed channel

$$\psi(x,z) = \frac{i}{D} \sum_{m=1}^{\infty} \frac{1}{\alpha_m} \sin \gamma_m z \sin \gamma_m z_s \; e^{i\alpha_m x} \quad . \qquad 4.2$$

Instead of the multimode acoustic field given by equation 4.2, let us first consider a single incident mode of order m encountering a region of internal wave activity. In order to apply the Rytov perturbation procedure the incident mode m must be decomposed into two traveling waves (ψ_{om}' and ψ_{om}'' in Fig. 2) which are propagating in the positive and negative z directions. The restruction to a single incident mode generally leads to a non-realistic solution for the acoustic-internal wave interaction since all effects of multi-mode summation are lost. Nevertheless, the solution will be of value since in many natural waveguides one mode is more strongly excited than others. In addition, the decomposition of the mode into two traveling waves leads to the geometrical optics problem of two ray interference in the waveguide whose solution has previously been determined (Porter et al., 1974).

From equation 3.14 we have the two first order equations

$$\nabla^2 W_m' + K_0^2 n_0^2 W_m' = -2K_0^2 n_0 \sigma \psi_{0m}' \qquad 4.3$$

and $$\nabla^2 W_m'' + K_0^2 n_0^2 W_m'' = -2K_0^2 n_0 \sigma \psi_{0m}'' \qquad 4.4$$

In the isospeed channel the depth-dependent index of refraction n_o is a constant equal to one but we shall retain it in the equations for generality. The incident mode ψ_{om} has been decomposed into two plane waves ψ_{om}' and ψ_{om}'' where

$$\psi_{om}' = \left[\sin \gamma_m z_s / 2\alpha_m D\right] \exp\left[i(\alpha_m x + \gamma_m z)\right] \qquad 4.5$$

and $$\psi_{om}'' = -\left[\sin \gamma_m z_s / 2\alpha_m D\right] \exp\left[i(\alpha_m x - \gamma_m z)\right] \qquad 4.6$$

The internal-wave-induced refractive index fluctuations, denoted by σ, are a function of space as well as of time.

In order to solve equations 4.3 and 4.4 we must first determine the boundary conditions which W_m' and W_m'' satisfy in the waveguide. The waveguide in Fig. 2 with a free surface and hard bottom requires that

$\psi = 0$ at $z = 0$ (pressure release surface)

and $\partial\psi/\partial z = 0$ at $z = D$ (zero vertical velocity) .

Since every mode in the waveguide can exist independently from each other, we then have

$$\psi_m = 0 \quad \text{at} \quad z = 0$$

and $$\partial\psi_m/\partial z = 0 \quad \text{at} \quad z = D \qquad 4.7$$

If we now consider equations 3.12, 3.14, 4.5 and 4.6, we can then determine the boundary conditions on W_m' and W_m''. At $z = 0$ we have

$$\psi_{om}' \exp\left(W_m'/\psi_{om}'\right) + \psi_{om}'' \exp\left(W_m''/\psi_{om}''\right) = 0 \quad .$$

But $\psi_{om}' = -\psi_{om}''$ at $z = 0$ (equations 4.5 and 4.6), so that

$$W_m' = -W_m'' \quad \text{at } z = 0 \quad . \qquad 4.8$$

At $z = 0$ we must also have continuity of particle velocity between the upward and downward traveling waves, so that

$$\frac{\partial\psi_m'}{\partial z} = \frac{\partial\psi_m''}{\partial z} \quad \text{at } z = 0 \quad .$$

Noting that $\dfrac{\partial\psi_{om}'}{\partial z} = \dfrac{\partial\psi_{om}''}{\partial z}$ at $z = 0$, we have

$$\frac{\partial W_m'}{\partial z} = \frac{\partial W_m''}{\partial z} \quad \text{at } z = 0. \qquad 4.9$$

At $z = D$ we can use the eigenvalue relation

$$\gamma_m = \left(m - \tfrac{1}{2}\right)\frac{\pi}{D}$$

to show that

$$\psi_{om}' = \psi_{om}''$$

and $$\partial\psi_{om}'/\partial z = -\partial\psi_{om}''/\partial z \quad \text{at } z = D \quad .$$

We can then use these two equations to prove that

$$W_m' = W_m'' \qquad \text{at } z = D \qquad 4.10$$

and $$\partial W_m'/\partial z = -\partial W_m''/\partial z \qquad \text{at } z = D \ . \qquad 4.11$$

To solve for W_m' and W_m'' it is convenient to introduce the functions

$$\hat{W} = W_m' + W_m'' \quad \text{and} \quad \tilde{W} = W_m' - W_m'' \qquad 4.12$$

which then satisfy the boundary conditions (combining equations 4.8 - 4.11)

$$\hat{W} = \partial\tilde{W}/\partial z = 0 \qquad \text{at } z = 0$$

and $$\partial\hat{W}/\partial z = \tilde{W} = 0 \qquad \text{at } z = D \ .$$

The two first order equations are now

$$\nabla^2\hat{W} + K_0^2 n_0^2 \hat{W} = -2K_0^2 n_0 \sigma\left(\psi_{0m}' + \psi_{0m}''\right) \qquad 4.13$$

and $$\nabla^2\tilde{W} + K_0^2 n_0^2 \tilde{W} = -2K_0^2 n_0 \sigma\left(\psi_{0m}' - \psi_{0m}''\right) \qquad 4.14$$

The solution to equations 4.13 and 4.14 can be found by two-dimensional Green's functions, where the Green's function for $\hat{W}$ will be different from that for $\tilde{W}$ due to the different boundary conditions. We then can write

$$\hat{W}(x,z,t) = -2K_0^2 n_0 \iint_{x_0 z_0} dx_0\, dz_0\, \sigma(x_0,z_0,t)\left[\psi_{0m}'(x_0,z_0) + \psi_{0m}''(x_0,z_0)\right] G_{\hat{W}}(x,z|x_0,z_0) \qquad 4.15$$

and $$\tilde{W}(x,z,t) = -2K_0^2 n_0 \iint_{x_0 z_0} dx_0\, dz_0\, \sigma(x_0,z_0,t)\left[\psi_{0m}'(x_0,z_0) - \psi_{0m}''(x_0,z_0)\right] G_{\tilde{W}}(x,z|x_0,z_0) \qquad 4.16$$

where the Green's functions

$$G_{\hat{w}}(x,z|x_0,z_0) \quad \text{and} \quad G_{\tilde{w}}(x,z|x_0,z_0)$$

satisfy $$\nabla^2 G_{\hat{w},\tilde{w}} + \varepsilon^2 G_{\hat{w},\tilde{w}} = -\delta(x-x_0)\delta(z-z_0). \qquad 4.17$$

In equation 4.17 δ is the Dirac delta function. Assuming only forward scattered waves, the appropriate Green's functions are now

$$G_{\hat{w}}(x,z|x_0,z_0) = \frac{i}{D}\sum_{n=1}^{\infty}\frac{1}{\alpha_n}\sin\gamma_n z\,\sin\gamma_n z_0\, e^{i\alpha_n(x-x_0)} \qquad 4.18$$

and $$G_{\tilde{w}}(x,z|x_0,z_0) = \frac{i}{D}\sum_{n=1}^{\infty}\frac{1}{\alpha_n}\cos\gamma_n z\,\cos\gamma_n z_0\, e^{i\alpha_n(x-x_0)} \qquad 4.19$$

Substituting equations 4.18 and 4.19 into 4.15 and 4.16, we can then determine the expressions for W_m' and W_m'':

$$W_m'(x,z,t) = \frac{iK_0^2 n_0 \sin\gamma_m z_s}{2\alpha_m D^2}\sum_{n=1}^{\infty}\frac{1}{\alpha_n}\int_0^D dz_0\left[e^{i\gamma_n z}\cos(\gamma_m-\gamma_n)z_0 + e^{-i\gamma_n z}\cos(\gamma_m+\gamma_n)z_0\right]$$
$$\cdot\int_0^x dx_0\,\sigma(x_0,z_0,t)\exp i\left[\alpha_m x_0 + \alpha_n(x-x_0)\right]$$

$$W_m''(x,z,t) = -\frac{iK_0^2 n_0 \sin\gamma_m z_s}{2\alpha_m D^2}\sum_{n=1}^{\infty}\frac{1}{\alpha_n}\int_0^D dz_0\left[e^{i\gamma_n z}\cos(\gamma_m+\gamma_n)z_0 + e^{-i\gamma_n z}\cos(\gamma_m-\gamma_n)z_0\right]$$
$$\cdot\int_0^x dx_0\,\sigma(x_0,z_0,t)\exp i\left[\alpha_m x_0 + \alpha_n(x-x_0)\right].$$

Recalling that

$$P_m' = W_m'/\psi_{om}' \quad , \quad P_m'' = W_m''/\psi_{om}'' \quad , \qquad \text{and}$$

$$\psi_m = \psi_{om}' \exp(P_m') + \psi_{om}'' \exp(P_m'')$$

we can now obtain an expression for the field in the waveguide due to the incident mode m:

$$\psi_m(x,z,t) = i \frac{\sin \gamma_m z_s \, e^{i\alpha_m x}}{\alpha_m D} \sin\left\{\gamma_m z - \frac{ik_0^2 n_0}{D} \sum_{n=1}^{\infty} \frac{1}{\alpha_n} \iint_{00}^{xD} dx_0 dz_0 \, \sigma \, h_{mn1}(z_0) e^{i(\alpha_n - \alpha_m)(x-x_0)}\right\}$$

$$\cdot \exp i\left\{\frac{k_0^2 n_0}{D} \sum_{n=1}^{\infty} \frac{1}{\alpha_n} \iint_{00}^{xD} dx_0 dz_0 \, \sigma \, h_{mn2}(z_0) e^{i(\alpha_n - \alpha_m)(x-x_0)}\right\}. \qquad 4.20$$

In deriving equation 4.20 we have used the trigonometric identity

$$e^{iA} - e^{iB} = 2i \sin\tfrac{1}{2}(A-B) \exp i\left[\tfrac{1}{2}(A+B)\right] .$$

The quantities $h_{mn1}(z_o)$ and $h_{mn2}(z_o)$ are given by

$$h_{mn1}(z_0) = \cos(\gamma_m - \gamma_n) z_0 \sin(\gamma_m - \gamma_n) z + \cos(\gamma_m + \gamma_n) z_0 \sin(\gamma_m + \gamma_n) z$$

and $$h_{mn2}(z_0) = \cos(\gamma_m - \gamma_n) z_0 \cos(\gamma_m - \gamma_n) z + \cos(\gamma_m + \gamma_n) z_0 \cos(\gamma_m + \gamma_n) z$$

Comparing equations 4.2 and 4.20 we can immediately ascertain that in the absence of internal waves and their associated refractive index fluctuations, the two equations become identical. In equation 4.20 we shall interpret the amplitude fluctuation for mode m as the modification to the eigenfunction so that $\sin(\gamma_m z)$ becomes

$$\sin\left\{\gamma_m z - \frac{ik_0^2 n_0}{D}\sum_{n=1}^{\infty}\frac{1}{\alpha_n}\int_0^{x_D}\int_0^{D} dx_0\, dz_0\, \delta h_{mn1}(z_0)\, e^{i(\alpha_n-\alpha_m)(x-x_0)}\right\}.$$

The phase fluctuation $S_m(x,z,t)$ is given by the expression

$$S_m(x,z,t) = \frac{k_0^2 n_0}{D}\sum_{n=1}^{\infty}\frac{1}{\alpha_n}\int_0^{x_D}\int_0^{D} dx_0\, dz_0\, \delta h_{mn2}(z_0)\, e^{i(\alpha_n-\alpha_m)(x-x_0)} \qquad 4.21$$

The expressions above that we interpret as amplitude and phase fluctuations contain real and imaginary parts. The imaginary amplitude term then becomes a phase fluctuation, while the imaginary phase term becomes an amplitude fluctuation. However, as we shall now show, the imaginary terms are quite small and we shall neglect them in the subsequent analysis.

Both the amplitude and phase fluctuations for one incident mode involve an infinite summation of scattered modes. We shall shortly demonstrate that the dominant terms in the summation are those with $n \approx m$. We can then ignore the $(\gamma_m+\gamma_n)$ terms in the expressions for h_{mn1} and h_{mn2}, since they will be rapidly varying in the z_o integral with their net effect being small.

Let us now examine the fluctuations arising from two scattered

modes, n = m + 1 and n = m - 1. Since

$$\gamma_m - \gamma_{m-1} = -(\gamma_m - \gamma_{m+1}) \quad \text{and} \quad \alpha_{m-1} - \alpha_m \approx -(\alpha_{m+1} - \alpha_m) \ ,$$

we can write the double integral for the amplitude fluctuations as

$$\frac{iK_0^2 \eta_0}{\alpha_m D} \int_0^{\chi D} \int_0 d\chi_0 \, dz_0 \, \sigma \left\{ \cos(\gamma_\Delta z_0) \sin(\gamma_\Delta z) \, e^{i\alpha_\Delta (\chi - \chi_0)} + \cos(-\gamma_\Delta z_0) \sin(-\gamma_\Delta z) \, e^{-i\alpha_\Delta (\chi - \chi_0)} \right\}$$

where we have set

$$\gamma_\Delta = \gamma_m - \gamma_{m-1} \ , \quad \alpha_\Delta = \alpha_{m-1} - \alpha_m \ , \quad \text{and}$$

$$\frac{1}{\alpha_{m-1}} \approx \frac{1}{\alpha_{m+1}} \approx \frac{1}{\alpha_m} \ .$$

The double integral can now be simplified to a form containing all real terms:

$$-\frac{2K_0^2 \eta_0}{\alpha_m D} \int_0^{\chi D} \int_0 d\chi_0 \, dz_0 \, \sigma \cos(\gamma_\Delta z_0) \sin(\gamma_\Delta z) \sin[\alpha_\Delta (\chi - \chi_0)] \ .$$

An analogous expression can be easily derived for the phase fluctuation. The above analysis can be generalized to any pair of scattered modes whose mode numbers are equidistant from the incident mode number. We are therefore justified in identifying the amplitude and phase fluctuation terms in equation 4.20.

In section 6 we shall show that the derivation and interpretation of amplitude and phase fluctuations in multimode propagation becomes quite complicated. Under several assumptions, however, the total phase rate fluctuation can be related to the phase rate fluctuations in the individual modes. We shall therefore concentrate our attention on the phase fluctuations and their time derivative.

Equation 4.21 indicates that the determination of various statistical quantities such as the mean-square phase fluctuations will involve a summation of scattered cross-mode terms. Each scattered mode will propagate through a different region of the random internal wave field. Due to the small vertical correlation scales of the internal waves, we shall assume the scattered modes to be uncorrelated from each other.

The nature of the acoustic-internal wave interaction process is revealed by considering the effects of the internal waves to be concentrated at a depth z_T(Figure 3). This situation corresponds to a two layered medium and approximates a highly stratified ocean. The Brunt-Väisälä frequency N(z) is assumed to be zero everywhere except at $z = z_T$.

The expression for the induced refractive index fluctuations is then

$$\sigma(x_o, z_o, t) = \Gamma(z_o)\,\delta(z_o - z_T)\,\sigma(x_o, t)$$

where δ is the Dirac delta function

and $\Gamma(z_o)$ is the magnitude of the refractive index fluctuations at $z = z_o$.

Integrating over depth with the delta function, we then have

$$S_m(x,z,t) = \frac{k_o^2 n_o}{D} \sum_{n=1}^{\infty} \Gamma(z_T)\, h_{mn2}(z_T)/\alpha_n \int_o^x dx_o\, \sigma(x_o,t)\, e^{i(\alpha_n - \alpha_m)(x - x_o)} \qquad 4.22$$

Assuming stationarity and horizontal homogeneity for the internal wave field, the mean-square value for the phase fluctuations is

$$\overline{S_m^2} = \overline{S_m(x,z,t)\, S_m^*(x,z,t)} \qquad 4.23$$

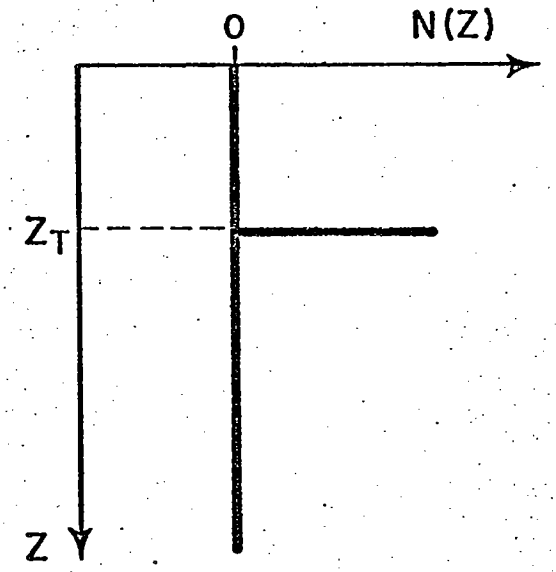

Figure 3: Brunt-Väisälä profile for a two fluid medium.

where the overbar $\overline{\quad}$ denotes statistical averages and the asterisk * indicates the complex conjugate.

If we assume the scattered cross-mode terms to be uncorrelated, the mean-square is given by

$$\overline{S_m^2}(x,z,t) = K_0^4 n_0^2 / D^2 \sum_{n=1}^{\infty} \Gamma^2(z_T) h_{mn2}^2(z_T)/\alpha_n^2 \iint_{00}^{xD} d\chi_0 \, d\chi_1 \, \rho_\sigma(\chi_2, t) e^{i(\alpha_m - \alpha_n)\chi_2} \qquad 4.24$$

where the correlation function for the refractive index fluctuations has been substituted:

$$\rho_\sigma(\chi_2, t) = \overline{\sigma(\chi_0, \tau)\, \sigma^*(\chi_1, \tau + t)} \qquad 4.25$$

with $x_2 = x_0 - x_1$.

Using the Wiener-Khintchine theorem we have

$$\rho_\sigma(\chi_2, t) = \iint_{-\infty}^{\infty} d\alpha_x \, d\omega \, F_\sigma(\alpha_x, \omega) e^{i(\alpha_x \chi_2 + \omega t)} \qquad 4.26$$

where $F_\sigma(\alpha_x, \omega)$ is the spectral density for the refractive index fluctuations. Substituting equation 4.26 into 4.24, we can then write

$$\overline{S_m^2} = \sum_{n=1}^{\infty} H_{mn}(z_T) \int_0^x d\chi_0 \int_0^x d\chi_1 \iint_{-\infty}^{\infty} d\alpha_x \, d\omega \, F_\sigma(\alpha_x, \omega) e^{i(\alpha_x + \alpha_m - \alpha_n)\chi_2} \qquad 4.27$$

where $$H_{mn}(z_T) = K_0^4 n_0^2 \Gamma^2(z_T) h_{mn2}^2(z_T) / D^2 \alpha_n^2 \, .$$

Let us now change the integration variables to x_2 and x_3 where

$$\chi_3 = \tfrac{1}{2}(\chi_0 + \chi_1) \, .$$

The Jacobian of the integral transformation is equal to one. If we assume that the correlation distance for $\rho_\sigma(x_2)$ is << x, then we can extend the integration limits on x_2 to $\pm \infty$ without contributing a significant error to the integral. The limits of integration on x_3 are 0 to x. Reversing the order of integration yields

$$\overline{S_m^2} = \sum_{n=1}^{\infty} H_{mn}(z_\tau) \int_0^x dx_3 \iint_{-\infty}^{\infty} d\alpha_x\, d\omega\, F_\sigma(\alpha_x, \omega) \int_{-\infty}^{\infty} dx_2\, e^{i(\alpha_x + \alpha_m - \alpha_n)x_2} \qquad 4.28$$

Recognizing that $$\int_{-\infty}^{\infty} dx_2\, e^{i(\alpha_x + \alpha_m - \alpha_n)x_2} = 2\pi\, \delta(\alpha_x + \alpha_m - \alpha_n),$$

we have $$\overline{S_m^2} = 2\pi x \sum_{n=1}^{\infty} H_{mn}(z_\tau) \iint_{-\infty}^{\infty} d\alpha_x\, d\omega\, F_\sigma(\alpha_x, \omega)\, \delta(\alpha_x + \alpha_m - \alpha_n). \qquad 4.29$$

The presence of the term

$$\delta(\alpha_x + \alpha_m - \alpha_n)$$

within the integral in equation 4.29 indicates that the spectral density for the acoustic phase will contain a series of "spikes" at wavenumbers where

$$\alpha_x = |\alpha_m - \alpha_n|.$$

A diffraction grating is therefore created whereby the acoustic field selects those internal waves whose wavenumber satisfies

$$\alpha_x = |\alpha_m - \alpha_n|$$

If the acoustic wave encounters an internal wave where this condition does not hold, the acoustic wave will pass through with no resultant scattering.

The magnitude of the various contributions at

$$\alpha_x = |\alpha_m - \alpha_n|$$

is a function of the term $H_{mn}(z_T)$ and of the refractive index spectral density $F_\sigma(\alpha_x, \omega)$. From equation 2.17 we can write

$$F_\sigma(\alpha_x, \omega) = N^4 \mu^2 g^{-2} F_\xi(\alpha_x, \omega) \quad . \qquad 4.30$$

Based on the discussion following equation 2.11 we are able to conclude that the refractive index spectral density is approximately proportional to α_x^{-2} throughout wavenumber space with the precise relation dependent on the 1972 or 1975 GM model. The interpretation and significance of the spectral density with the condition that

$$\alpha_x = |\alpha_m - \alpha_n|$$

is shown on the figure below.

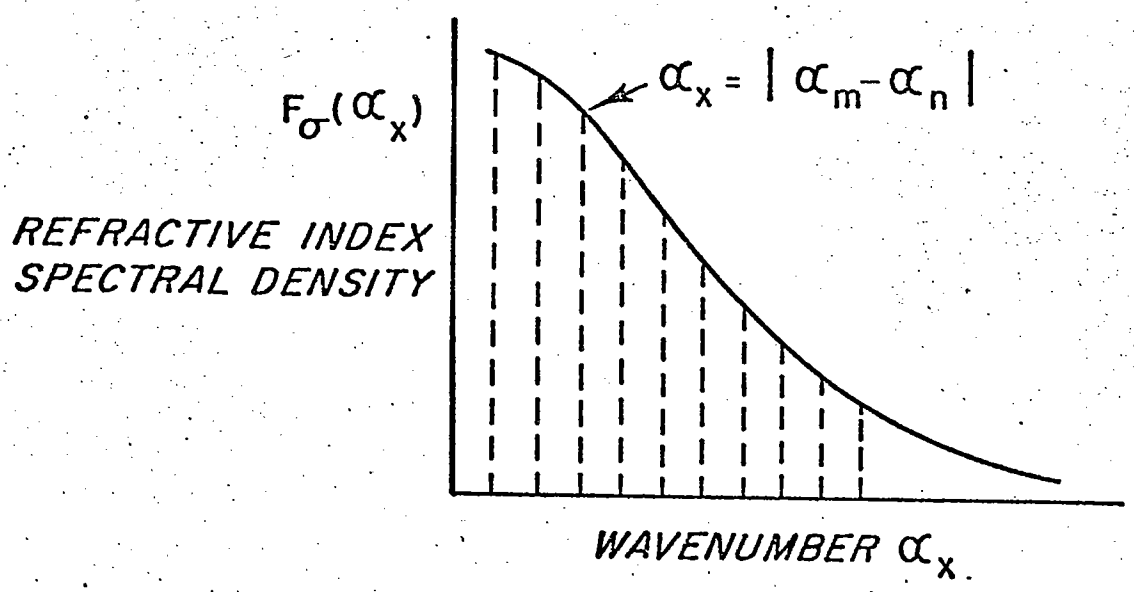

Figure 4: Horizontal wavenumber dependence for the refractive index spectral density. Smaller wavenumbers are dominant in the acoustic interaction.

Absolute value signs are used since internal waves can travel in the $\pm x$ direction. In Figure 4 only the positive α_x values have been sketched. It is immediately evident that the smaller α_x values will contribute more to the phase fluctuations than do the larger α_x values. This implies that the scattered modes with $\alpha_n \approx \alpha_m$ (or n approximately equal to m) form the dominant contribution to the scattered field.

Let us now further examine the significance of equation 4.29. It is immediately evident that the mean-square phase fluctuations increase linearly with range. This is a result of the weak scattering theory and suggests a finite region of validity for the predicted acoustic fluctuations. From the definition of $H_{mn}(z_T)$ we see that the mean-square phase fluctuations (and its spectral density) is approximately proportional to the acoustic frequency.

The parameter $\Gamma(z_T)$ represents the effective change in vertical acoustic path length due to the refractive index inhomogeneities. It is a concept which Porter, et al. (1974) have called the "acoustic thickness" and is defined as the integrated refractive index fluctuations over depth:

$$\int_z \sigma \, dz \; .$$

An acoustic wave propogating vertically through the waveguide will then experience a change in phase proportional to the acoustic thickness. Because of the multimode structure of the internal wave field with its short vertical correlation scales, we shall use the rms behavior of the refractive index fluctuations (as described in

section 2) to calculate the acoustic thickness.

In equation 4.29 we have made the implicit assumption that the horizontally propagating internal waves cause most of the acoustic scattering. In the variable-sound-speed waveguide of section 7 we shall see that acoustic waves trapped by the waveguide propagate almost horizontally. Since the induced refractive index fluctuations are assumed to be horizontally homogeneous, an acoustic wave passing through a vertically propagating internal wave will encounter an essentially homogeneous medium, so that very little scattering is experienced. As such, most of the acoustic scattering is caused by the horizontally propagating internal waves. The precise structure of the vertical internal wave scales is then not crucial in the determination of the acoustic fluctuations.

In this section we have treated the interaction of an acoustic wave with a random internal wave field in an isospeed two dimensional waveguide. The concept of the internal wave field acting as a diffraction grating has been discussed. The relationship between mean-square phase fluctuations and internal wave statistics has been derived.

Three dimensional waveguides will be discussed in sections 5 and 7. We shall show that the interaction process and the resulting acoustic fluctuations are quite similar to those found in the two dimensional waveguide.

5. THREE DIMENSIONAL ISOSPEED WAVEGUIDE

The derivation and solution of the scattered field in the three dimensional isospeed waveguide closely parallels that of the two dimensional isospeed waveguide. The introduction of cylindrical waves with their associated Hankel functions significantly complicates the mathematics in the three dimensional waveguide. We shall rely upon the result of the previous section that most of the acoustic fluctuations occur for scattered modes with mode number approximately equal to that of the incident mode. We shall defer the calculation of various statistical acoustic quantities to the variable-sound-speed waveguide in section 7.

Assuming cylindrical symmetry with a CW point source located at $r = r_s$ and $z = z_s$, the equation for the zero order velocity potential ψ_o is

$$\frac{1}{r}\left[\frac{\partial}{\partial r}\left(r\frac{\partial \psi_0}{\partial r}\right)\right] + \frac{\partial^2 \psi_0}{\partial z^2} + k_0^2 n_0^2 \psi_0 = -\frac{1}{2\pi r}\delta(r-r_s)\delta(z-z_s). \qquad 5.1$$

Equation 5.1 is recognized as the equation for the Green's function in a wave duct whose solution is given by (Tolstoy, 1973, p. 300)

$$\psi_0(r,z) = \frac{i}{4}\sum_m h_m(z)\, h_m(z_s)\, H_0^{(1)}\left[\alpha_m |r-r_s|\right] \qquad 5.2$$

where $H_o^{(1)}$ is the zero order Hankel function of the first kind and $h_m(z)$ is the orthonormal eigenfunction with eigenvalue α_m. For the isospeed channel of depth D with a hard bottom and free surface the velocity potential is

$$\psi_0(r,z) = \frac{i}{2D}\sum_{m=1}^{\infty} \sin(\gamma_m z)\sin(\gamma_m z_s)\, H_0^{(1)}(\alpha_m r) \qquad 5.3$$

where we have taken $r_s = 0$. The eigenfunctions are given by

$$h_m(z) = (2/D)^{1/2} \sin(\gamma_m z)$$

where $\gamma_m = (m-\frac{1}{2})\pi/D$ and $\alpha_m^2 + \gamma_m^2 = k_o^2 n_o^2$.

The first order equations are again

$$\nabla^2 W_m' + k_o^2 n_o^2 W_m' = -2k_o^2 n_o \sigma \psi_{om}' \qquad 5.4$$

and $$\nabla^2 W_m'' + k_o^2 n_o^2 W_m'' = -2k_o^2 n_o \sigma \psi_{om}'' .$$

Using the auxiliary functions

$$\hat{W} = W_m' + W_m'' \quad \text{and} \quad \tilde{W} = W_m' - W_m'' ,$$

the appropriate Green's functions are

$$G_{\hat{W}}(r,z|r_o,z_o) = \frac{i}{2D} \sum_{n=1}^{\infty} \sin(\gamma_n z) \sin(\gamma_n z_o) H_o^{(1)}[\alpha_n |r-r_o|] \qquad 5.5$$

and $$G_{\tilde{W}}(r,z|r_o,z_o) = \frac{i}{2D} \sum_{n=1}^{\infty} \cos(\gamma_n z) \cos(\gamma_n z_o) H_o^{(1)}[\alpha_n |r-r_o|] .$$

With a small amount of manipulation we can obtain expressions for the scattered waves:

$$P_m'(r,z,t) = \frac{ik_o^2 n_o}{2D} \sum_{n=1}^{\infty} \int_0^r \int_0^D dr_o\, dz_o\, \sigma F_{mn}(r_o) f_{mn1}(z_o)$$

$$P_m''(r,z,t) = \frac{ik_o^2 n_o}{2D} \sum_{n=1}^{\infty} \int_0^r \int_0^D dr_o\, dz_o\, \sigma F_{mn}(r_o) f_{mn2}(z_o) \qquad 5.6$$

where $$F_{mn}(r_o) = H_o^{(1)}(\alpha_m r_o) H_o^{(1)}[\alpha_n |r-r_o|] \Big/ H_o^{(1)}(\alpha_m r) ,$$

$$f_{mn1}(z_o) = \cos(\gamma_m - \gamma_n) z_o\, e^{-i(\gamma_m-\gamma_n)z} + \cos(\gamma_m+\gamma_n) z_o\, e^{-i(\gamma_m+\gamma_n)z} ,$$

and $$f_{mn2}(z_o) = \cos(\gamma_m - \gamma_n) z_o\, e^{i(\gamma_m-\gamma_n)z} + \cos(\gamma_m+\gamma_n) z_o\, e^{i(\gamma_m+\gamma_n)z} .$$

It should be noted that in equation 5.6 backscattered waves are assumed to be insignificant. The total field at the receiver is equal to

$$\psi_m(r,z,t) = \frac{i \sin \gamma_m z_s}{2D} H_0^{(1)}(\alpha_m r) \sin\left\{\gamma_m z - \frac{ik_0^2 n_0}{2D} \sum_{n=1}^{\infty} \int_0^r \int_0^D dr_0 dz_0 \, \sigma F_{mn}(r_0) h_{mn1}(z_0)\right\}$$

$$\cdot \exp i\left\{\frac{k_0^2 n_0}{2D} \sum_{n=1}^{\infty} \int_0^r \int_0^D dr_0 dz_0 \, \sigma F_{mn}(r_0) h_{mn2}(z_0)\right\} \qquad 5.7$$

where $$h_{mn1}(z_0) = \frac{i}{2}\left[f_{mn1}(z_0) - f_{mn2}(z_0)\right]$$

and $$h_{mn2}(z_0) = \frac{1}{2}\left[f_{mn1}(z_0) + f_{mn2}(z_0)\right] .$$

From equation 5.7 the phase fluctuation $S_m(r,z,t)$ is

$$S_m(r,z,t) = \frac{k_0^2 n_0}{2D} \sum_{n=1}^{\infty} \int_0^r \int_0^D dr_0 dz_0 \, \sigma(r_0,z_0,t) F_{mn}(r_0) h_{mn2}(z_0) . \qquad 5.8$$

If we assume that the effects of the internal waves are concentrated at a single depth z_T so that

$$\sigma(r_0,z_0,t) = \Gamma(z_0)\, \delta(z_0 - z_T)\, \sigma(r_0,t) ,$$

we then have

$$S_m(r,z,t) = \frac{k_0^2 n_0}{2D} \sum_{n=1}^{\infty} \Gamma(z_T) h_{mn2}(z_T) \int_0^r dr_0 \, \sigma F_{mn}(r_0) . \qquad 5.9$$

Because of the large internal wavelengths in comparison to the acoustic wavelengths, the acoustic fluctuations are effectively caused by forward

scattering only. As such only that portion of the medium close to the propagation vector joining the source and receiver will contribute appreciably to the scattered field.

We now rotate the coordinate system so that the x axis is the horizontal projection of the line joining the source and receiver. The source is located at $\vec{r}_s(o,o,z_s)$ while the receiver is located at $\vec{r}(x,o,z)$. A scattering point has the coordinate $\vec{r}_o(x_o,y_o,z_o)$ (for a delta function in depth, $z_o = z_T$ only) where $x_o >> y_o$ and $|x-x_o| >> |y-y_o| = y_o$. In the horizontal plane we also have the relations

$$r_o^2 = x_o^2 + y_o^2 = x_o^2\left(1+y_o^2/x_o^2\right) \Rightarrow r_o \approx x_o + y_o^2/2x_o ,$$

$$r = x, \quad \text{and} \quad |r-r_o| \approx x - x_o + y_o^2/[2(x-x_o)] .$$

The asymptotic expansion for the Hankel function is given by

$$H_0^{(1)}(\alpha_m r) \approx \left[\frac{2}{\pi\alpha_m r}\right]^{1/2} e^{i\left(\alpha_m r - \frac{\pi}{4}\right)}$$

This expression is valid for $\alpha_m r >> 1$ or equivalently for ranges r greater than a few acoustic wavelengths. Since transmission ranges in long range propagation are on the order of hundreds of kilometers, almost all the internal wave fluctuations will occur in regions where the Hankel function expansion is valid. We shall therefore use the asymptotic expansion for $F_{mn}(r_o)$ throughout the region from o to r.

The expression for $F_{mn}(r_o)$ can now be written as

$$F_{mn}(r_o) = \left[\frac{2}{\pi\alpha_n}\right]^{1/2} e^{-i\pi/4} \left[\frac{r}{r_o|r-r_o|}\right]^{1/2} \exp i\left[\alpha_n|r-r_o| - \alpha_m(r-r_o)\right] . \qquad 5.10$$

We shall use a zero order approximation in the amplitude coefficient of the

exponential and a first order expansion on the exponential itself. We then have

$$F_{mn}(r_0) = \left(\frac{2}{\pi\alpha_n}\right)^{1/2} e^{-i\frac{\pi}{4}} \left[\frac{\chi}{\chi_0(\chi-\chi_0)}\right]^{1/2} \exp i\left\{\alpha_n\left[\chi-\chi_0+\frac{y_0^2}{2(\chi-\chi_0)}\right]-\alpha_m\left[\chi-\chi_0-\frac{y_0^2}{2\chi_0}\right]\right\} \qquad 5.11$$

The integration over x_o is taken from 0 to x while the limits on y_o may be extended to $\pm\infty$ since in the region where y_o is large, the value of the exponential will rapidly oscillate with its net value being zero.

The expression for the phase fluctuation is

$$S_m(r,z,t) = \frac{K_0^2 n_0}{2D} \sum_{n=1}^{\infty} \Gamma(z_\tau) h_{mn2}(z_\tau) \left[\frac{2\chi}{\pi\alpha_n}\right]^{1/2} e^{-i\pi/4} \int_0^{\chi} [\chi_0(\chi-\chi_0)]^{-1/2} d\chi_0$$

$$\cdot \int_{-\infty}^{\infty} dy_0\, \sigma \exp i\left\{(\alpha_n-\alpha_m)(\chi-\chi_0)+\frac{\alpha_n y_0^2}{2(\chi-\chi_0)}+\frac{\alpha_m y_0^2}{2\chi_0}\right\}. \qquad 5.12$$

Assuming stationarity and horizontal homogeneity for the internal wave field, let us determine the mean-square phase fluctuations

$$\overline{S_m^2} = \overline{S_m(r,z,t)\, S_m^*(r,z,t)}$$

Taking uncorrelated scattered cross-mode terms, we now have

$$\overline{S_m^2} = \frac{K_0^4 n_0^2 \chi}{2\pi D^2} \sum_{n=1}^{\infty} \Gamma^2(z_\tau) h_{mn2}^2(z_\tau)/\alpha_n \int_0^{\chi}\int_0^{\chi} [\chi_0\chi_1(\chi-\chi_0)(\chi-\chi_1)]^{-1/2} d\chi_0 d\chi_1$$

$$\cdot \int_{-\infty}^{\infty}\int dy_0 dy_1\, \rho_\sigma \exp i\left\{(\alpha_m-\alpha_n)\chi_2+\frac{\alpha_n}{2}\left[\frac{y_0^2}{\chi-\chi_0}-\frac{y_1^2}{\chi-\chi_1}\right]+\frac{\alpha_m}{2}\left[\frac{y_0^2}{\chi_0}-\frac{y_1^2}{\chi_1}\right]\right\}. \qquad 5.13$$

where $$\rho_\sigma(x_2, y_2, z, \tau) = \overline{\sigma(x_0, y_0, z, t)\,\sigma^*(x_1, y_1, z, t+\tau)}$$

and $x_2 = x_0 - x_1$.

If we now substitute $y_0 = y_1 + y_2$, the integrals over y_1 and y_2 become

$$\exp i\left[(\alpha_m - \alpha_n)x_2\right] \iint_{-\infty}^{\infty} dy_2\, dy_1\, \rho_\sigma \exp i\left\{\frac{\alpha_n}{2}\left[\frac{y_1^2(x_0-x_1) + 2y_1y_2(x-x_1) + y_2^2(x-x_1)}{(x-x_0)(x-x_1)}\right]\right.$$

$$\left. + \frac{\alpha_m}{2}\left[\frac{y_1^2(x_1-x_0) + 2y_1y_2x_1 + y_2^2x_1}{x_0x_1}\right]\right\} .$$

The integration over y_1 can be performed directly as it is of the form

$$J = \int_{-\infty}^{\infty} \exp i\left[ay^2 + by + c\right] dy \quad .$$

Evaluating this integral yields (Chernov, 1960, p. 158-159)

$$J = \exp i\left[c - \frac{b^2}{4a}\right]\left[\frac{i\pi}{a}\right]^{1/2} .$$

Therefore, with

$$a = \left[\alpha_n x_0 x_1 x_2 - \alpha_m x_2 (x-x_0)(x-x_1)\right] \Big/ 2x_0x_1(x-x_0)(x-x_1) ,$$

$$b = \left[\alpha_n x_0 y_2 + \alpha_m y_2 (x-x_0)\right] \Big/ x_0(x-x_0) ,$$

and $$c = y_2^2\left[\alpha_n x_0 + \alpha_m(x-x_0)\right] \Big/ 2x_0(x-x_0) ,$$

the expression for $\overline{s_m^2}$ becomes

$$\overline{S_m^2} = \sum_{n=1}^{\infty} L_{mn}(z_T) \iint_{00}^{xx} dx_0\, dx_1 \left\{ x_2 \left[\alpha_n x_0 x_1 - \alpha_m (x-x_0)(x-x_1) \right] \right\}^{-1/2} e^{i(\alpha_m - \alpha_n) x_2}$$

$$\cdot \int_{-\infty}^{\infty} dy_2\, \rho_\sigma (x_2, y_2, z, \tau) \exp \left[i F y_2^2 \right] . \qquad 5.14$$

In equation 5.14 we have used a shorthand notation, where

$$L_{mn}(z_T) = (i 2\pi)^{1/2} \left[k_0^4 n_0^2 \chi \Gamma^2(z_T) h_{mn2}^2(z_T) / 2\pi \alpha_n D^2 \right]$$

and $$F = - \frac{\alpha_n^2 x_0 x_1 + \alpha_m^2 (x-x_1)(x-x_0) - \alpha_n \alpha_m \left[2 x_0 x_1 - x(x_0 + x_1) \right]}{2 x_2 \left[\alpha_n x_0 x_1 - \alpha_m (x-x_0)(x-x_1) \right]} .$$

Recognizing that $\rho_\sigma (x_2, y_2, z, \tau)$ can be expressed in terms of its spectral density by the Wiener-Khintchine relation

$$\rho_\sigma (x_2, y_2, z, \tau) = \iiint_{-\infty}^{\infty} d\alpha_x\, d\alpha_y\, d\omega\, F_\sigma (\alpha_x, \alpha_y, \omega, z) \exp i \left[\alpha_x x_2 + \alpha_y y_2 + \omega \tau \right] ,$$

we have

$$\overline{S_m^2} = \sum_{n=1}^{\infty} L_{mn}(z_T) \iiint_{-\infty}^{\infty} d\alpha_x\, d\alpha_y\, d\omega\, F_\sigma (\alpha_x, \alpha_y, \omega, z)$$

$$\cdot \iint_{00}^{xx} dx_0 dx_1 \frac{\exp i \left[(\alpha_m - \alpha_n + \alpha_x) x_2 \right]}{\left\{ x_2 \left[\alpha_n x_0 x_1 - \alpha_m (x-x_0)(x-x_1) \right] \right\}^{1/2}} \int_{-\infty}^{\infty} dy_2 \exp i \left[F y_2^2 + \alpha_y y_2 \right] . \qquad 5.15$$

The integration over y_2 can be performed by the same technique as that for y_1 to give

$$\overline{S_m^2} = \sum_{n=1}^{\infty} R_{mn}(z_T) \int_{-\infty}^{\infty}\int_{-\infty}^{\infty}\int_{0}^{x}\int_{0}^{x} d\alpha_x\, d\alpha_y\, d\omega\, dx_0\, dx_1\, F_0 E^{-1} \exp i\left[(\alpha_x+\alpha_m-\alpha_n)x_2 - \frac{\alpha_y^2}{4F}\right] \quad 5.16$$

where $$R_{mn}(z_T) = \left[\frac{2\pi}{i}\right]^{1/2} L_{mn}(z_T) = \frac{k_0^4 \eta_0^2 \chi \Gamma^2(z_T) h_{mn2}^2(z_T)}{\alpha_n D^2}$$

and $$E = \left\{\alpha_n^2 x_0 x_1 + \alpha_m^2 (x-x_0)(x-x_1) - \alpha_n \alpha_m \left[2x_0 x_1 - x(x_0+x_1)\right]\right\}^{1/2}.$$

If we now let $\alpha_n = \alpha_m + \Delta_n$ where Δ_n can be positive or negative, then

$$-\frac{\alpha_y^2}{4F} = \frac{\alpha_y^2 \chi_2 \left[(\alpha_m+\Delta_n)x_0 x_1 - \alpha_m (x-x_0)(x-x_1)\right]}{2\left\{(\alpha_m^2 + 2\alpha_m\Delta_n + \Delta_n^2)x_0 x_1 + \alpha_m^2 (x-x_0)(x-x_1) - \alpha_m(\alpha_m+\Delta_n)(2x_0 x_1 - x_0 x - x x_1)\right\}}$$

$$= \frac{\alpha_y^2 \chi_2 \left[-\alpha_m x(x-x_0-x_1) + \Delta_n x_0 x_1\right]}{2\left[\alpha_m^2 x^2 + \alpha_m \Delta_n x(x_0+x_1) + \Delta_n^2 x_0 x_1\right]}.$$

The two dimensional problem suggests that the dominant terms in the summation are when $n \approx m$. Let us therefore take $\alpha_n \approx \alpha_m$ so that Δ_n is a first order correction term. To zero order, we then have

$$\left|\alpha_y^2/4F\right| = \alpha_y^2 \chi_2 (x-x_0-x_1)/2\alpha_m x.$$

Over the main region of integration for α_y we have $\alpha_y x_2 \sim \alpha_x x_2 \lesssim 1$, so that

$$\left|\alpha_y^2 \chi_2 (x-x_0-x_1)/2\alpha_m x\right| \lesssim \left|\alpha_y (x-x_0-x_1)/2\alpha_m x\right| \sim \alpha_y/\alpha_m << 1.$$

Since $\alpha_y^2/4F$ is << 1, we shall assume that the exponential term

$$\exp i\left[-\alpha_y^2/4F\right]$$

is approximately equal to one. A similar expansion of $\alpha_n = \alpha_m + \Delta_n$ can be performed on the term E:

$$E = \left\{(\alpha_m^2 + 2\alpha_m\Delta_n + \Delta_n^2)\chi_0\chi_1 + \alpha_m^2(\chi^2 - \chi\chi_1 - \chi\chi_0 + \chi_0\chi_1) - \alpha_m(\alpha_m+\Delta_n)(2\chi_0\chi_1 - \chi\chi_0 - \chi\chi_1)\right\}^{1/2}$$

$$= \left\{\alpha_m^2\chi^2 + \alpha_m\Delta_n\chi(\chi_0+\chi_1) + \Delta_n^2\chi_0\chi_1\right\}^{1/2} \approx \alpha_m\chi .$$

With these two expansions the expression for $\overline{S_m^2}$ becomes

$$\overline{S_m^2} = \frac{K_0^4\eta_0^2}{D^2}\sum_{n=1}^{\infty}\frac{\Gamma^2(z_T)h_{mn_2}^2(z_T)}{\alpha_n\alpha_m}\int_{-\infty}^{\infty}\int_{0}^{\chi}\int_{0}^{\chi} d\alpha_x\, d\alpha_y\, d\omega\, dx_0\, dx_1\, F_\sigma\, e^{i(\alpha_m-\alpha_n+\alpha_x)\chi_2} . \qquad 5.17$$

Let us now change the integration variables to $x_2 = x_o - x_1$ and $x_3 = 1/2(x_o + x_1)$. If we assume that the correlation distance for $\rho_\sigma(x_2)$ is << x, we can extend the integration limits on x_2 to $\pm\infty$. The limits of integration on x_3 are o to x.

Integration over x_3 yields

$$\overline{S_m^2} = \frac{K_0^4\eta_0^2\chi}{D^2}\sum\frac{\Gamma^2(z_T)h_{mn_2}^2(z_T)}{\alpha_n\alpha_m}\int_{-\infty}^{\infty} d\alpha_x\, d\alpha_y\, d\omega\, F_\sigma\int_{-\infty}^{\infty} dx_2\, e^{i(\alpha_m-\alpha_n+\alpha_x)\chi_2} \qquad 5.18$$

Recognizing that $\int_{-\infty}^{\infty} dx_2\, e^{i(\alpha_m-\alpha_n+\alpha_x)\chi_2} = 2\pi\,\delta(\alpha_x+\alpha_m-\alpha_n)$,

we have

$$\overline{S_m^2} = \sum_{n=1}^{\infty} G_{mn}(z_T)\int_{-\infty}^{\infty} d\alpha_x\, d\alpha_y\, d\omega\, F_\sigma(\alpha_x,\alpha_y,\omega,z)\,\delta(\alpha_x+\alpha_m-\alpha_n) \qquad 5.19$$

where $G_{mn}(z_T) = 2\pi K_0^4 n_0^2 \chi \Gamma^2(z_T) h_{mn2}^2(z_T) / [\alpha_m \alpha_n D^2]$.

Equation 5.19 is almost identical to the analogous expression in the two dimensional waveguide (equation 4.39). In equation 5.19 α_x is the projection of the horizontal internal wavenumber upon the propagation path between the source and receiver. The presence of the delta function indicates that only those internal waves whose wavenumber projection upon the propagation path is equal to the difference between an incident and scattered mode wavenumber will affect the acoustic fluctuations.

The condition that $\alpha_x = |\alpha_m - \alpha_n|$ has a physical interpretation in terms of ray theory. In the isospeed waveguide

$$\alpha_m^2 = K_0^2 n_0^2 - \gamma_m^2 \quad \text{and} \quad \alpha_n^2 = K_0^2 n_0^2 - \gamma_n^2$$

where $\gamma_m = (m - \frac{1}{2})\frac{\pi}{D}$ and $\gamma_n = (n - \frac{1}{2})\frac{\pi}{D}$.

Subtracting and rearranging terms we have

$$\alpha_m - \alpha_n = (\gamma_n - \gamma_m)(\gamma_n + \gamma_m)/(\alpha_m + \alpha_n) \quad .$$

The analysis in the two dimensional waveguide has revealed that the $n \approx m$ terms are the dominant terms in the summation. Taking $\gamma_n + \gamma_m \approx 2\gamma_m$ and $\alpha_m + \alpha_n \approx 2\alpha_m$ we have

$$\alpha_x = \alpha_m - \alpha_n \approx (\gamma_n - \gamma_m)\gamma_m / \alpha_m = [(n-m)\pi/D] \tan\theta$$

where θ is the horizontal propagation angle.

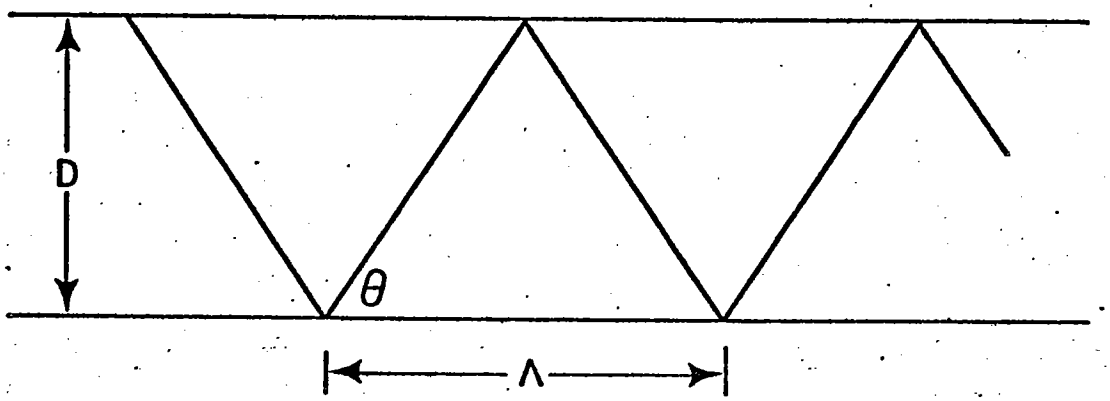

Figure 5: Ray geometry in isospeed waveguide; width D, ray angle θ, and ray cycle length Λ.

The ray cycle length Λ is

$$\Lambda = \frac{2D}{\tan\theta} = \frac{2\pi(n-m)}{\alpha_m - \alpha_n} = \frac{2\pi(n-m)}{\alpha_x} = (n-m)\lambda_x \qquad 5.20$$

where λ_x is the projection of the internal wavelength along the transmission path. Large acoustic phase fluctuations are therefore possible when the ray cycle length is an integer multiple of λ_x.

The relationship between ray cycle length and internal wavelength has also been deduced by ray theories which treat the acoustic-internal wave interaction. DeFerrari (1974) has found that the acoustic field will be most sensitive to those internal waves whose horizontal wavelength is equal to the ray cycle length. Porter, et al. (1974) have found that amplification of the phase fluctuations can occur if the ray cycle length is a multiple of the projection of the internal wavelength along the propagation path.

Let us now assume horizontal isotropy for the internal wave field so that

$$F_\delta(\alpha,\omega,z) = 2\pi\alpha\, F_\delta(\alpha_x,\alpha_y,\omega,z) \qquad 5.21$$

where $\alpha_x = \alpha\cos\phi$ and $d\alpha_x d\alpha_y = \alpha\, d\alpha\, d\phi$.

For convenience we shall let $\Delta = |\alpha_n - \alpha_m|$ where the absolute value signs are used since α_x can take on positive and negative values. Substituting equation 5.21 into 5.19 yields

$$\overline{S_m^2} = \sum_{n=1}^{\infty} \frac{G_{mn}(z_T)}{2\pi} \int_{-\infty}^{\infty} d\omega \int_0^{\infty} d\alpha\, F_\delta(\alpha,\omega,z) \int_0^{2\pi} \delta(\alpha\cos\phi - \Delta)\, d\phi . \qquad 5.22$$

The integral over ϕ can be evaluated by substituting

$$\delta[f(\phi)] = \frac{\sum_i \delta(\phi-\phi_i)}{|f'(\phi_i)|} \qquad 5.23$$

where ϕ_i is a root of $f(\phi) = 0$, and $f'(\phi)$ is the derivative of f with respect to ϕ . Letting

$$f(\phi) = \alpha\cos\phi - \Delta \quad , \quad \text{so that}$$

$$f'(\phi) = -\alpha\sin\phi \quad \text{and} \quad \phi_i = \cos^{-1}(\Delta/\alpha),$$

we can write

$$\int_0^{2\pi} d\phi\ \delta(\alpha\cos\phi - \Delta) = \frac{2}{(\alpha^2-\Delta^2)^{1/2}} \qquad 5.24$$

The expression for the mean-square phase fluctuations now becomes

$$\overline{S_m^2} = \sum_{n=1}^{\infty} \frac{G_{mn}(z_T)}{\pi} \int_{-\infty}^{\infty} d\omega \int_{0}^{\infty} d\alpha \; \frac{F_\sigma(\alpha,\omega,z)}{(\alpha^2-\Delta^2)^{1/2}} \qquad 5.25$$

Recognizing that the mean-square phase fluctuation is related to its spectral density $F_{s_m}(\alpha,\omega,z)$ by

$$\overline{S_m^2} = \int_{-\infty}^{\infty}\int_{0}^{\infty} d\omega \, d\alpha \, F_{s_m}(\alpha,\omega,z) \qquad 5.26$$

we can write

$$F_{s_m}(\alpha,\omega,z) = \sum_{n=1}^{\infty} \frac{G_{mn}(z_T)}{\pi} \; \frac{1}{(\alpha^2-\Delta^2)^{1/2}} \, F_\sigma(\alpha,\omega,z). \qquad 5.27$$

In terms of the phase rate spectral density $F_{\dot{s}_m}(\alpha,\omega,z)$, we have

$$F_{\dot{s}_m}(\alpha,\omega,z) = \sum_{n=1}^{\infty} \frac{G_{mn}(z_T)}{\pi} \; \frac{1}{(\alpha^2-\Delta^2)^{1/2}} \, F_{\dot{\sigma}}(\alpha,\omega,z) \qquad 5.28$$

where $$F_{\dot{\sigma}}(\alpha,\omega,z) = \omega^2 F_\sigma(\alpha,\omega,z) \; . \qquad 5.29$$

In equation 5.27 and 5.28 it is important to note that the phase and phase rate statistics for incident mode m can be directly related to the internal wave statistics. As we shall see in the next section, this direct relationship does not exist for phase (or amplitude) fluctuations in multimode propagation although a modified relationship is preserved with phase rate. As such, acoustic phase rate fluctuations will be emphasized in the remainder of this thesis.

6. MULTIMODE WAVEGUIDES

The previous sections have determined the acoustic fluctuations that result from the interaction of a random internal wave field with a single incident normal mode. For long range propagation in the ocean, however, a multimode description (multipath description in ray theory) is usually necessary to represent the received signal adequately. The number of modes that contain significant energy at the receiver depend upon many factors including the acoustic frequency, the range of propagation, the type of waveguide, the locations of source and receiver, etc. In some cases one, two, or three modes are sufficient to describe the acoustic field, while in other situations several hundred modes may be necessary. Generally, in short range studies a large number of modes must be used while fewer modes may be employed in long range propagation. This is in direct contrast to ray theory where several rays can adequately represent short range propagation while many rays are necessary for long ranges.

In a multimode environment the presence of internal waves creates two overlapping phenomena which lead to amplitude and phase fluctuations. Firstly, as is evidenced by the single mode sections, the internal wave field will induce amplitude and phase fluctuations on each of the incident modes. In addition, the induced acoustic fluctuations will cause a time varying multimode interference at any point in space. Therefore, the measured acoustic fluctuations are due to the direct interaction of the internal wave inhomogeneities with the individual modes as well as the spatial and temporal modification of the multimode structure. The relationship and relative importance of these two mechanisms has recently been

explored in the context of ray theory (DeFerrari and Leung, 1975). They recognized that the relationship between internal waves and acoustic fluctuations is complicated by the multipath process. They suggest that acoustic phase fluctuations are caused by two factors. The internal wave field linearly modulates the acoustic phase, while time-varying multipath interference non-linearly induces fluctuations in both amplitude and phase. For a two ray interference situation Porter, et al., (1974) predicted that acoustic phase fluctuations would be the mean of the individual phase terms while amplitude fluctuations would exhibit non-linearities.

The effect of multimode interference on acoustic fluctuations for two modes and three or more modes will be described. One of the most significant differences is that the character of the multimode interference markedly changes when more than two modes are being considered. The linear relationship between induced refractive index fluctuations and acoustic phase fluctuations no longer holds for three or more modes.

Relationships can also be established between internal wave fluctuations and phase rate fluctuations (time rate of change of phase fluctuations). If we assume that the phase fluctuations for each path are statistically independent of each other, then the total phase rate variation becomes a weighted sum of the contributions from the individual paths.

In examining the multimode waveguide we will first investigate the three dimensional isospeed waveguide with two incident modes m and ℓ. From equation 5.7 we have

$$\psi = \psi_m + \psi_\ell = \frac{\sin\gamma_m z_s}{D}\left[\frac{1}{2\pi\alpha_m r}\right]^{1/2} e^{i\pi/4} \sin\left\{\gamma_m z - \frac{ik_0^2 n_0}{2D}\sum_{n=1}^{\infty}\int_0^{r_D}\int_0^{D} dr_0\, dz_0\, \sigma F_{mn}(r_0) h_{mn1}(z_0)\right\}$$

$$\cdot \exp i\left\{\alpha_m r + \frac{k_0^2 n_0}{2D}\sum_{n=1}^{\infty}\int_0^{r_D}\int_0^{D} dr_0\, dz_0\, \sigma F_{mn}(r_0) h_{mn2}(z_0)\right\}$$

$$+ \frac{\sin\gamma_\ell z_s}{D}\left[\frac{1}{2\pi\alpha_\ell r}\right]^{1/2} e^{i\pi/4} \sin\left\{\gamma_\ell z - \frac{ik_0^2 n_0}{2D}\sum_{n=1}^{\infty}\int_0^{r_D}\int_0^{D} dr_0\, dz_0\, \sigma F_{\ell n}(r_0) h_{\ell n1}(z_0)\right\}$$

$$\cdot \exp i\left\{\alpha_\ell r + \frac{k_0^2 n_0}{2D}\sum_{n=1}^{\infty}\int_0^{r_D}\int_0^{D} dr_0\, dz_0\, \sigma F_{\ell n}(r_0) h_{\ell n2}(z_0)\right\} \qquad 6.1$$

where we have used the asymptotic form of the Hankel function. As a first consideration let us assume that the internal waves only affect the phase terms and that the mode amplitudes A_m and A_ℓ are approximately equal to each other. With $A = A_m = A_\ell$,

$$\beta_m = \frac{k_0^2 n_0}{2D}\sum_{n=1}^{\infty}\int_0^{r_D}\int_0^{D} dr_0\, dz_0\, \sigma F_{mn}(r_0) h_{mn2}(z_0),$$

and

$$\beta_\ell = \frac{k_0^2 n_0}{2D}\sum_{n=1}^{\infty}\int_0^{r_D}\int_0^{D} dr_0\, dz_0\, \sigma F_{\ell n}(r_0) h_{\ell n2}(z_0)$$

the expression for the total field is

$$\psi = A\left\{\exp i\left[\alpha_m r + \beta_m\right] + \exp i\left[\alpha_\ell r + \beta_\ell\right]\right\}. \qquad 6.2$$

Noting that

$$e^{ia} + e^{ib} = 2\cos\left[\tfrac{1}{2}(a-b)\right]\exp i\left[\tfrac{1}{2}(a+b)\right],$$

we can write ψ as

$$\psi = 2A \cos\left[\frac{1}{2}(\alpha_m - \alpha_\ell)r + \frac{1}{2}(\beta_m - \beta_\ell)\right] \exp i\left[\frac{1}{2}(\alpha_m + \alpha_\ell)r + \frac{1}{2}(\beta_m + \beta_\ell)\right]. \quad 6.3$$

Since the horizontal wave number α_m is approximately equal to α_ℓ, the internal wave induced phase fluctuation is given by

$$S = \frac{1}{2}(\beta_m + \beta_\ell) \quad 6.4$$

while the amplitude fluctuation is

$$\chi = 2 \cos\left[\frac{1}{2}(\alpha_m - \alpha_\ell)r + \frac{1}{2}(\beta_m - \beta_\ell)\right]. \quad 6.5$$

In equation 6.5 we have used the signed amplitude convention, that is permitting the amplitude to become negative. The total phase variation is seen as the mean of the phases for the two modes and as such is linearly proportional to the internal wave refractive index variation. The presence of the cosine in the amplitude term reveals the non-linearity of the interaction process. It is interesting to note that phase modulated terms have been transformed into amplitude terms in the two mode summation. The reverse process also takes place when we allow the internal wave field to affect the amplitude terms.

Let us now consider the two mode summation where the internal waves affect both the phase and amplitude terms. The expression for the total field is now

$$\psi = A(1+\mu_m)\exp i(\alpha_m r + \beta_m) + A(1+\mu_\ell)\exp i(\alpha_\ell r + \beta_\ell) \quad 6.6$$

where μ_m and μ_ℓ are the amplitude fluctuations for mode m and ℓ respectively. In order to express ψ in the form $\psi = R\exp(i\nu)$ we must use the relation for the sum of two vectors of arbitrary magnitude and phase. Consider the equation

$$Be^{i\gamma} = Ce^{i\alpha} + De^{i\beta}$$

where all the terms are defined on the figure below:

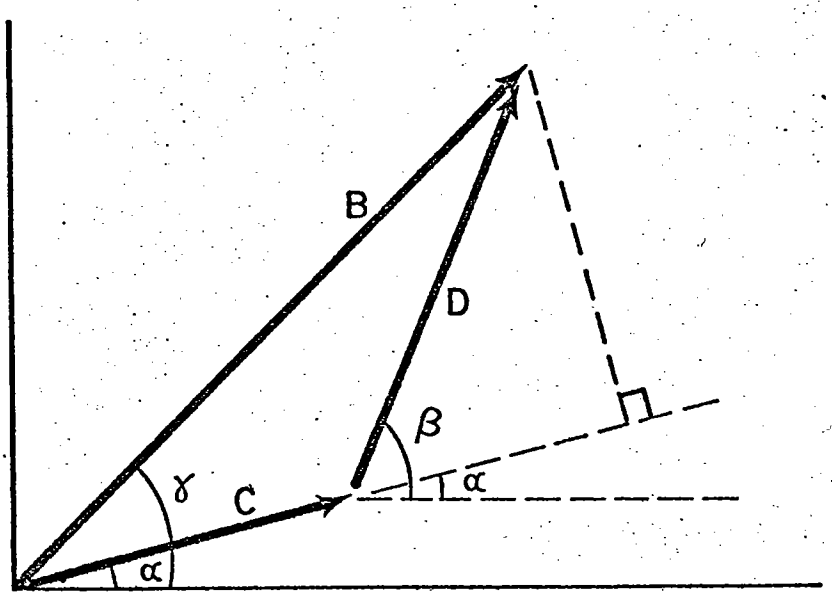

Figure 6: Summation of two vectors of arbitrary magnitude and phase.

From the law of cosines we have

$$B^2 = C^2 + D^2 - 2CD\cos(\pi + \alpha - \beta) .$$

But noting that $\cos(\pi + \alpha - \beta) = -\cos(\alpha - \beta)$,

we can write

$$B = \left[C^2 + D^2 + 2CD\cos(\alpha - \beta)\right]^{1/2}. \qquad 6.7$$

From simple trigonometry the expression for γ is

$$\gamma = \alpha + \mathrm{Tan}^{-1}\left\{D\sin(\beta-\alpha)/[C + D\cos(\beta-\alpha)]\right\}. \qquad 6.8$$

Expanding equation 6.6 and using equation 6.7 and 6.8 we have

$$\psi = A\left\{\exp i(\alpha_m r + \beta_m) + \exp i(\alpha_\ell r + \beta_\ell) + \mu_m \exp i(\alpha_m r + \beta_m) + \mu_\ell \exp i(\alpha_\ell r + \beta_\ell)\right\}$$

$$= 2A\cos\left[\tfrac{1}{2}(\alpha_m - \alpha_\ell)r + \tfrac{1}{2}(\beta_m - \beta_\ell)\right]\exp i\left[\tfrac{1}{2}(\alpha_m + \alpha_\ell)r + \tfrac{1}{2}(\beta_m + \beta_\ell)\right] + A\eta e^{i\theta}$$

where $\eta = \left[\mu_m^2 + \mu_\ell^2 + 2\mu_m\mu_\ell\cos(\theta_m - \theta_\ell)\right]^{1/2}$,

$$\theta_m = \alpha_m r + \beta_m,$$

$$\theta_\ell = \alpha_\ell r + \beta_\ell,$$

and $$\theta = \alpha_m + \mathrm{Tan}^{-1}\left\{\frac{\mu_\ell \sin(\theta_\ell - \theta_m)}{\mu_m + \mu_\ell\cos(\theta_\ell - \theta_m)}\right\}$$

If we now let $\chi = \frac{1}{2}(\alpha_m + \alpha_\ell)r + \frac{1}{2}(\beta_m + \beta_\ell)$

and $Y = \cos\left[\frac{1}{2}(\alpha_m - \alpha_\ell)r + \frac{1}{2}(\beta_m - \beta_\ell)\right]$

then we can write

$$\psi = R \exp i\nu = 2AY \exp i\chi + A\eta \exp i\theta .$$

Again using equations 6.7 and 6.8 we have

$$R = A\left[4Y^2 + \eta^2 + 4Y\eta\cos(\chi - \theta)\right]^{1/2} \qquad 6.9$$

and

$$\nu = \chi + \mathrm{Tan}^{-1}\left\{\eta\sin(\theta-\chi)/[2Y + \eta\cos(\theta-\chi)]\right\} . \qquad 6.10$$

If we again assume that $\alpha_m \approx \alpha_\ell$, the total phase fluctuation S is given by

$$S = \frac{1}{2}(\beta_m + \beta_\ell) + \mathrm{Tan}^{-1}\left\{\eta\sin(\theta-\chi)/[2Y + \eta\cos(\theta-\chi)]\right\} . \qquad 6.11$$

In contrast to equation 6.4 we now see that the phase fluctuation is no longer simply the average phase for the two modes but now contains in addition a complicated non-linear term arising from the amplitude modulation on the two modes. It can be easily verified that as the amplitude modulation approaches zero the result from equation 6.11 approaches that of 6.4.

It was previously mentioned that the character of multimode interference markedly changes when more than two modes are considered. This is most easily observed by treating three modes with equal amplitude and assuming that the internal wave field only affects the phase components of the various modes. With incident modes k, ℓ, and m the total field is

$$\psi = A\left\{\exp i\theta_k + \exp i\theta_\ell + \exp i\theta_m\right\} \qquad 6.12$$

where $\theta_k = \alpha_k r + \beta_k$,

$\theta_\ell = \alpha_\ell r + \beta_\ell$,

and $\theta_m = \alpha_m r + \beta_m$.

Combining two of the exponential terms we have

$$\psi = A \left\{ A_1 \exp i\theta_1 + \exp i\theta_m \right\} \qquad 6.13$$

where $A_1 = 2 \cos \frac{1}{2} (\theta_k - \theta_\ell)$

and $\theta_1 = \frac{1}{2} (\theta_k + \theta_\ell)$.

Now using expressions 6.7 and 6.8 we can obtain the amplitude and phase for the total field:

$$\psi = A_2 \exp i\theta_2 \qquad 6.14$$

where $A_2 = A \left[A_1^2 + 1 + 2A_1 \cos (\theta_1 - \theta_m) \right]^{1/2}$

and $\theta_2 = \theta_1 + \mathrm{Tan}^{-1} \left\{ \sin (\theta_m - \theta_1) / \left[A_1 + \cos (\theta_m - \theta_1) \right] \right\}$

$$= \frac{1}{2} (\theta_k + \theta_\ell) + \mathrm{Tan}^{-1} \left\{ \frac{\sin \left[\theta_m - \frac{1}{2} (\theta_k + \theta_\ell) \right]}{A_1 + \cos \left[\theta_m - \frac{1}{2} (\theta_k + \theta_\ell) \right]} \right\} .$$

From equation 6.14 we can see that the total phase fluctuation is not equal to the mean of the phases for the individual modes. As such we can generally

conclude that for multimode propagation with three or more modes the internal wave field induces non-linear amplitude and phase fluctuations. The direct relationships between acoustic fluctuation statistics and internal wave statistics for single mode propagation are not applicable in multimode situations.

The non-linear acoustic-internal wave interaction makes it quite difficult to determine the relative contribution of any particular mode to the total acoustic fluctuations. However, under the assumptions that the amplitude in any mode is constant or slowly varying in comparison to its phase variations and that the fluctuations in every mode are statistically independent from each other, the nature of the interaction becomes greatly simplified. We will now examine the phase rate fluctuation for multimode propagation under these conditions and subsequently discuss the significance of the above two assumptions.

The total field received is given by

$$\psi = R \exp i\mathcal{V} = \sum_m R_m \exp i\mathcal{V}_m$$

$$= \mathcal{U} + i\mathcal{V} = \sum_m \mathcal{U}_m + i\mathcal{V}_m \qquad 6.15$$

where $\mathcal{U}$ and $\mathcal{V}$ are the quadrature components of the signal such that

$$\mathcal{U} = R\cos\mathcal{V} = \sum_m R_m \cos\mathcal{V}_m \quad \text{and} \quad \mathcal{V} = R\sin\mathcal{V} = \sum_m R_m \sin\mathcal{V}_m .$$

In terms of $\mathcal{U}$ and $\mathcal{V}$ the amplitude and phase of the signal are

$$R = \left[U^2 + V^2\right]^{1/2} \qquad 6.16$$

and $$\nu = \mathrm{Tan}^{-1}\left[V/U\right] = \mathrm{Tan}^{-1}\left[\sum_m R_m \sin\nu_m \Big/ \sum_m R_m \cos\nu_m\right] .$$

The phase rate $\dot{\nu}$ (time derivative of the phase ν) is

$$\dot{\nu} = \frac{d\nu}{dt} = \frac{d}{dt}\left[\mathrm{Tan}^{-1}(V/U)\right] \qquad 6.17$$

$$= \frac{1}{1+\frac{V^2}{U^2}}\,\frac{d}{dt}\left(\frac{V}{U}\right) = \frac{U\dot{V} - V\dot{U}}{R^2}$$

If we now invoke the condition that the modal amplitude R_m is slowly varying in comparison to the modal phase ν_m, we can write $\dot{\nu}$ as

$$\dot{\nu} = \frac{\sum_\ell \sum_m \left(R_\ell R_m \dot{\nu}_m \cos\nu_\ell \cos\nu_m + R_\ell R_m \dot{\nu}_\ell \sin\nu_\ell \sin\nu_m\right)}{\sum_\ell \sum_m \left[R_\ell R_m \left(\cos\nu_\ell \cos\nu_m + \sin\nu_\ell \sin\nu_m\right)\right]} \qquad 6.18$$

Due to the statistical nature of the internal wave field, the phases and phase rates of the various modes in equation 6.18 are random variables which we assume to have zero mean. If we now assume statistical independence between the phases in different modes and calculate the total mean-square phase rate, we have

$$\overline{\dot{\nu}^2} = \sum_m \overline{\dot{\nu}_m^2}\,\overline{\left(R_m^2\right)}^2 \Big/ \sum_m \overline{\left(R_m^2\right)}^2 \qquad 6.19$$

In equation 6.19 we must assume that either the modal amplitudes are statistically independent from the phase rate or the statistical average is taken over a time that is short compared to the amplitude fluctuation rate but long compared to that of the phase. Examining equation 6.19 we see that the total phase rate fluctuation is a weighted average of the component phase

rates. The term $\overline{\sum_m (R_m^2)^2}$ is a normalization factor associated with the total mean-square power in the signal. The relative contribution of each mode to the total phase rate fluctuation depends on both the phase rate for that mode as well as the power contained in the mode. The power in any given mode is a function of how strongly that mode is excited by the waveguide. For the special cases of equal phase rate fluctuation for each mode or equal power in each mode, equation 6.19 reduces to

$$\overline{\dot{\nu}^2} = \overline{\dot{\nu}_m^2} \quad .$$

Let us now discuss the two assumptions that were used to derive equation 6.19. In mathematical terms the assumption that R_m is slowly varying in comparison to ν_m implies

$$\dot{R}_m << R_m \dot{\nu}_m \quad . \qquad 6.20$$

This is essentially a weak scattering condition in that we are assuming small amplitude fluctuations for a single mode propagating through the waveguide. The condition given by 6.20 is obtained by considering the time derivative of one mode and assuming that phase fluctuations are dominant over those of amplitude. We have

$$\psi_m = R_m \exp i\nu_m$$

and

$$\dot{\psi}_m = i\dot{\nu}_m R_m \exp i\nu_m + \dot{R}_m \exp i\nu_m$$

$$= \psi_m \left[i\dot{\nu}_m + \dot{R}_m / R_m \right]$$

from which 6.20 directly follows. It is important to remember that although we assume that the rate of amplitude changes slowly for a particular mode, the total multimode amplitude can change quite rapidly due to the multimode interference. This is caused by the transformation of phase to amplitude modulated terms as was noted previously.

We have also assumed statistical independence between amplitudes and phases in the various modes while deriving equation 6.19. The internal wave induced refractive index fluctuations constitute a random variable in space and time. Since each incident mode interacts with the random field at different points in space and time, it is reasonable to expect independence between the acoustic fluctuations in different modes. We also assume that the amplitude and phase fluctuations in a given mode are statistically independent. The independence is suggested by the different type of mechanism causing the respective fluctuations. Amplitude fluctuations within a mode are caused by scattering and redistribution of energy upon encountering the inhomogeneities. This is a localized effect which occurs in the region of refractive index inhomogeneities. Phase fluctuations are due to an integrated change in travel time along the entire propagation path. The inhomogeneities cause sound speed fluctuations and subsequently travel time fluctuations for the traveling wave.

In the next section a variable sound speed waveguide will be considered which is representative of deep water acoustic propagation. Equation 6.19 will be used to obtain an estimate of the multimode phase rate fluctuations and comparisons will be made with experimental results.

7. VARIABLE SOUND SPEED WAVEGUIDE

The basic characteristics of the interaction process between acoustic and internal waves are revealed by the isospeed waveguide in the previous sections. The isospeed waveguide with a free surface and a hard bottom represents a reasonable approximation to shallow water propagation studies. In deep water propagation a waveguide is established due to the depth variation of sound speed. To first order sound speed increases linearly with temperature and pressure. As such, a minimum sound speed can be established within the water column (typically on the order of 1000 meters in the North Atlantic). The waveguide that is created is fairly weak with the minimum sound speed varying from the maximum by approximately 3%.

Because of this natural waveguide structure and the relatively small absorption of sound at low frequencies by sea water, acoustic energy can propagate for hundreds of kilometers in the ocean. The waveguide will tend to refract an acoustic wave towards the region of the sound speed minimum. Sound that encounters the sea surface or sea floor will undergo scattering and/or attenuation. It is reasonable to propose then that most of the received acoustic energy in long range studies has traveled through the water column along totally refractive paths.

It will be assumed that the waveguide is horizontally homogeneous and isotropic in the absence of internal waves. Cylindrical symmetry will be used in determining the static acoustic field. Any range dependencies for the static sound speed distribution will be neglected. The assumptions of horizontal homogeneity and isotropy will permit the internal-wave-induced sound speed fluctuations to be directly superimposed on the static sound speed profile.

With the transition from the isospeed waveguide with a free surface and a hard bottom to the variable sound speed waveguide it is necessary to consider a more realistic depth distribution of internal waves. In the isospeed waveguide we artificially lumped the acoustic effects of the internal waves in a thin layer at depth z_T. This was a convenient representation which could be employed due to the peculiarities of the isospeed waveguide. With an isospeed medium the waveguide characteristics are established as a result of the perfectly reflecting boundaries. For an acoustic wave to travel through the waveguide, it must pass through the entire width of the guide and reflect off one of the boundaries. Therefore, every mode will encounter the entire depth-distributed internal wave field whose net depth effect can be conveniently represented by a thin layer at z_T.

In the sound speed depth-dependent waveguide the representation of the internal wave field as a thin layer is not valid. The energy traveling in different modes (or rays) does not pass through the entire or identical part of the waveguide. Since the intensity of the induced refractive index fluctuation varies with depth, we would expect the magnitude of the acoustic fluctuations to be different in each mode.

The internal wave model in section 2 represented the induced refractive index fluctuations σ as a random variable which is horizontally homogeneous and isotropic and temporally stationary. In the vertical direction σ fluctuates rapidly and randomly due to the relatively short vertical wavelength and the small vertical correlation scales of the internal wave field. We are then able to smooth the refractive index fluctuations over depth by using its root-mean-square behavior while leaving intact the horizontal and slowly varying depth dependencies. The justification for this smoothing

procedure is that the vertical internal wavenumbers are significantly larger than horizontal ones at a given frequency due to the anisotropy of the oceans. From equation 2.14 the rms depth dependency of σ was found to be proportional to $N^{3/2}$ where N is the local Brunt-Väisälä frequency. Using the Garrett and Munk exponentially decaying profile $N(z) = N_o \exp(-z/B)$ where B is a scale depth and z is positive downwards, we find that

$$\overline{\sigma^2}^{1/2} \propto \exp(-3z/2B) .$$

This is a fairly reasonable representation for the actual depth variation of the refractive index fluctuations, and we shall use it in the subsequent analysis.

In determining the acoustic fluctuations resulting from the interaction of the internal wave field with one incident mode in the depth-dependent sound speed waveguide, we shall follow the same general procedure as in the isospeed waveguide. The important differences to recognize are that both the static sound speed profile and the internal wave field possess depth dependencies and that the waveguide traps energy without reflection off the boundaries.

The Green's function in a cylindrically symmetric waveguide with a CW point source at r_o, z_o is given by equation 5.2

$$G(r,z|r_0,z_0) = \frac{i}{4} \sum_n h_n(z) h_n(z_0) H_0^{(1)}[\alpha_n |r-r_0|] \qquad 7.1$$

where $h_n(z)$ is an orthonormal eigenfunction with eigenvalue α_n. If we assume that the eigenfunctions are not orthonormal but only orthogonal, the Green's function becomes

$$G(r,z|r_0,z_0) = \frac{i}{4} \sum_n d_n(z) d_n(z_0) \nu_n^{-1} H_0^{(1)}[\alpha_n |r - r_0|] \qquad 7.2$$

where $d_n(z)$ is an orthogonal eigenfunction and

ν_n is a normalization factor $= \int_{-\infty}^{\infty} d_n^2(z)\,dz$.

The zero order or static solution $\psi_o(r,z)$ is found by assuming a source located at $r_o = 0$, $z_o = z_s$ so that

$$\psi_0(r,z) = \frac{i}{4} \sum_m d_m(z)\, d_m(z_s)\, \nu_m^{-1} H_0^{(1)}(\alpha_m r) \quad . \qquad 7.3$$

We wish to determine the acoustic fluctuations for a single mode m. The eigenfunction $d_m(z)$ creates a standing wave pattern in the z direction. Separating $d_m(z)$ into upward and downward traveling waves $d_m'(z)$ and $d_m''(z)$, we can apply equation 5.4 where

$$\psi_{om}'(r,z) = \frac{i}{4}\, d_m(z_s)\, \nu_m^{-1}\, d_m'(z)\, H_0^{(1)}(\alpha_m r)$$

and $$\psi_{om}''(r,z) = \frac{i}{4}\, d_m(z_s)\, \nu_m^{-1}\, d_m''(z)\, H_0^{(1)}(\alpha_m r) \quad . \qquad 7.4$$

Each of the traveling waves causes scattered waves to be created in the waveguide. For the scattered waves to travel to long distances they must be trapped by the waveguide as modes. The same wave trapping condition exists for all modes in the waveguide, so that the Green's function for W_m' and W_m'' are identical and are given by equation 7.2. Recalling that $p_m' = W_m'/\psi_{om}'$ and $p_m'' = W_m''/\psi_{om}''$, we can then write

$$P_m'(r,z,t) = 2K_0^2 \iint_{r_0 z_0} dr_0\, dz_0\, n_0(z_0)\, \sigma(r_0,z_0,t)\, G(r,z|r_0,z_0)\, \psi_{0m}'(r_0,z_0) \Big/ \psi_{0m}'(r,z)$$

7.5

$$\text{and} \quad P_m''(r,z,t) = 2K_0^2 \iint_{r_0 z_0} dr_0\, dz_0\, n_0(z_0)\, \sigma(r_0,z_0,t)\, G(r,z|r_0,z_0)\, \psi_{0m}''(r_0,z_0) \Big/ \psi_{0m}''(r,z).$$

The total field due to incident mode m is then

$$\psi_m(r,z,t) = \psi_{0m}' \exp(P_m') + \psi_{0m}'' \exp(P_m'')$$

$$= \frac{i}{4}\, d_m(z_s)\, \nu_m^{-1}\, H_0^{(1)}(\alpha_m r) \left\{ d_m' e^{P_m'} + d_m'' e^{P_m''} \right\}. \qquad 7.6$$

In equation 7.5 the limits of integration on r_o and z_o have been deliberately left indefinite. If we consider only forward scattering, the limits of integration should be 0 to r. If backscattering is included in the analysis, the integration limits will be $-\infty$ to $+\infty$. The limits of integration on z_o are more subtle and will shortly be discussed in some detail.

In proceeding from equation 7.6 it becomes necessary to use a specific form for the eigenfunction $d_m(z)$ and its components $d_m'(z)$ and $d_m''(z)$. The exact form of the eigenfunction is dependent upon the nature of the static sound speed profile. We recall that the eigenfunctions satisfy the Helmholtz equation

$$\frac{d^2}{dz^2}\left[d_m(z)\right] + \gamma_m^2 d_m = 0 \qquad 7.7$$

where $\gamma_m(z)$ is the vertical wavenumber = $\left[k_o^2 n_o^2(z) - \alpha_m^2\right]^{1/2}$.
Exact solutions to equation 7.7 have been found for only several specific forms of $\gamma_m(z)$. With an arbitrary sound speed profile $n_o(z)$, an approximate solution to equation 7.7 must be used. The most commonly used approximation (and the one which will be used here) is known as the WKB (Wentzel, Kramers, Brillouin) solution. An n_o^2-bilinear sound speed profile will be used to obtain numerical results. With an appropriate choice of coefficients this profile can give an adequate representation for the sound speed distribution in deep water. In addition it allows eigenvalues to be easily determined and the exact eigenfunction solution is known. This will then permit us to determine the validity of the WKB solution and to obtain an estimate of the inherent error.

The WKB approximation to the Helmholtz equation is known also in the literature as the phase-integral method. It has been shown to be the first term in an asymptotic expansion to the exact solution (Bremmer, 1951). The relationship between ray theory and WKB mode theory is quite close. Tindle and Guthrie (1974) has used the WKB approximation to show that ray effects are due to the constructive interference of neighboring normal modes. The WKB approximation is also used as a method of modifying ray theory to include phase information. The general WKB solution to equation 7.7 has the form

$$d_m(z) = \gamma_m^{-1/2}(z)\left\{C_1 \exp\left[i\int_{z'}^{z}\gamma_m\,dz\right] + C_2 \exp\left[-i\int_{z'}^{z}\gamma_m\,dz\right]\right\} \qquad 7.8$$

where C_1, C_2, and z' are constants, two of which are independent. The phase integral $\int_{z'}^{z}\gamma_m\,dz$ represents the change in phase for a wave traveling from an arbitrary point z' to point z. From equation 7.8 we see that the

WKB approximation yields upward and downward going traveling waves for the eigenfunctions. This type of solution can then be directly applied to equations 7.4 - 7.6.

Although the WKB approximation is a wave-type solution, it suffers from many of the same limitations as in ray theory. The WKB solution is applicable as long as the physical properties of the medium do not change appreciably over a vertical wavelength. In mathematical terms this implies that (Tolstoy and Clay, 1966)

$$\gamma^{-1} \left| \frac{d}{dz} (\ln \gamma) \right| << 1 \quad . \qquad 7.9$$

From this relation and equation 7.8 it is immediately evident that the WKB solution diverges near a turning point, i.e. where $\gamma = 0$. On the other hand, exact solutions to the Helmholtz equation exhibit no unusual characteristics near $\gamma = 0$. Examining equation 7.7 we see that the turning point marks the transition from a region of oscillating solutions ($\gamma^2 > 0$) to exponential ones ($\gamma^2 < 0$).

The failure of the WKB approximation near the turning point can also be understood on physical grounds. The WKB solution is equivalent to assuming that total reflection takes place at the turning points while refraction occurs elsewhere. The depth-dependent sound speed is assumed solely to cause a change in phase along the transmission path. WKB theory neglects the continuous reflection or backscatter that also occurs, an assumption which is valid provided the parameters of the medium vary little over a vertical wavelength. Near the turning point the vertical wavelength becomes very large, so that backscatter is no longer small and cannot be neglected. This results in the divergence of the WKB amplitude term while the phase part of

the solution remains finite. Examination of the exact solution near the turning point indicates that a $-\pi/2$ phase shift occurs upon total reflection at the turning point (Tolstoy, 1968). This phase shift must then be superimposed on the WKB phase term when a turning point is encountered.

The characteristic equation in the variable sound speed waveguide can be obtained from the resonance condition that a wave traveling an entire cycle in the z direction must advance in phase by 2π radians to remain in phase. Using the phase integral we have

$$\int_{z_\ell}^{z_u} \gamma_m \, dz = \left(m + \tfrac{1}{2}\right)\pi \quad \text{for} \quad m = 0, 1, 2, \ldots \qquad 7.10$$

where z_u, z_ℓ are the upper and lower turning points, respectively, for mode m. Referencing the integrals to the upper and lower turning points and incorporating the constants into the normalization factor, the WKB solution becomes (Furry, 1947; Carter, 1963; Porter, 1973)

$$d_m(z) = \begin{cases} (-1)^m \tfrac{1}{2} |\gamma_m|^{-1/2} \exp\left[-\int_z^{z_\ell} |\gamma_m| \, dz\right] & , \; z > z_\ell \\ \gamma_m^{-1/2} \cos\left[\int_z^{z_u} \gamma_m \, dz - \frac{\pi}{4}\right] & , \; z_\ell > z > z_u \\ \tfrac{1}{2} |\gamma_m|^{-1/2} \exp\left[-\int_{z_u}^{z} |\gamma_m| \, dz\right] & , \; z < z_u \end{cases} \qquad 7.11$$

We have taken $z = 0$ at the surface and have measured z positive downwards. The normalization factor ν_m can then be approximated by

$$\nu_m \approx \frac{1}{2} \int_{z_\ell}^{z_u} \gamma_m^{-1}(z)\, dz \qquad 7.12$$

The solutions given by equation 7.11 are good approximations when z is well away from the turning points. Since the solutions are exponentially decaying outside the turning points, we can roughly assume that $d_m(z) = 0$ for $z > z_\ell$ and $z < z_u$. The amplitude of the oscillatory solution diverges as z approaches a turning point. By examining the exact solution in this region we can place a bound on $\gamma_m^{-\frac{1}{2}}$ and assume that the phase part of the solution remains valid.

Let us now reconsider equation 7.6 using the WKB solutions discussed above. We will use the shorthand notation

$$\theta_m(z_u, z) = \int_z^{z_u} \gamma_m\, dz \,.$$

The expressions for $d_m(z)$, $d_m'(z)$, and $d_m''(z)$ can immediately be recognized:

$$d_m(z) = \gamma_m^{-1/2}(z) \cos\left[\theta_m(z_u, z) - \frac{\pi}{4}\right]$$

$$d_m'(z) = \frac{1}{2}\gamma_m^{-1/2}(z) \exp i\left[\theta_m(z_u, z) - \frac{\pi}{4}\right] \qquad 7.13$$

and $$d_m''(z) = \frac{1}{2}\gamma_m^{-1/2}(z) \exp -i\left[\theta_m(z_u, z) - \frac{\pi}{4}\right] .$$

The expressions in equation 7.13 are assumed to be valid for $z_\ell > z > z_u$ and equal to zero outside these limits. With these expressions equation 7.4 becomes

$$\psi_{om}'(r,z) = \frac{i\cos\varepsilon_m(z_s)}{8\nu_m\gamma_m^{1/2}(z)\gamma_m^{1/2}(z_s)}\, H_0^{(1)}(\alpha_m r)\exp i\varepsilon_m(z) \qquad 7.14$$

and

$$\psi_{om}''(r,z) = \frac{i\cos\varepsilon_m(z_s)}{8\nu_m\gamma_m^{1/2}(z)\gamma_m^{1/2}(z_s)}\, H_0^{(1)}(\alpha_m r)\exp -i\varepsilon_m(z)$$

where

$$\varepsilon_m(z) = \left[\theta_m(z_u,z) - \frac{\pi}{4}\right].$$

The Green's function of equation 7.2 with the WKB approximation is

$$G(r,z\,|\,r_0,z_0) = \frac{i}{4}\sum_{n=0}^{\infty}\frac{\cos\varepsilon_n(z)\cos\varepsilon_n(z_0)}{\nu_n\gamma_n^{1/2}(z_0)\gamma_n^{1/2}(z)}\, H_0^{(1)}\left[\alpha_n|r-r_0|\right] \qquad 7.15$$

The expressions for p_m' and p_m'' (equation 7.5) are

$$P_m'(r,z,t) = \frac{iK_0^2}{2}\sum_{n=0}^{\infty}\frac{\gamma_m^{1/2}(z)\cos\varepsilon_n(z)}{\gamma_n^{1/2}(z)\,\nu_n}\iint_{r_0 z_0} dr_0 dz_0\, f_{mn1}(z_0)\,F_{mn}(r_0)\,\sigma(r_0,z_0,t) \qquad 7.16$$

and

$$P_m''(r,z,t) = \frac{iK_0^2}{2}\sum_{n=0}^{\infty}\frac{\gamma_m^{1/2}(z)\cos\varepsilon_n(z)}{\gamma_n^{1/2}(z)\,\nu_n}\iint_{r_0 z_0} dr_0 dz_0\, f_{mn2}(z_0)\,F_{mn}(r_0)\,\sigma(r_0,z_0,t)$$

where $$f_{mn1}(z_0) = \frac{n_0(z_0)\cos\varepsilon_n(z_0)}{\gamma_m^{1/2}(z_0)\gamma_n^{1/2}(z_0)} \exp i\left[\varepsilon_m(z_0) - \varepsilon_m(z)\right]$$

$$f_{mn2}(z_0) = \frac{n_0(z_0)\cos\varepsilon_n(z_0)}{\gamma_m^{1/2}(z_0)\gamma_n^{1/2}(z_0)} \exp -i\left[\varepsilon_m(z_0) - \varepsilon_m(z)\right]$$

and $$F_{mn}(r_0) = H_0^{(1)}(\alpha_m r_0)\, H_0^{(1)}\left[\alpha_n |r - r_0|\right] \Big/ H_0^{(1)}(\alpha_m r).$$

Substituting equations 7.13 and 7.16 into 7.6, we have

$$\psi_m(r,z,t) = \frac{i\cos\varepsilon_m(z_s)\, H_0^{(1)}(\alpha_m r)}{4\nu_m \gamma_m^{1/2}(z_s)\gamma_m^{1/2}(z)} \cos\left\{\varepsilon_m(z) + \right.$$

$$\left. \frac{K_0^2}{4}\sum_{n=0}^{\infty} \frac{\gamma_m^{1/2}(z)\cos\varepsilon_n(z)}{\gamma_n^{1/2}(z)\,\nu_n} \iint_{r_0 z_0} dr_0 dz_0\, \sigma F_{mn}(r_0)\left[f_{mn1}(z_0) - f_{mn2}(z_0)\right]\right\}$$

$$\cdot \exp i\left\{\frac{K_0^2}{4}\sum_{n=0}^{\infty} \frac{\gamma_m^{1/2}(z)\cos\varepsilon_n(z)}{\gamma_n^{1/2}(z)\,\nu_n} \iint_{r_0 z_0} dr_0 dz_0\, \sigma F_{mn}(r_0)\left[f_{mn1}(z_0) + f_{mn2}(z_0)\right]\right\} \quad 7.17$$

where we have used the trigonometric identity

$$e^{iA} + e^{iB} = 2\cos\left[\tfrac{1}{2}(A-B)\right] \exp i\left[\tfrac{1}{2}(A+B)\right].$$

The expression given in equation 7.17 is very similar to the corresponding expression (equation 5.7) in the isospeed waveguide. The eigenfunctions are

modified as an amplitude fluctuation and the phase fluctuation S_m is

$$S_m(r,z,t) = \sum_{n=0}^{\infty} B_{mn}(z) \iint_{r_0 z_0} dr_0\, dz_0\, F_{mn}(r_0)\, D_{mn}(z_0)\, \sigma(r_0, z_0, t) \qquad 7.18$$

where $$B_{mn}(z) = \frac{K_0^2\, \gamma_m^{1/2}(z) \cos \varepsilon_n(z)}{2\, \gamma_n^{1/2}(z)\, \nu_n}$$

and $$D_{mn}(z_0) = \frac{\eta_0(z_0) \cos \varepsilon_n(z_0)}{\gamma_m^{1/2}(z_0)\, \gamma_n^{1/2}(z_0)} \cos\left[\theta_m(z_u, z_0) - \theta_m(z_u, z)\right] .$$

Comparing equations 5.7 and 7.18, we can notice that the horizontal range dependences are identical for both expressions. The asymptotic expansions of equations 5.10 and 5.11 can again be used and the analysis for the horizontal fluctuations can proceed in an identical manner. The dominant terms in the summation will again occur when $n \approx m$ and the interaction process will select those internal waves whose wavenumber projection upon the transmission path is equal to the difference between the wavenumbers of a scattered and incident wave.

The condition that $\alpha_x = |\alpha_m - \alpha_n|$ has the same physical interpretation in terms of ray theory in the variable sound speed channel as it does in the isospeed waveguide. As in section 5, we shall assume that $n \approx m$. The ray cycle length $h(\phi_o)$ is given by

$$h(\phi_o) = 2 \int_{z_\ell}^{z_u} \frac{\partial \chi}{\partial z}\, dz = 2 \int_{z_\ell}^{z_u} \cos \phi_o \Big/ \left[n_0^2(z) - \cos^2 \phi_o\right]^{1/2} dz \qquad 7.19$$

where ϕ_o is the ray angle at $c = c_0$.

Defining $\rho(\phi_o)$ as $\int_{z_\ell}^{z_u} [n_o^2(z) - \cos^2\phi_o]^{1/2} dz$,

we can write the resonance condition

$$\int_{z_\ell}^{z_u} \gamma_m dz = (m+\tfrac{1}{2})\pi \quad \text{as}$$

$$(m+\tfrac{1}{2})\pi = K_{om}\,\rho(\phi_{om}) = \frac{\omega_m}{c_o}\,\rho(\phi_{om}) \,. \qquad 7.20$$

Differentiating 7.20 with respect to ω, we have

$$\frac{d}{d\omega}\left[\frac{\omega}{c_o}\,\rho(\phi_o)\right] = \frac{\rho(\phi_o)}{c_o} + \frac{\omega}{c_o}\,\frac{\partial\rho}{\partial\phi_o}\,\frac{d\phi_o}{d\omega} = 0 \qquad 7.21$$

where $\dfrac{\partial\rho}{\partial\phi_o} = \int_{z_\ell}^{z_u} \cos\phi_o \sin\phi_o \left[n_o^2(z) - \cos^2\phi_o\right]^{-1/2} dz = \frac{1}{2}\sin\phi_o\, h(\phi_o)$.

Substituting this expression into 7.21, we have

$$-\frac{d\omega}{\omega} = \frac{h(\phi_o)}{2\rho(\phi_o)}\sin\phi_o\, d\phi_o \,. \qquad 7.22$$

If we now integrate equation 7.22 while requiring $n \approx m$ so that $\beta(\phi_o)$ and $h(\phi_o)$ are approximately constant, we have

$$\ln\frac{\omega_n}{\omega_m} = \frac{h(\phi_{om})}{2\rho(\phi_{om})}\left[\cos\phi_{on} - \cos\phi_{om}\right] \qquad 7.23$$

Now taking $\omega_n \approx \omega_m$ and $\phi_{on} \approx \phi_{om}$, equation 7.23 can be approximated as

$$\omega_n - \omega_m = \frac{\omega_m h(\phi_{om})}{2\rho(\phi_{om})} \left[\phi_{om} - \phi_{on}\right] \sin\phi_{om} \quad . \qquad 7.24$$

Noting that equation 7.20 gives

$$\omega_n - \omega_m = \frac{c_o}{\beta(\phi_{om})} (n-m)\pi \quad , \qquad 7.25$$

the relationship for cycle length becomes

$$h(\phi_{om}) = \frac{2\pi(n-m)}{K_o(\phi_{om} - \phi_{on})\sin\phi_{om}} \quad . \qquad 7.26$$

Considering the quantity $|\alpha_m - \alpha_n|$, we have

$$|\alpha_m - \alpha_n| = K_o\left|\cos\phi_{om} - \cos\phi_{on}\right| \approx K_o\left|(\phi_{on} - \phi_{om})\sin\phi_{om}\right| \quad . \qquad 7.27$$

The projection of the internal-wave wavelength is given by

$$\lambda_x = \frac{2\pi}{\alpha_x} = \frac{2\pi}{|\alpha_m - \alpha_n|} \approx \frac{2\pi}{K_o\left|(\phi_{on} - \phi_{om})\sin\phi_{om}\right|} \quad . \qquad 7.28$$

Comparing equations 7.26 and 7.28, we see that the interaction process tends to select those internal waves whose wavelength projection along the transmission path is an integral fraction of the ray cycle length.

In section 6 we discussed the non-linearities inherent to the phase and amplitude fluctuations due to the multimode structure of the received signal. It was apparent that the relationship between the induced refractive index

fluctuations and the acoustic fluctuations was quite complicated. Examination of the phase rate fluctuation revealed that it could be expressed as a weighted average of the phase rate fluctuation in each mode. Each of these modal phase rate fluctuations could be related to the internal wave fluctuations. In the discussion that follows we shall then determine the modal phase rate fluctuation $\dot{S}_m$ in a variable sound speed waveguide.

From equation 7.18 we can write

$$\dot{S}_m(r,z,t) = \sum_{n=0}^{\infty} B_{mn}(z) \iint_{r_0 z_0} dr_0\, dz_0\, F_{mn}(r_0) D_{mn}(z_0)\, \dot{\sigma}(r_0, z_0, t) \qquad 7.29$$

where $F_{mn}(r_o)$ is expressed by equation 7.16, and $B_{mn}(z)$ and $D_{mn}(z_o)$ are given by equation 7.18. In determining various statistical quantities such as the root mean square phase rate, we shall introduce several approximations and expansions for computational convenience. Except for a first order expansion on the exponential term of $F_{mn}(r_o)$, all the approximations are taken on the coefficients of $B_{mn}(z)$ and $D_{mn}(z_o)$. For numerical calculations we shall use an asymmetric n_o^2 -bilinear sound speed profile which is representative for North Atlantic water. This will permit a comparison to be made with experimental acoustic fluctuation data and previous theoretical calculations. The n_o^2 -bilinear profile also enables eigenvalues to be easily calculated. In addition exact eigenfunction solutions are known (in terms of Airy functions) so that the amount of error introduced by the WKB approximation can be determined.

Let us now examine the various terms in equation 7.29 and discuss the approximations we shall use in determining the rms phase rate fluctuation.

The expressions for $B_{mn}(z)$ and $D_{mn}(z_o)$ are

$$B_{mn}(z) = \frac{K_o^2 \gamma_m^{1/2}(z) \cos \varepsilon_n(z)}{2 \gamma_n^{1/2}(z) \nu_n}$$

and

$$D_{mn}(z_o) = \frac{n_o(z_o) \cos \varepsilon_n(z_o)}{\gamma_m^{1/2}(z_o) \gamma_n^{1/2}(z_o)} \cos\left[\theta_m(z_u, z_o) - \theta_m(z_u, z)\right] .$$

From the definition of θ_m we can immediately write

$$\cos\left[\theta_m(z_u, z_o) - \theta_m(z_u, z)\right] = \cos\left[\theta_m(z, z_o)\right] .$$

For a typical sound speed profile the index of refraction n_o will vary by only 3 percent over the entire water column. We shall then assume n_o to be a constant, denote it by $\bar{n}_o$, and remove it from the integral over z_o. Using the condition that the dominant terms in the summation are those where $n \approx m$, we can take

$$\gamma_n^{1/2}(z) \approx \gamma_m^{1/2}(z) \quad \text{so that}$$

$$\gamma_m^{1/2}(z) / \gamma_n^{1/2}(z) \approx 1 .$$

The product of $\gamma_m^{\frac{1}{2}}(z_o)\gamma_n^{\frac{1}{2}}(z_o)$ in the denominator of $D_{mn}(z)$ arises from the use of the WKB approximation and gives the eigenfunction amplitudes. It was previously mentioned that the WKB solution diverges near a turning point, that is where $\gamma_m^2 = 0$. If we examine the exact eigenfunction solution for the n_o^2 -bilinear profile, we notice that the behavior of the Airy function

(which is shown below) remains finite in the region near $\gamma_m^2 = 0$

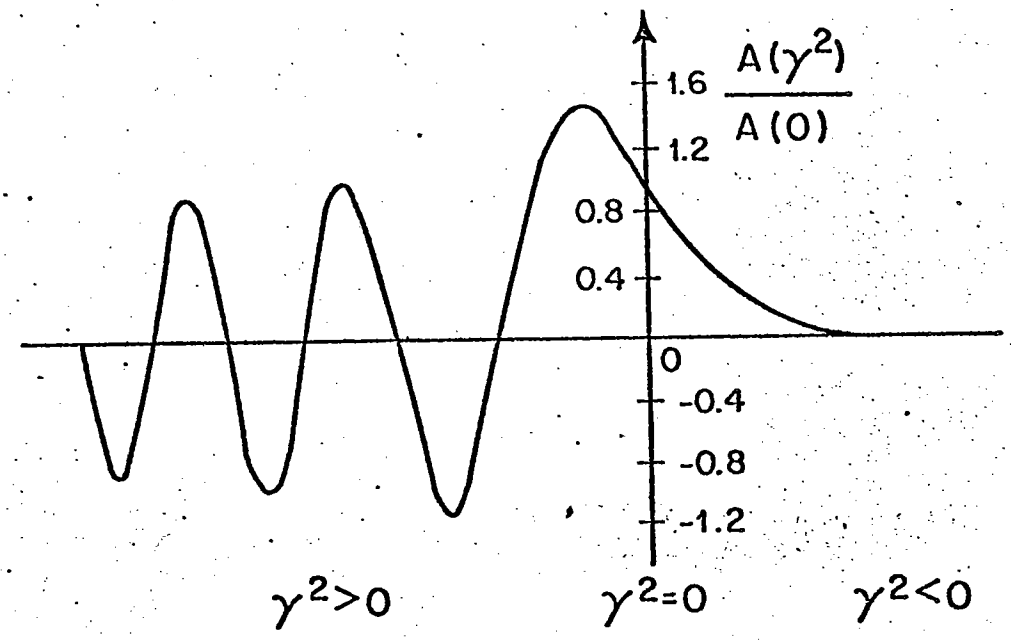

Figure 7: Airy Function behavior in region near the turning point.

As we approach the turning point from the oscillatory region the amplitude increases slightly. In the WKB solution (equation 7.11) this increase in amplitude is caused by the $\gamma_m^{-\frac{1}{2}}$ term. Close to the turning point the WKB solution indicates that the eigenfunction amplitude will rapidly increase and become infinite at $\gamma_m = 0$. On the other hand the exact solution reveals an amplitude maximum and an exponential decrease as the turning point is approached. We shall use the following scheme to approximate the eigenfunction amplitudes. The actual values of $\gamma_m^{\frac{1}{2}}(z_o)$ and $\gamma_n^{\frac{1}{2}}(z_o)$ in the denominator of

$D_{mn}(z_o)$ will be used if the condition

$$\left| \int_{z'}^{z_u, z_\ell} \gamma \, dz \right| > 2$$

is satisfied (Porter and Leslie, 1975). When this expression is not satisfied (implying z' is close to one of the turning points), we shall use a constant value for $\gamma^{-\frac{1}{2}}(z_o)$ throughout the region between z' and the turning point. It is important to note that while the above approximate procedure is used to calculate the eigenfunction amplitude, the actual depth variations of γ_m and γ_n are used in the sinusoidal terms since they remain finite. The approximate expressions for $B_{mn}(z)$ and $D_{mn}(z_o)$ are now

$$B_{mn}(z) \approx \left(K_o^2 / 2\nu_n\right) \cos\left[\theta_n(z_u, z) - \pi/4\right]$$

7.30

and $$D_{mn}(z_o) \approx \bar{n}_o \gamma_m^{-1/2}(z_o) \gamma_n^{-1/2}(z_o) \cos\left[\theta_n(z_u, z_o) - \frac{\pi}{4}\right] \cos\left[\theta_m(z, z_o)\right] .$$

Substituting these expressions in equation 7.29, we have

$$\dot{S}_m(r, z, t) \approx \sum_{n=0}^{\infty} \left(K_o^2 \bar{n}_o / 2\nu_n\right) \cos\left[\theta_n(z_u, z) - \pi/4\right] \cdot$$

$$\iint_{r_o z_o} dr_o \, dz_o \, F_{mn}(r_o) \, \dot{\delta}(r_o, z_o, t) \, \frac{\cos \varepsilon_n(z_o) \cos\left[\theta_m(z, z_o)\right]}{\gamma_m^{1/2}(z_o) \, \gamma_n^{1/2}(z_o)} \quad . \qquad 7.31$$

In order to calculate the rms phase rate fluctuation, we must square equation 7.31, average the result, and take the square root. We shall assume the internal wave field to be horizontally isotropic and shall use the rms

behavior of the refractive index fluctuations in the vertical direction. Because the magnitude of the mean-square refractive index fluctuations is proportional to $N^3(z)$, most of the acoustic phase rate fluctuations will occur in shallow water where N(z) is greatest. We shall use an internal wave vertical correlation scale of 100 meters which is typical in shallow water (Munk and Zachariasen, 1976). If we let

$$L_{mn}(r, z_0, t) \equiv \int_{r_0} dr_0 \, F_{mn}(r_0) \, \dot{\delta}(r_0, z_0, t)$$

then $\overline{L_{mn}^2}$ can be determined by the procedure described from equation 5.9 to equation 5.25. We can therefore express $\overline{L_{mn}^2}$ as

$$\overline{L_{mn}^2} = \frac{8\pi\chi}{\alpha_n \alpha_m} \int_{-\infty}^{\infty}\int\int\int d\alpha_x \, d\alpha_y \, d\omega \, F_{\dot{\delta}}(\alpha_x, \alpha_y, \omega) \, \delta(\alpha_x + \alpha_m - \alpha_n) \qquad 7.32$$

where $F_{\dot{\delta}}(\alpha_x, \alpha_y, \omega, z) = \omega^2 F_{\delta}(\alpha_x, \alpha_y, \omega, z)$.

Applying the condition of horizontal isotropy we can write

$$\overline{L_{mn}^2} = \frac{8\chi}{\alpha_n \alpha_m} \int_{-\infty}^{\infty} d\omega \int_0^{\infty} d\alpha \, \frac{F_{\dot{\delta}}(\alpha, \omega, z)}{(\alpha^2 - \Delta^2)^{1/2}} \qquad 7.33$$

To proceed further we must substitute a specific form for the spectral density $F_{\dot{\sigma}}(\alpha, \omega, z)$. For convenience we shall use the GM72 form of $F_{\dot{\sigma}}(\alpha, \omega, z)$, so that from equation 2.18 we have

$$F_{\dot{\delta}72}(\alpha, \omega) = \frac{4\varepsilon B^3 N_0^2 \omega_i \mu^2 N^3}{j\pi q^2 \omega} \qquad 7.34$$

The substitution of equation 7.34 into equation 7.33 permits us to determine the mean-square phase rate fluctuation. We now have

$$\overline{L_{mn}^2} = \frac{32\chi B^3 E \mu^2 N^3 N_0^2 \omega_i}{\pi j g^2 \alpha_n \alpha_m} \int_{\omega_i}^{N} \frac{d\omega}{\omega} \int_{\Delta}^{j\alpha^{(1)}} \frac{d\alpha}{(\alpha^2 - \Delta^2)^{1/2}} \quad . \qquad 7.35$$

In equation 7.35 the lower limit of integration on α has been replaced by Δ, since α must be $\geq \Delta$ for real internal waves to contribute to the acoustic fluctuation. We must similarly replace the lower limit of integration on ω by ω_Δ, where the dispersion relation gives

$$\omega_\Delta = \left\{ \omega_i^2 + \left(\frac{2BN_0\Delta}{j} \right)^2 \right\}^{1/2} \quad . \qquad 7.36$$

The physical interpretation for these changes in the limits of integration is shown in the figure below [adapted from Garrett and Munk (1972, Fig. 7)].

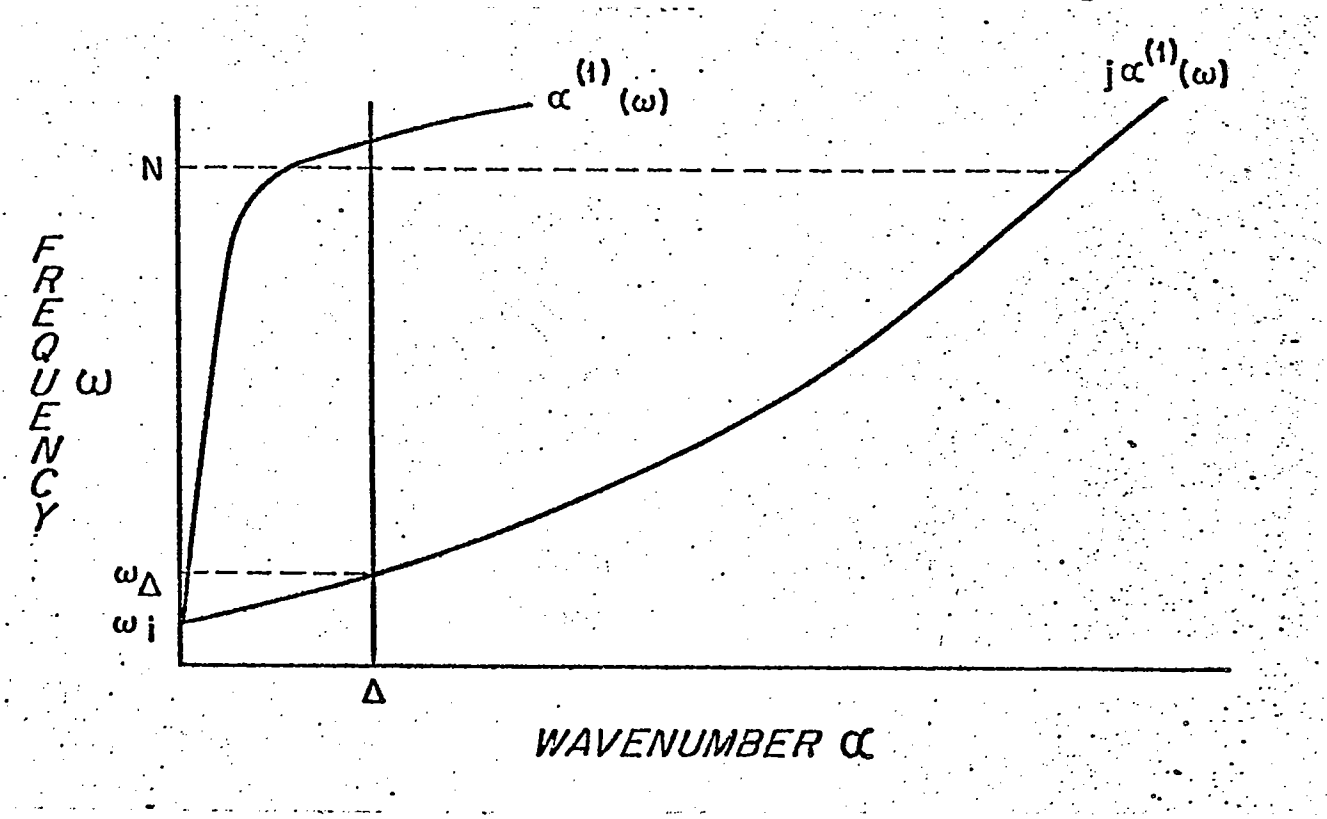

Figure 8: Region of integration in frequency-wavenumber space for equation 7.35.

The integral over α within equation 7.35 can be evaluated analytically so that

$$\int_{\Delta}^{j\alpha^{(1)}} \frac{d\alpha}{(\alpha^2-\Delta^2)^{1/2}} = \ln\left\{\frac{j\alpha^{(1)}+\sqrt{[j\alpha^{(1)}]^2-\Delta^2}}{\Delta}\right\} = \text{Cosh}^{-1}\frac{j\alpha^{(1)}}{\Delta} \quad . \qquad 7.37$$

Equation 7.35 can now be written as

$$\overline{L_{mn}^2} = \frac{QN^3}{\alpha_n}\int_{\omega_\Delta}^{N} d\omega\, \omega^{-1}\,\text{Cosh}^{-1}\frac{j\alpha^{(1)}}{\Delta} \qquad 7.38$$

where $$j\alpha^{(1)} = \frac{j(\omega^2-\omega_i^2)^{1/2}}{2BN_0}$$

and $$Q = \frac{32\chi B^3 E\mu^2 N_0^2 \omega_i}{\pi j g^2 \alpha_m} \quad .$$

We must now consider the integral

$$\int_{\omega_\Delta}^{N} d\omega\, \omega^{-1}\,\text{Cosh}^{-1}\frac{j\alpha^{(1)}}{\Delta} \quad .$$

We notice from equation 7.36 that ω_Δ is always greater than ω_i . Since the lower limit of integration is ω_Δ , we shall approximate $j\alpha^{(1)}$ over the entire integration region by

$$j\alpha^{(1)} = j\omega/2BN_0 \quad .$$

The ω integral can now be written as

$$\int_{\omega_\Delta}^{N} d\omega\, \omega^{-1}\,\text{Cosh}^{-1}\frac{\omega}{a}$$

where $$a = 2BN_0\Delta/j = \left(\omega_\Delta^2 - \omega_i^2\right)^{1/2} .$$

This integral has been evaluated (Dwight, 1961, p. 171) so that

$$\int_{\omega_\Delta}^{N} d\omega\, \omega^{-1}\, \mathrm{Cosh}^{-1}\frac{\omega}{a}\, d\omega =$$

$$\frac{1}{2}\left[\ln\frac{2\omega}{a}\right]^2 + \frac{1}{2^3}\frac{a^2}{\omega^2} + \frac{1\cdot 3\, a^4}{2\cdot 4^3\omega^4} + \ldots \Bigg|_{\omega_\Delta}^{N} . \qquad 7.39$$

Since a is always less than ω, we shall retain the first two terms in the summation. Equation 7.38 now becomes

$$\overline{L_{mn}^2} = \frac{QN^3}{2\alpha_n}\left\{\left[\ln\frac{jN}{BN_0\Delta}\right]^2 - \left[\ln\frac{j\omega_a}{BN_0\Delta}\right]^2 + \left[\frac{BN_0\Delta}{j}\right]^2\left[\frac{1}{N^2} - \frac{1}{\omega_a^2}\right]\right\} . \qquad 7.40$$

Assuming uncorrelated scattered cross-mode terms, we can now write the mean-square phase rate fluctuation as

$$\overline{\dot{S}_m^2} = \frac{Q}{2}\sum_{n=0}^{\infty}\frac{K_0^4\,\bar{n}_0^2\cos^2\varepsilon_n(z)}{4\alpha_n\nu_n^2} \cdot$$

$$\iint_{z_0 z_1} dz_0\, dz_1\, N^3(z_3)\, L(z_3)\rho_0(z_2)\, \frac{M_{mn}(z_0)M_{mn}(z_1)}{\gamma_m^{1/2}(z_0)\gamma_m^{1/2}(z_1)\gamma_n^{1/2}(z_0)\gamma_n^{1/2}(z_1)} . \qquad 7.41$$

In equation 7.41 we have let

$$z_2 = z_0 - z_1 \quad , \quad z_3 = \frac{1}{2}\left(z_0 + z_1\right) ,$$

$$L(z_3) = \left[\ln \frac{jN}{BN_0\Delta}\right]^2 - \left[\ln \frac{j\omega_\Delta}{BN_0\Delta}\right]^2 + \left[\frac{BN_0\Delta}{j}\right]\left[\frac{1}{N^2} - \frac{1}{\omega_\Delta^2}\right],$$

and $$M_{mn}(z_0) = \cos \mathcal{E}_n(z_0) \cos\left[\theta_m(z, z_0)\right] .$$

We shall now introduce a correlation function of the form

$$\rho_{\dot{\sigma}}(z_2) = \exp\left[-z_2^2/\ell_z^2\right] \qquad 7.42$$

where ℓ_z is the vertical correlation scale.

Equation 7.42 is not meant to model precisely the vertical fluctuations of internal waves, but rather it allows a reasonable model for the internal wave fluctuations which can be easily integrated.

Let us change the integration variables from z_0, z_1 to z_2, z_3. The integration limits on z_2 can be extended to $\pm \infty$ without contributing a significant error, since ℓ_z is much less than the width of the waveguide (the distance between the upper and lower turning points) for all but the lowest order modes. Using trigonometric identities we can write $M_{mn}(z_0)M_{mn}(z_1)$ as

$$M_{mn}(z_0)M_{mn}(z_1) = \frac{1}{4}\left\{\cos \theta_n(z_1, z_0) + \sin\left[\theta_n(z_u, z_0) + \theta_n(z_u, z_1)\right]\right\}$$

$$\cdot \left\{\cos \theta_m(z_1, z_0) + \cos\left[\theta_m(z, z_0) + \theta_m(z, z_1)\right]\right\} , \qquad 7.43$$

Since most of the contribution to the integral over z_2 occurs for small z_2, we can simplify equation 7.43 to

$$M_{mn}(z_0)\,M_{mn}(z_1) \approx \frac{1}{4}\Big\{\cos\gamma_n z_2 \cos\gamma_m z_2 + \cos\gamma_n z_2 \cos\big[2\theta_m(z,z_3)\big] + \cos\gamma_m z_2 \sin\big[2\theta_n(z_u,z_3)\big] + \sin\big[2\theta_n(z_u,z_3)\big]\cos\big[2\theta_m(z,z_3)\big]\Big\}.$$

We can also use the same argument to write

$$\gamma_m^{-1/2}(z_0)\,\gamma_m^{-1/2}(z_1)\,\gamma_n^{-1/2}(z_0)\,\gamma_n^{-1/2}(z_1) \approx \gamma_m^{-1}(z_3)\,\gamma_n^{-1}(z_3)\,.$$

Equation 7.41 is now

$$\overline{\dot{S}_m^2} = \frac{Q}{2}\sum_{n=0}^{\infty} \frac{k_0^4\,\bar{n}_0^2\cos^2\mathcal{E}_n(z)}{4\alpha_n\nu_n^2} \cdot \int_{z_3} dz_3\,\frac{N^3(z_3)\,L(z_3)}{\gamma_m(z_3)\,\gamma_n(z_3)} \int_{-\infty}^{\infty} dz_2\,M_{mn}(z_0)\,M_{mn}(z_1)\exp\big[-z_2^2/\ell_z^2\big] \qquad 7.44$$

To perform the integration over z_2, we shall use (Dwight, 1961, p. 236)

$$\int_{-\infty}^{\infty}\big[\cos bx\big]\exp\big[-\beta^2x^2\big]\,dx = \frac{\sqrt{\pi}}{\beta}\exp\Big[-\frac{b^2}{4\beta^2}\Big]$$

Noting that $\gamma_n, \gamma_m >> \gamma_n - \gamma_m$, we can write

$$\int_{-\infty}^{\infty} dz_2\, M_{mn}(z_0) M_{mn}(z_1) \exp\left[-z_2^2/\ell_z^2\right] \approx$$

$$\ell_z \sqrt{\pi} \left\{ \frac{1}{8} \exp\left[-\frac{(\gamma_n - \gamma_m)^2 \ell_z^2}{4} \right] + \frac{1}{4} \sin\left[2\theta_n(z_u, z_3)\right] \cos\left[2\theta_m(z, z_3)\right] \right\}.$$

The expression for the mean-square phase rate fluctuation finally becomes

$$\overline{\dot{S}_m^2} = \frac{Q}{2} \ell_z \sqrt{\pi} \sum_{n=0}^{\infty} \frac{K_0^4 \bar{n}_0^2}{4 a_n \nu_n^2} \int_{z_3} dz_3 \, \frac{N^3(z_3) L(z_3) T(z_3)}{\gamma_m(z_3) \gamma_n(z_3)} \qquad 7.45$$

where $T(z_3) = \frac{1}{8} \exp\left[-\frac{(\gamma_n - \gamma_m)^2 \ell_z^2}{4} \right] + \frac{1}{4} \sin\left[2\theta_n(z_u, z_3)\right] \cos\left[2\theta_m(z, z_3)\right]$.

Equation 7.45 is in a form which can be directly evaluated to determine the phase rate fluctuation for one incident mode. Since the variable-sound-speed waveguide can sustain multimode propagation, we must use equation 6.19 to compute the total mean-square phase rate fluctuation at any point in the waveguide. The actual procedure that was used to calculate the total mean-square phase rate fluctuation was as follows:

(a) using the WKB approximation, determine which incident modes are strongly excited at the receiver.

(b) using equation 7.45, calculate the phase rate fluctuations for each incident mode.

(c) using the weighted average concept from equation 6.19, determine the total mean-square phase rate fluctuation.

In order to compare the calculated values with actual experimental data, we have used an asymmetric n_o^2 bilinear-sound-speed profile which leads to convenient representations for the various depth-dependent quantities in equation 7.45. For simplification in the mathematics the depth axis has been shifted so that z = 0 at the sound speed minimum, z > 0 above the minimum, and z < 0 below the minimum. The n_o^2 profile can be written as

$$n_o^2(z) = \begin{cases} 1 - q_u z & \text{for } z > 0 \\ 1 + q_\ell z & \text{for } z < 0 \end{cases} \qquad 7.46$$

where q_u and q_ℓ are the slopes of the profile for z > 0 and z < 0 respectively. Figure 9 schematically pictures the n_o^2 profile and the shifted coordinate system.

Expressions such as $\theta_m(z_u, z)$, the characteristic equation of the wave-guide (equation 7.10), and the normalization factor (equation 7.12) can be easily determined using equation 7.46. For example, with

$$\gamma_m(z) = K_0 \left[n_o^2(z) - \cos^2 \phi_m \right]^{1/2}$$

where ϕ_m is the horizontal propagation angle, equation 7.10 becomes

$$\left(m + \tfrac{1}{2}\right)\pi = \int_{z_\ell}^{z_u} \gamma_m \, dz = \int_0^{z_u} \gamma_m \, dz + \int_{z_\ell}^{0} \gamma_m \, dz$$

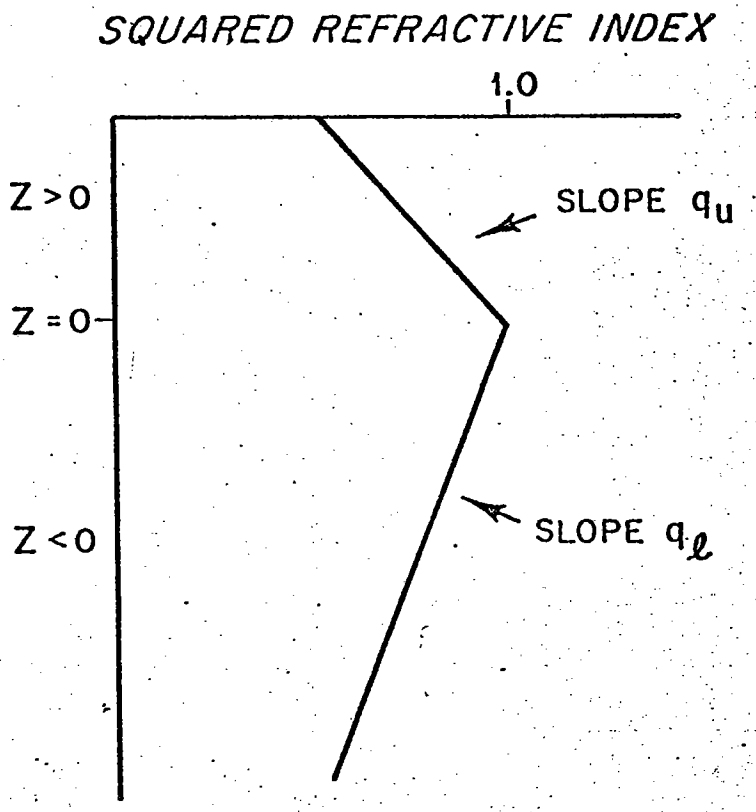

Figure 9: Bilinear squared-refractive-index profile with depth origin shifted to sound channel axis.

$$\left(m+\tfrac{1}{2}\right)\pi = K_0 \int_0^{z_u} \left[\sin^2\phi_m - q_u z\right]^{1/2} dz + K_0 \int_{z_\ell}^{0} \left[\sin^2\phi_m + q_\ell z\right]^{1/2} dz$$

$$\left(m+\tfrac{1}{2}\right)\pi = \frac{2K_0 \sin^3\phi_{0m}}{3}\left[\frac{1}{q_u} + \frac{1}{q_\ell}\right] \qquad 7.47$$

where ϕ_{om} is the horizontal propagation angle at z = 0.

The actual integral over z_3 in equation 7.45 is performed numerically using the trapezoidal rule. The limits of integration on z_3 are controlled by two independent factors. The first, which is solely acoustic in nature, is based on the assumption that the acoustic field for any mode is equal to zero outside its turning points. For a given incident and scattered mode the region of integration on z_3 will be over those depths where the amplitude of either mode does not equal zero. The second factor is due to the frequency limits imposed on the internal waves. From equation 7.38 we noted that $N(z_3)$ must always be greater than ω_Δ. For an exponentially decaying N, a depth will be reached where $N(z_3) = \omega_\Delta$. Below this depth the internal wave effects will be zero. The limits of integration on z_3 must therefore be chosen so as to satisfy both of these factors.

With the coordinate system in Figure 9 the exponentially decaying Brunt-Väisälä frequency is written as

$$N(z_3) = N_0 \exp\left[(z_3 - z_s)/B\right] \qquad 7.48$$

where z_s is the actual depth of the sound channel axis.

In equation 7.48 we choose the 1/e depth B to be 1300 meters and set N_o equal to 3 cycles/hr (5.2×10^{-3} rad/sec). The inertial frequency ω_i is taken as 7.3×10^{-5} rad/sec (at 30^o latitude). From an estimated rms refractive index fluctuation of 5×10^{-4} at the top of the main thermocline (Munk and Zachariasen, 1976), we set the value of the dimensionless parameter μ to be 24.5.

For actual calculations we have chosen a sound-speed profile representative of the region between Eleuthera and Bermuda. We have picked a sound speed minimum of 1492 m/s (at 1300 m), a surface speed of 1540 m/s, and a bottom speed of 1542 m/s (at 5000 m). The appropriate slopes in Figure 9 are then $q_u = 4.72 \times 10^{-5}$ m^{-1} and $q_\ell = 1.72 \times 10^{-5}$ m^{-1}.

In evaluating equation 7.45, we note that an infinite summation of scattered modes n is necessary to calculate the mean-square phase rate fluctuation for incident mode m. We recall sections 4 and 5 where we argued that the dominant terms in the summation are for $n \approx m$. With equation 7.45 we can verify that this claim is in fact true. Figure 10 shows the percent of the total phase rate fluctuation for mode m versus the number of scattered modes displaced from mode m. The curve shown is an average of the curves from several widely spaced incident modes (modes 50, 100, and 200). We can see that over 95% of the contribution to the mean-square phase rate fluctuation occurs from scattered modes whose mode number is within 10 of the incident mode. In determining $\overline{\dot{s}_m^2}$ we shall then replace the infinite summation by

$$\sum_{n=m-10}^{m+10} .$$

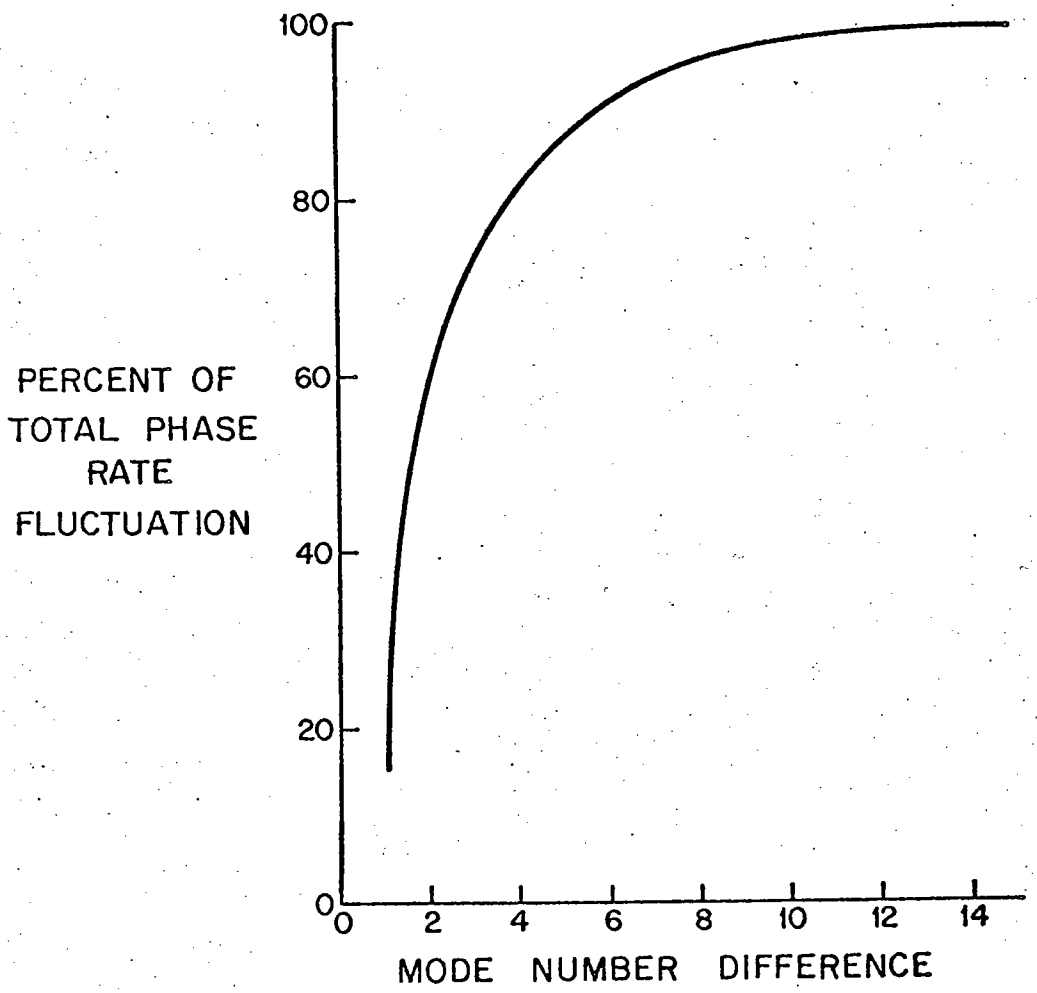

Figure 10: Relative contribution of scattered modes to the modal phase rate fluctuation. Over 95% of the contribution occurs for scattered modes with a mode number within 10 of the incident mode. The curve shown is an average for three incident modes (modes 50, 100, 200).

The condition that $\alpha_x = |\alpha_m - \alpha_n|$ allows us to determine the horizontal scales of internal waves that are most important in the acoustic interaction process. If we choose an incident mode number of 100, for example, we find that internal waves whose horizontal wavelength projection along the propagation path is less than 5 km contribute less than 5% to the total phase rate fluctuation.

Munk and Zachariasen (1976) have developed a theoretical model based upon ray techniques to explain acoustic-internal wave interactions in the ocean. They have compared experimental data from the MIMI transmissions between Eleuthera and Bermuda (Clark and Kronengold, 1974) with their theoretical predictions for the rms phase rate fluctuation. Although Munk and Zachariasen do not compute $\left[\overline{\dot{S}^2}\right]^{\frac{1}{2}}$ at a given depth, they do calculate the rms phase rate fluctuation for a single axial ray and for a single surface limited ray (a ray whose upper turning point is at the sea surface). For a range of 550 km and an acoustic frequency of 406 Hz they find that

$$\left[\overline{\dot{S}^2}\right]^{1/2} = \begin{cases} 2.9 \times 10^{-3} \text{ rad/sec for axial ray} \\ 4.6 \times 10^{-3} \text{ rad/sec for surface limited ray.} \end{cases}$$

The actual MIMI experimental value for a source and receiver on the sound channel axis is

$$\left[\overline{\dot{S}^2}\right]^{1/2} = 2.8 \times 10^{-3} \text{ rad/sec.}$$

With a source at 406 Hz, a range of 550 km, and the n_o^2 bilinear profile chosen above, the multimode rms phase rate fluctuation has been determined using equations 7.45 and 6.19. The depth dependency has been

plotted in Figure 11. It can be seen that the calculated values compare favorably with those of Munk and Zachariasen. The computed value at the sound channel axis is approximately one-half that of the experimental value.

The larger phase rate values at shallow and deep water can be explained by the following argument. The separation between the upper and lower turning point of a mode is proportional to its mode number (see equation 7.47). Due to the exponential Brunt-Väisälä profile, most of the refractive index fluctuation energy is in shallow water. We would therefore expect the higher order modes, which have a shallower upper turning point, to contain more internal-wave-induced fluctuation energy than the lower order modes. On the other hand, lower order modes contain most of the acoustic energy for receiver depths close to the sound channel axis. The resultant depth dependence of $\left[\overline{\dot{S}^2}\right]^{\frac{1}{2}}$ in Figure 11 is then evident.

Close examination of Figure 11 suggests that the minimum value of the phase rate fluctuation occurs several hundred meters below the sound speed minimum. The calculated phase rate fluctuations for a receiver above the sound channel axis are greater than the fluctuations for a receiver at the same sound speed below the axis. The skewness about the sound channel axis is due to the depth dependence of the Brunt-Väisälä profile with its associated refractive index fluctuations. This conclusion is based upon a comparison of calculated phase rate fluctuations from profiles with constant and exponentially decaying Brunt-Väisälä frequencies. The precise depth dependency of the phase

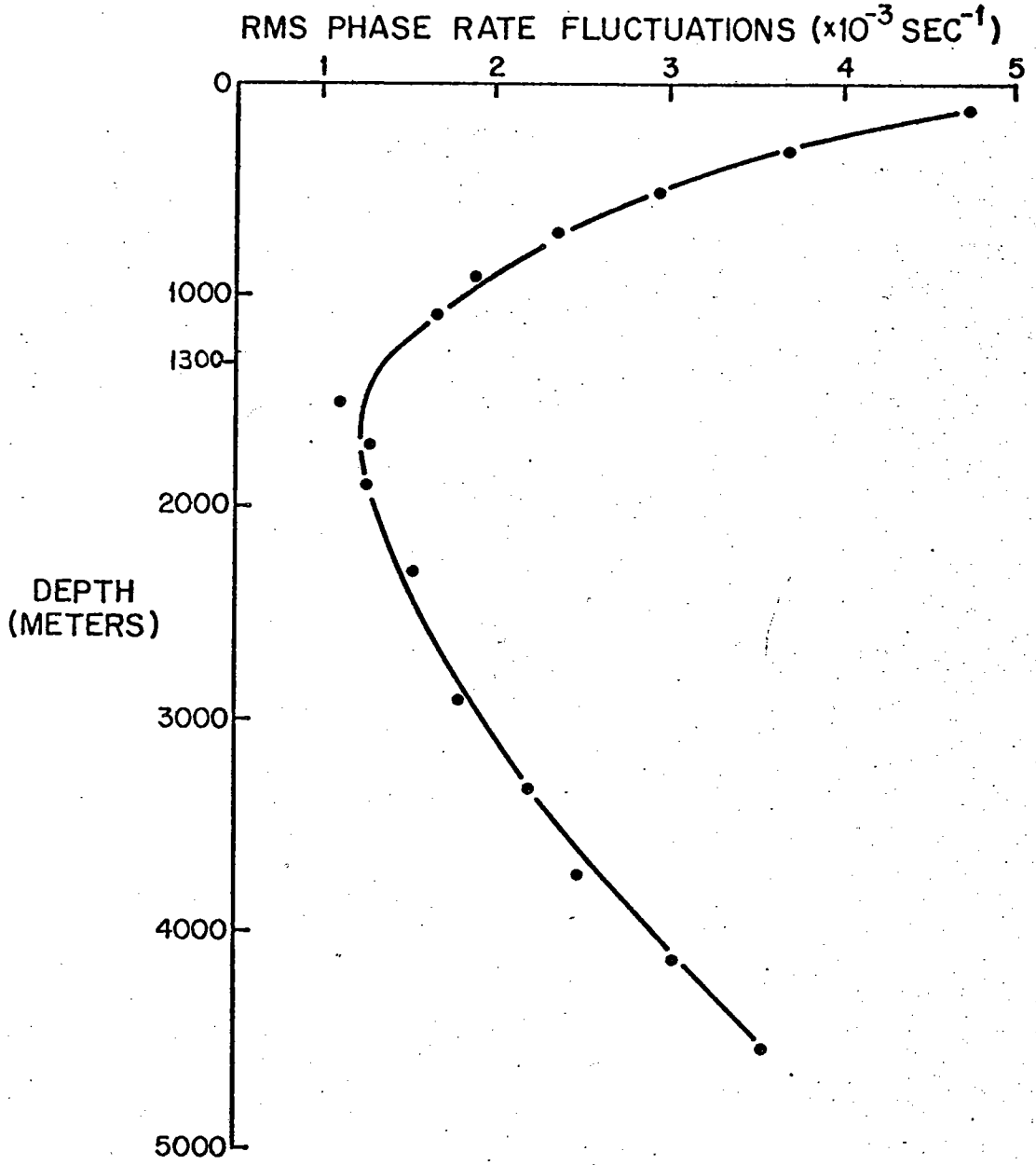

Figure 11: Depth dependence of the multimode rms phase rate fluctuation at a range of 550 km. The source is at the axis of the sound channel (1300 meters) and has a frequency of 406 Hz. The solid line is a visual fit for the computed points.

rate fluctuations is thus a function of the depth distribution of the induced refractive index fluctuations.

Experimental data also suggests that the depths for the minimum sound speed and the minimum phase rate fluctuation do not coincide (Porter and Spindel, 1976). The Porter and Spindel data was taken at a range of 264 km with a source at 1100 meters and a frequency of 220 Hz. With a minimum sound speed of 1495 m/s (at 1100 m) and bilinear slopes of $q_u = 5.24 \times 10^{-5}\ m^{-1}$ and $q_\ell = 1.48 \times 10^{-5}\ m^{-1}$, we have calculated the rms phase rate fluctuations. A comparison of the measured and predicted values at several receiver depths is shown below:

Depth	Measured	Calculated
500 m	6.6×10^{-3} r/s	1.0×10^{-3} r/s
1000 m	4.3×10^{-3} r/s	0.7×10^{-3} r/s
1500 m	2.7×10^{-3} r/s	0.6×10^{-3} r/s

Before we explain possible reasons for the discrepancy between the calculated and measured values, we should note that the smallest phase rate fluctuations occur for the 1500 meter receiver depth (400 meters below the sound channel axis). Unfortunately there is no data for deeper depths. This data is then consistent with the profile in Figure 11.

The MIMI data mentioned above used fixed sources and fixed receivers. The Porter and Spindel experiment used a fixed source and drifting receivers with typical velocities along the propagation vector of 500 meters/hr. The drifting receivers are probably the reason for the large difference between the computed and measured values. Two possible explanations can be used to explain the large measured phase rate fluctuations. Due

to the resulting Doppler shift, increased spectral levels in the refractive index fluctuations will be experienced by the drifting receiver (Garrett and Munk, 1972, section 8). Secondly, the actual horizontal displacement will cause a different multipath structure to be encountered as the receiver moves through space. This will also create an increase in the acoustic fluctuations. It should be noted that the expressions derived here are directly applicable only to fixed sources and fixed receivers.

Other statistical quantities such as the frequency spectrum of the phase rate fluctuations can be easily obtained from the above derivation. Noting that

$$\overline{\dot{S}_m^2} = \int_\omega F_{\dot{S}_m}(\omega)\, d\omega \,,$$

we can use equation 7.45 and 7.38 to write

$$F_{\dot{S}_m}(\omega) = \frac{1}{\omega} \operatorname{Cosh}^{-1} \frac{j\alpha^{(1)}}{\Delta} \left\{ Q\, \ell_z \sqrt{\pi} \sum_{n=0} \frac{K_0^4 \bar{n}_0^2}{4 a_n \nu_n^2} \cdot \int_{z_3} dz_3 \, \frac{N^3(z_3)\, T(z_3)}{\gamma_m(z_3)\, \gamma_n(z_3)} \right\} \qquad 7.49$$

In equation 7.49 we recall that

$$j\alpha^{(1)}(\omega) = \frac{j(\omega^2 - \omega_i^2)^{1/2}}{2BN_0} \,.$$

For a given value of ω, there are several important points to consider in evaluating equation 7.49. No internal wave contributions exist for $\omega < \omega_\Delta$, where ω_Δ is a function of modes m and n (equation 7.36). As the scattered mode number n changes in equation 7.49, the minimum value of ω causing acoustic fluctuations will also change. For high frequencies the value of ω may exceed $N(z_3)$ over part of the z_3 region of integration. When this occurs we must change the upper limit of integration to the depth where $\omega = N(z_3)$.

In Figure 12 we have determined the frequency spectrum of the phase rate fluctuations for a single incident mode. As in Figure 11 we have used a source at 1300 meters with a frequency of 406 Hz and have calculated the frequency spectrum at a range of 550 Km. We have chosen a receiver depth of 300 meters and have selected a strongly excited incident mode (mode 304). The solid line in Figure 12 is a plot of the calculated values from equation 7.49. The inertial frequency ω_i and the peak Brunt-Väisälä N_o are indicated in the figure. We note that over much of the frequency range the slope of the phase rate spectrum is between -0.5 and -1.0. At high frequencies it is approximately -1.0 with a sharp cutoff beyond the Brunt-Väisälä frequency at the upper turning point of the mode. For a multimode frequency spectrum the mid-frequency dependence will be the same as in Figure 12 while the high and low frequency characteristics will be slightly modified. For example, the high-frequency cutoff will be more gradual since the maximum Brunt-Väisälä frequency will be different for each mode.

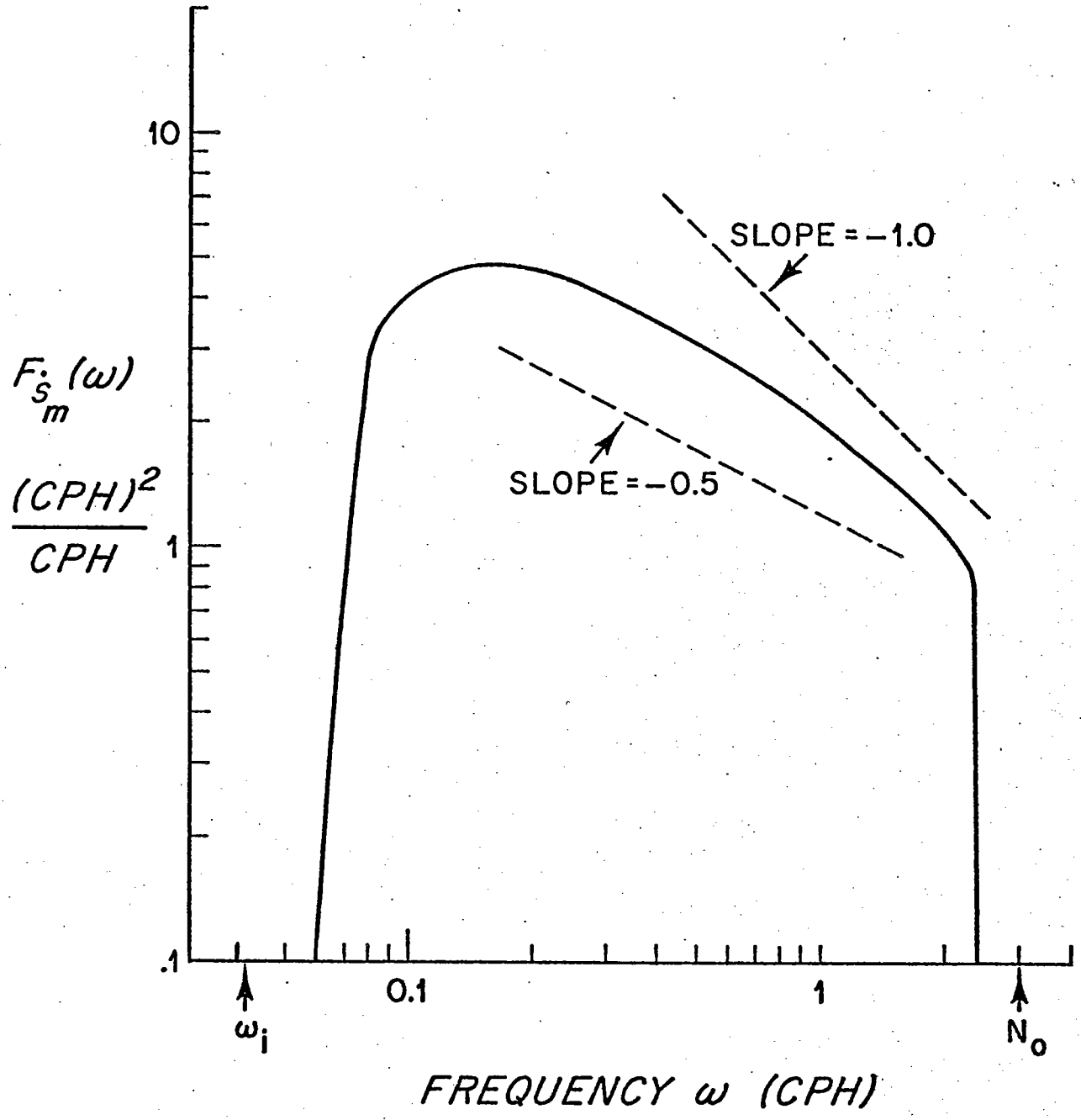

Figure 12: Phase rate frequency spectrum for single incident mode. Source frequency is 406 Hz, source depth is 1300 meters, receiver depth is 300 meters, range is 550 km, incident mode number is 304, peak Brunt-Väisälä frequency N_o is 3 cycles/hr (CPH), and inertial frequency ω_i is 0.042 CPH.

The frequency spectrum predicted by Figure 12 compares favorably with experimental results. Dyson et al. (1976) show that the slope of the spectrum for the MIMI data is between 0 and -1 and approaches -1 for high frequencies. Porter and Spindel (1976) find that the slope of their data is constant with a value slightly less than one over much of the internal wave frequency band with a sharp cutoff in the region of the largest Brunt-Väisälä frequency for the water column. Theoretical estimates using ray acoustics have been made for the frequency spectrum of the phase fluctuations. For a single path Munk and Zachariasen (1976) have predicted a constant ω^{-3} dependence (ω^{-1} for phase rate), while Porter et al. (1974) have found an ω^{-2} dependence (ω^{0} for phase rate) for a two-ray interference. It appears that the estimate of the frequency spectrum for phase rate fluctuations using acoustic wave techniques agrees better with the actual data.

The prediction of acoustic fluctuations in this thesis have all been based on the assumption that the acoustic-internal wave interaction can be modeled as a weak scattering process. The solutions indicate that quantities such as the mean-square phase fluctuations or the phase-rate frequency spectrum are linearly proportional to range. Since we have neglected back-scattering and multiple-scattering effects in our derivation, it is important to determine the region of validity for our expressions.

We shall use the criterion that the solutions are valid when the phase fluctuations arising from one incident mode are less than $\pi/2$ radians. It should be noted that we are not requiring that the total

phase fluctuation (see section 6) be less than $\pi/2$ radians. We can obtain a rough estimate for the range of validity by examining equation 4.24:

$$\overline{S_m^2} = K_0^4 \eta_0^2 / D^2 \sum_{n=1}^{\infty} \Gamma^2(z_T) h_{mn2}^2(z_T) / \alpha_n^2 \iint_{0}^{\chi} \int_{0}^{\chi} dx_0 dx_1 \, \rho_6(x_2) \, e^{i(\alpha_m - \alpha_n)x_2} \qquad 4.24$$

Let us now choose a correlation function of the form

$$\rho_6(x_2) = \exp\left(-x_2^2/\ell_H^2\right) \qquad 7.50$$

where ℓ_H is the horizontal correlation scale

and $x_2 = x_0 - x_1$.

Changing the integration variables to x_2 and x_3 [where $x_3 = \frac{1}{2}(x_0 + x_1)$] and noting that $\ell_H << x$, so that the limits on the x_2 integral can be extended to $\pm\infty$, we can write

$$\overline{S_m^2} = \frac{K_0^4 \eta_0^2 \chi}{D^2} \sum_{n=1}^{\infty} \frac{\Gamma^2(z_T) h_{mn2}^2(z_T)}{\alpha_n^2} \int_{-\infty}^{\infty} \exp\left[-x_2^2/\ell_H^2 + i(\alpha_m - \alpha_n)x_2\right] dx_2 \qquad 7.51$$

The integral over x_2 has been evaluated (Gradshteyn and Ryzhik, 1965, p. 307) so that

$$\overline{S_m^2} = \frac{K_0^4 \eta_0^2 \chi \ell_H \pi^{1/2} \Gamma^2(z_T)}{D^2} \sum_{n=1}^{\infty} \frac{h_{mn2}^2(z_T)}{\alpha_n^2} \exp\left[-\frac{(\alpha_m - \alpha_n)^2}{4} \ell_H^2\right] . \qquad 7.52$$

In equation 7.52, $\Gamma^2(z_T)$ is the square of the acoustic thickness. From section 2, we can write

$$\overline{\sigma^2}^{1/2}(z) = (5 \times 10^{-4}) \frac{N^{3/2}(z)}{N_0^{3/2}} .$$

Using the exponentially decaying Brunt-Väisälä profile (equation 2.3) and integrating over depth, we have

$$\Gamma^2(z_T) \approx \left[(5 \times 10^{-4}) \left(\frac{2B}{3} \right) \right]^2$$

where B is the 1/e depth.

Since only a few of the scattered modes contribute appreciably to the summation, we can write

$$\overline{S_m^2} \approx \frac{K_0^4 n_0^2 \Gamma^2(z_T) \chi \ell_H \pi^{1/2}}{\alpha_n^2 D^2} \approx \frac{K_0^2 \Gamma^2(z_T) \chi \ell_H \pi^{1/2}}{D^2} \qquad 7.53$$

The requirement that $\overline{S_m^2}^{1/2} < \pi/2$ or $\overline{S_m^2} < \pi^2/4$ implies

$$\chi < \frac{\pi^2 D^2}{4 K_0^2 \Gamma^2(z_T) \ell_H \pi^{1/2}} \qquad 7.54$$

Choosing parameters consistent with other parts of this thesis, we have B = 1300 meters, D = 5000 meters, and ℓ_H = 1000 meters. With source frequencies of 406 Hz and 220 Hz we find that the range of validity is

$$x_{406} < 65 \text{ km.}$$
$$x_{220} < 221 \text{ km.} \qquad 7.55$$

If we relax our phase requirement to $\overline{S_m^2}^{1/2} < \pi$, the ranges of validity will increase by a factor of 4. It should be noted that the estimates given here are conservative, since we have chosen the maximum possible values in equation 7.52.

The calculations performed earlier in this section at a range of 550 km are probably beyond the region of applicability of the weak scattering theory. Nevertheless, there appears to be a fairly close agreement between the measured and calculated values.

Experimental data with acoustic frequencies at 220 Hz and 406 Hz (Porter and Spindel, 1976) indicates that weak scattering theory is still valid at a range of 250 km. The theoretical calculations (equation 7.49) show that the frequency spectra of the phase rate fluctuation is proportional to the square of acoustic frequency. A comparison of the spectra from 220 Hz and 406 Hz sources indicates that the 406 Hz spectral levels are consistently 5-6 dB greater. The actual ratio is then approximately 3.55 as compared to the predicted ratio of 3.4. Since strong scattering theory (Tatarski, 1971) does not predict this same acoustic frequency dependence, it

is reasonable to assume that weak scattering theory is still valid for this range.

8. CONCLUSIONS

This thesis investigated the nature of acoustic-internal wave interaction using acoustic wave techniques. The study did not attempt to prove that all or even most of the acoustic fluctuations in long range propagation are the direct or indirect result of internal waves. Horizontal currents, tides, microstructure, as well as internal waves can all cause significant acoustic fluctuations. For the space and tide scales of interest here, internal waves are likely to have a considerable influence on sound propagation. Using a statistical internal wave model the relationship between the induced refractive index fluctuations and the acoustic fluctuations has been explored.

With weak scattering theory in an acoustic waveguide, we have found that the internal wave field acts as a diffraction grating to the acoustic wave. Together with the properties of the waveguide, the internal waves only permit selected scattered acoustic waves to propagate to long ranges with little attenuation. With a random wavenumber distribution of internal waves the acoustic field performs a spatial filtering of the internal wave field. Acoustic fluctuations become a statistical average with a bias toward particular spatial internal wavelengths.

The multimode nature of acoustic propagation greatly complicates the relationship between internal waves and acoustics. Single mode propagation permits linear relationships to be established between the statistics of acoustic fluctuations and those of internal waves. Multimode propagation induces non-linearities to the acoustic phase and amplitude fluctuations which preclude their comparison to internal wave statistics.

With the assumptions of statistical independence between the amplitude and phase fluctuations within a mode and between different modes, we found that the total phase rate fluctuation was a weighted average of the individual phase rate fluctuations in each mode. Each of the modal phase rate fluctuations can be related to the internal wave fluctuations, so that a direct relationship exists between the multi-mode phase rate statistics and the internal statistics.

Comparisons have been made between measured and predicted phase rate fluctuations for long range acoustic propagation. The theoretical estimates have been based upon the Garrett and Munk 1972 internal wave model. Considering the approximations and uncertainties in the acoustic and internal wave models, the correspondence between the theoretical and actual values is quite surprising. The theory also compares favorably with a weak scattering theory based upon geometrical optic techniques. The depth variation of rms phase rate fluctuation suggests that the influence of internal waves on acoustics is minimal at a depth several hundred meters below the sound channel axis.

The frequency spectrum for the phase rate fluctuation was also examined. Due to the multimode propagation the observed spectrum is a weighted average of the spectrum in each mode. Each of these component spectra can then be related to the internal wave statistics. We found that over a wide frequency band the calculated phase rate spectrum for a single mode is proportional to $\omega^{-\frac{1}{2}}$ and approaches ω^{-1} at high frequencies.

Several improvements could be made in the theory to provide a better estimate for the phase rate fluctuations. With the n_o^2 bilinear profile the exact Airy function solution could be substituted for the WKB approximation. More realistic sound-speed profiles would also give better results. Any more sophisticated acoustic model would probably cause a substantial increase in computer execution time. With the WKB approximation and the bilinear profile in takes approximately 5 minutes on a Hewlett-Packard 2100 computer to obtain an estimate of the phase rate fluctuations due to one incident mode. Several modifications in the internal wave model might also be considered. The GM75 model could be used instead of the GM72 model to obtain the same phase rate estimates. We would expect the results to be comparable although long internal wavelengths would be slightly more energetic in the interaction process. The vertical structure of internal waves might also be considered more closely. We have shown that the horizontal scales of internal waves cause most of the phase fluctuations, but the vertical scales are obviously important in determining the correlation distances for a vertical acoustic array.

The significance of the nature and effect of multimode acoustic propagation is critical in any acoustic study. It would be highly desirable,for example, to predict the acoustic fluctuations for a moving receiver (or due to a moving source) which is traveling through a time and space varying multimode structure. An understanding of the interaction process between refractive index inhomogeneities and multimode propagation must be a central concern in any future study.

In summary, the major contributions of this thesis include the following:

1. Treatment of acoustic-internal wave interaction in a waveguide using acoustic wave techniques.
2. Interpretation of the interaction process of a diffraction grating.
3. Confirmation that large acoustic fluctuations result when the ray cycle length is an integral multiple of internal wave lengths along the acoustic propagation path.
4. Recognition that amplitude and phase fluctuations in an inhomogeneous waveguide cannot be linearly related to internal wave statistics. Under the assumption of statistical independence between amplitude and phase fluctuations within a mode and between different modes, the total phase rate fluctuation is a weighted sum of the phase rate fluctuations in the individual modes. The individual modal phase rate fluctuations can be related to the internal wave statistics.
5. Determination of the frequency spectrum for the phase rate fluctuation. Over much of the frequency band the frequency spectrum is proportional to $\omega^{-\frac{1}{2}}$; at high frequencies it is approximately proportional to ω^{-1}.
6. Determination of the depth dependence of the mean-square phase rate fluctuation. Largest fluctuations occur for shallow and deep receivers. With a source on the sound channel axis, the minimum fluctuations occur several hundred meters below the sound channel axis.

REFERENCES

Baer, R.N., and M.J. Jacobson, "Effect of a Rossby Wave on the Phase of an Underwater Acoustic Signal," J. Acoust. Soc. Am., 56, 809-816 (1974).

Barakos, P.A., "On the Theory of Acoustic Wave Scattering and Refraction by Internal Waves," Report No. 649, U.S. Navy Underwater Sound Laboratory, Fort Trumbull, New London, Conn., 178 pp, 1965.

Barkhatov, A.N. and Y.N. Cherkashin, "Measurements of the Back-Scattering of Sound by an Internal Wave," Sov. Phys. Acoust., 8, 41-43 (1962).

Barkhatov, A.N. and Y.N. Cherkashin, "Deformation of a Beam of Sound by an Internal Wave at the Boundary Between Two Liquids," Sov. Phys. Acoust., 9, 86-87 (1963).

Batchelor, G.K., "Wave Scattering Due to Turbulence," Symposium on Naval Hydrodynamics, Washington, D.C., September 24-28, 1956.

Benilov, A.Y., "Experimental Data on Small-Scale Ocean Turbulence," Izv. Atmos. Oceanic Phys., 5, 288-299 (1969).

Bremmer, H., "The W.K.B. Approximation as the First Term of a Geometric-Optical Series," Commun. Pure Appl. Math., 4, 105-115 (1951).

Brown, W.P., Jr., "Validity of the Rytov Approximation," J. Opt. Soc. Am., 57, 1539-1543 (1967).

Carter, A., Multi-Mode Acoustic Propagation in an Inhomogeneous Bounded Medium, Ph.D. Thesis, Brown University, Providence, R.I., 1963.

Chernov, L.A., Wave Propagation in a Random Medium, Dover Publications, Inc., New York, 1960.

Chuprov, S.D., "On the Observation of a Sound Signal in the Presence of Internal Waves," Izv. Atmos. Oceanic Phys., 2, 334-335 (1966).

Clark, J.G., and M. Kronengold, "Long-Period Fluctuations of CW Signals in Deep and Shallow Water," J. Acoust. Soc. Am., 56, 1071-1083 (1974).

Clay, C.S., "Effect of a Slightly Irregular Boundary on the Coherence of Waveguide Propagation," J. Acoust. Soc. Am., 36, 833-837 (1964).

Deferrari, H.A., "Effects of Horizontally Varying Internal Wavefields on Multipath Interference for Propagation Through the Deep Sound Channel," J. Acoust. Soc. Am., 56, 40-46 (1974).

DeFerrari, H., and R. Leung, "Spectrum of Phase Fluctuations Caused by Multipath Interference," J. Acoust. Soc. Am., 58, 604-607, (1975).

DeWolf, D.A., "Validity of Rytov's Approximation," J. Opt. Soc. Am., 57, 1057-1058 (1967).

Dwight, H.B., Tables of Integrals and Other Mathematical Data, The Macmillan Co., Toronto, Ontario, 1961.

Dyson, F., W. Munk, and B. Zetler, "An Interpretation in Terms of Internal Waves and Tides of Multipath Scintillations Eleuthera to Bermuda," J. Acoust. Soc. Am., in press (1976).

Eckart, C., Hydrodynamics of Oceans and Atmospheres, Pergamon Press, New York, 1960.

Ellison, T.H., "The Propagation of Sound Waves Through a Medium with Very Small Random Variations in Refractive Index," J. Atmos. Terr. Phys., 2, 14-21 (1951).

Ewart, T.E., "Acoustic Fluctuations in the Open Ocean: A Measurement Using a Fixed Refractive Path," J. Acoust. Soc. Am., in press (1976).

Franchi, E.R., and M.J. Jacobson, "Ray Propagation in a Channel with Depth-Variable Sound Speed and Current," J. Acoust. Soc. Am., 52, 316-331 (1972).

Franchi, E.R., and M.J. Jacobson, "An Environmental-Acoustics Model for Sound Propagation in a Geostrophic Flow," J. Acoust. Soc. Am., 53, 835-847 (1973).

Furry, W.H., "Two Notes on Phase-Integral Methods," Phys. Rev., 71, 360-371 (1947).

Garrett, C. and W. Munk, "Space-Time Scales of Internal Waves," Geophys. Fluid Dynam., 2, 225-264 (1972).

Garrett, C. and W. Munk, "Space-Time Scales of Internal Waves: A Progress Report," J. Geophys. Res., 80, 291-297 (1975).

Gradshteyn, I.S. and I.M. Ryzhik, Table of Integrals, Series, and Products, Academic Press, New York, 1965.

Heidbreder, G.R., "Multiple Scattering and the Method of Rytov," J. Opt. Soc. Am., 57, 1477-1479 (1957).

Isakovich, M.A., "Scattering of Acoustic Waves at Small Inhomogeneities in a Waveduct," Sov. Phys. Acoust, 3, 35-45 (1957).

Katz, E.J., "Effect of the Propogation of Internal Water Waves on Underwater Sound Transmission," J. Acoust. Soc. Am., 42, 83-87 (1967).

Keller, J.B., "Accuracy and Validity of the Born and Rytov Approximations," J. Opt. Soc. Am., 59, 1003-1004 (1969).

Kennedy, R.M., "Phase and Amplitude Fluctuations in Propagating Through a Layered Ocean," J. Acoust. Soc. Am., 46, 737-745 (1969).

Lapin, A.D., "Scattering of Sound Waves in Irregular Waveguides," Sov. Phys. Acoust., 4, 272-279 (1958).

Lee, O.S., "Effect of an Internal Wave on Sound in the Ocean," J. Acoust. Soc. Am., 33, 677-681 (1961).

Liebermann, L., "The Effect of Temperature Inhomogeneities in the Ocean on the Propagation of Sound," J. Acoust. Soc. Am., 23, 563-570 (1951).

Liu, C.H., "Wave Propagation in a Random Medium with Stratified Background," Radio Sci., 3, 551-559 (1968).

Malyuzhinets, G.D., "Sound Scattering by Nonuniformities in a Layer of Discontinuity in the Sea," Sov. Phys. Acoust., 5, 68-74 (1959).

Mintzer, D., "Wave Propagation in a Randomly Inhomogeneous Medium I, II, III," J. Acoust. Soc. Am., 25, 922-927, 1107-1111 (1953); 26, 186-190 (1954).

Mooers, C.N.K., "Sound-Velocity Perturbations Due to Low-Frequency Motions in the Ocean," J. Acoust. Soc. Am., 57, 1067-1075 (1975).

Munk, W.H., and F. Zachariasen, "Sound Propagation Through a Fluctuating Stratified Ocean: Theory and Observation," J. Acoust. Soc. Am., 59, 818-838 (1976).

Nayfeh, A.H., Perturbation Methods, Wiley-Interscience, New York, 1973.

Nayfeh, A.H., "Sound Waves in Two-Dimensional Ducts with Sinusoidal Walls," J. Acoust. Soc. Am., 56, 768-770 (1974).

Neubert, J.A., "Asymptotic Solution of the Stochastic Helmholtz Equation for Turbulent Water," J. Acoust. Soc. Am., 48, 1203-1211 (1970).

Phillips, O.M., The Dynamics of the Upper Ocean, Cambridge University Press, London, 1969.

Pierce, A.D., "Extension of the Method of Normal Modes to Sound Propagation in an Almost-Stratified Medium," J. Acoust. Soc. Am., 37, 19-27 (1965).

Pisareva, V.V., "Limits of Applicability of the Method of 'Smooth' Perturbations in the Problem of Radiation Propagation Through a Medium Containing Inhomogeneities," Sov. Phys. Acoust., 6, 81-86 (1960).

Porter, R.P., "Transmission and Reception of Transient Signals in a SOFAR Channel," J. Acoust. Soc. Am., 54, 1081-1091 (1973).

Porter, R.P., and H.D. Leslie, "Energy Evaluation of Wide-Band SOFAR Transmission," J. Acoust. Soc. Am., 58, 812-822 (1975).

Porter, R.P., and R.C. Spindel, "Acoustic Fluctuations and Internal Waves - Are Their Spectra Related?," J. Acoust. Soc. Am., 59, S57 (1976).

Porter, R.P., R.C. Spindel, and R.J. Jaffee, "Acoustic-Internal Wave Interaction at Long Ranges in the Ocean," J. Acoust. Soc. Am., 56, 1426-1436 (1974).

Samuels, J.C., "On Propagation of Waves in Slightly Rough Ducts," J. Acoust. Soc. Am., 31, 319-325 (1959).

Sancer, M.I., and Varvatsis, A.D., "A Comparison of the Born and Rytov Methods," Proc. IEEE, 58, 140-141 (1970).

Sanford, T.B., "Observations of Strong Current Shears in the Deep Ocean and Some Implications on Sound Rays," J. Acoust. Soc. Am., 56, 1118-1121 (1974).

Schmeltzer, R.A., "Means, Variances, and Covariances for Laser Beam Propagation Through a Random Medium," Quart. Appl. Math., 24, 339-354 (1966).

Spindel, R.C., R.P. Porter, and R.J. Jaffee, "Long-Range Sound Fluctuations with Drifting Hydrophones," J. Acoust. Soc. Am., 56, 440-446 (1974).

Stanford, G.E., "A Model for Signal Fluctuations Induced by Internal Waves," Tech. Mem. TA 113-189-71, Naval Underwater Systems Center, Newport, R.I., 17 pp., 1971.

Stanford, G.E., "Low-Frequency Fluctuations of a CW Signal in the Ocean," J. Acoust. Soc. Am., 55, 968-977 (1974).

Steinberg, J.C., J.G. Clark, H.A. DeFerrari, M. Kronengold, and K. Yacoub, "Fixed-System Studies of Underwater Acoustic Propagation," J. Acoust. Soc. Am., 52, 1521-1536 (1972).

Strohbehn, J.W., "Comments on Rytov's Method," J. Opt. Soc. Am., 58, 139-140 (1968).

Tatarski, V.I., Wave Propagation in a Turbulent Medium, Dover Publications, Inc., New York, 1961.

Tatarski, V.I., The Effects of the Turbulent Atmosphere on Wave Propagation, TT 68-50464, National Technical Information Service, Springfield, Va., 1971.

Taylor, L.S., "On Rytov's Method," Radio Sci., 2, 437-441 (1967).

Tindle, C.T., and K.M. Guthrie, "Rays As Interfering Modes in Underwater Acoustics," J. Sound Vib., 34, 291-295 (1974).

Tolstoy, I., "Phase Changes and Pulse Deformation in Acoustics," J. Acoust. Soc. Am., 44, 675-683 (1968).

Tolstoy, I., Wave Propagation, McGraw-Hill, New York, 1973.

Tolstoy, I. and C.S. Clay, Ocean Acoustics: Theory and Experiment in Underwater Sound, McGraw-Hill, New York, 1966.

Urick, R.J., G.R. Lund, and D.L. Bradley, "Observations of Fluctuation of Transmitted Sound in Shallow Water," J. Acoust. Soc. Am., 45, 683-690 (1969).

Weinberg, N.L., J.G. Clark, and R.P. Flanagan, "Internal Tidal Influence on Deep-Ocean Acoustic-Ray Propagation," J. Acoust. Soc. Am., 56, 447-458 (1974).

Weston, D.E., and H.W. Andrews, "Acoustic Fluctuations Due to Shallow-Water Internal Waves," J. Sound Vib., 31, 357-367 (1973).

Weston, D.E. A.A. Horrigan, S.J.L. Thomas, and J. Revie, "Studies of Sound Transmission Fluctuations in Shallow Coastal Waters," Phil. Trans. Roy. Soc. London, A 265, 567-606 (1969).

VITA

Richard Jay Jaffee was born in Worcester, Massachusetts on October 10, 1948. He prepared for college at Classical High School (Worcester, Mass.) from 1963-1966. He attended Brown University from 1966-1970 and received the degree of Bachelor of Science in electrical engineering in June, 1970. He graduated magna cum laude and was elected to Tau Beta Pi and Sigma Xi. He entered the Massachusetts Institute of Technology and Woods Hole Oceanographic Institution joint program in ocean engineering in 1970. He is a candidate for the degree of Doctor of Philosophy in ocean engineering, June 1976.